GLASS FIBER REINFORCED POLYMER COMPOSITE CONNECTION BETWEEN CONCRETE WALL PANELS UNDER CYCLIC SHEAR

by

Trevor K. Nye

A thesis submitted to the faculty of
The University of Utah
in partial fulfillment of the requirements for the degree of

Master of Science

Department of Civil and Environmental Engineering

The University of Utah

August 2017

THE UNIVERSITY OF UTAH GRADUATE SCHOOL

STATEMENT OF THESIS APPROVAL

The thesis of **Trevor K. Nye**

has been approved by the following supervisory committee members:

Chris P. Pantelides	, Chair	**12/21/16** Date Approved
Lawrence D. Reaveley	, Member	**12/21/16** Date Approved
Clayton A. Burningham	, Member	**12/21/16** Date Approved
	, Member	Date Approved
	, Member	Date Approved

and by **Michael Ernest Barber**, Chair of the Department of **Civil and Environmental Engineering**

and by David B. Kieda, Dean of The Graduate School.

ABSTRACT

Glass fiber reinforced polymer (GFRP) composites offer several advantages over welded steel plate connections when used in the connection of vertical joints between concrete wall panels. These advantages include resistance to corrosion, higher tensile strength, and ability to conform to uneven surfaces. In the present research, push-off tests and wall tests were carried out to understand the behavior of GFRP composite connections between concrete elements. Push-off tests were performed to understand direct shear transfer capability when using different concrete surface preparation methods. Wall tests were performed to understand the behavior of different GFRP composite connections under simulated seismic loads, or cyclic shear. Ultimately, the GFRP composite connections displayed little ductility, but demonstrated outstanding displacement and load capacity.

Push-off tests were performed for a GFRP composite connection between two L-shaped concrete elements. Each of the six groups of surface preparation included three specimens each, resulting in eighteen push-off specimens. A compressive load at the top and bottom of the specimen introduced direct shear in the GFRP composite connections. Specimens with concrete surface preparation using only a high-pressure wash demonstrated superior load and displacement capacities.

Wall tests were performed for GFRP composite connections between two concrete panels, with the connection only applied on one side of the joint. A lateral load

was applied at the top of the wall pair, while restraining the horizontal movement at the base and the vertical movement of each panel, inducing shear in the connection. Tests from group one (using unidirectional lamina) included eight specimens and concluded that the use of application pressure and CFRP anchors significantly increased load, displacement, and shear capacity of the GFRP composite connection. Also, fewer layers and CFRP anchor use increased the amount of energy dissipated during simulated seismic loads. Tests from group two (using bidirectional lamina) included six specimens and concluded that the use of GFRP anchors significantly increased load, displacement, and shear capacity of the GFRP composite connection. Also, the use of epoxy-putty adhesive had a significant effect on the load capacity; and full seam coverage and GFRP anchor use increased the amount of energy dissipated during simulated seismic loads.

TABLE OF CONTENTS

LIST OF TABLES

Tables

ACKNOWLEDGEMENTS

I would like to acknowledge the guidance and support from Dr. Chris Pantelides, Dr. Larry Reaveley, and Dr. Clayton Burningham during this important time in my education; their friendship and instruction have been crucial.

I want to thank the Department of Civil and Environmental Engineering, Forterra Structural and Specialty Products, Sika Corporation, and Structural Technologies for their support and donation of time and materials.

Additional thanks to my fellow students and mentors MJ Ameli, Joel Parks, Vanessa McEntee, and Ryan Barton. I express my gratitude to Mark Bryant for his sincere dedication to all students in the department.

CHAPTER 1

INTRODUCTION

Fiber reinforced polymer (FRP) composites have been used to construct many lightweight structures in the aerospace and sporting industry. FRP composites have also been used in repair or strengthening of concrete structural members, but herein is used as a connection between individual concrete elements. The interest in using Glass fiber reinforced polymer (GFRP) composite for a connection lies within its resistance to corrosion, higher tensile strength, and ability to conform to uneven surfaces.

In Chapter 2, past FRP research is presented. Research included surface preparation methods, CFRP shear transfer between concrete elements, and CFRP performance as a retrofit to the current welded steel plate connection.

In Chapter 3, GFRP composite connection under monotonic vertical shear is investigated. Two L-shaped concrete elements had surface preparation performed and oriented as to perform a push-off, or shear transfer, test. The two elements were connected with a GFRP composite to form a specimen. The GFRP composite was a unidirectional glass fiber fabric saturated with epoxy resin and applied to each face of the specimen to create the connection. The axial monotonic force was applied to each specimen and increased until failure of the GFRP composite connection occurred. A total of eighteen shear transfer tests were performed, only varying in surface preparation. The objective was to understand how each surface preparation affects the GFRP composite

connection as the only shear resistance mechanism between the two concrete elements.

In Chapter 4, the first group of eight wall tests was performed using a unidirectional GFRP composite connection under cyclic shear. Concrete wall panels had surface preparation performed on the connection area and erected next to another. Two walls were connected with a GFRP composite to form a specimen. The GFRP composite was a unidirectional glass fiber fabric saturated with epoxy resin and applied the full height of the specimen on one face to create the connection. Horizontal restraint on the specimen and vertical restraint on individual wall panels were installed to force shear in the connection. The quasi-static cyclic force, simulating seismic loads, was applied in the horizontal direction near the top of each wall system and displacements increased until failure of the connection occurred. Variables of the test program included: varying concrete surface preparation methods, applying pressure during epoxy resin curing, changing the number of unidirectional GFRP lamina, and using CFRP composite anchors. Research sought to evaluate how GFRP connection affects the horizontal load and displacement capacity of the specimen, as well as energy dissipation and shear capacity in the connection.

In Chapter 5, the second group of six wall tests was performed using a bidirectional GFRP composite connection under cyclic shear. Experiments were performed similar to the first group of wall tests. Variables of the test program included: applying epoxy-putty adhesive in the joint in-between the two panels, changing the number and coverage of bidirectional GFRP lamina, and using GFRP composite anchors. Research continued to evaluate how GFRP connection affects the horizontal load and displacement capacity of the specimen, as well as the shear capacity in the connection.

In Chapter 6 and 7, the conclusions for the entire research are presented and future considerations for investigation are proposed.

CHAPTER 2

LITERATURE REVIEW

2.1 FRP Connection and Reinforcement History

FRP has proven to benefit reinforced concrete shear transfer mechanisms (Lin et al 2016), as well as the shear friction capacity of concrete (Saenz et al 2005). The benefits of different concrete surface preparation methods and bonding agents have proven to increase the surface stress on a FRP connection, which implies a better FRP-to-concrete bond (Pantelides et al 2003).

In precast concrete wall applications, a field-installed connection is typically used to develop shear transfer and composite action between panels (Hofheins et al 2002). The connection is formed by a welded steel plate between steel embeds in each wall. Embeds consist of welding deformed reinforcing bars to steel angles. The deformed rebar provide development into the concrete wall and the steel angle provides a welding surface for connection to another wall panel. It was shown that connecting precast concrete wall panels through this mechanical anchorage has shortcomings with respect to corrosion and seismic performance. Existing walls may not have sufficient capacity to resist current design seismic loads and require retrofit. Although the existing mechanical anchorage connection provides the necessary continuity, premature failure of the connection may occur, as observed by Strigel et al. (2000) and Hofheins et al. (2002). Failure of the loose plate steel connector includes fracture of the weld from steel plate to rebar and embedded

rebar debonding from concrete. Performance of the welded plate steel connection also degrades from long-term corrosion effects. Unidirectional CFRP composite lamina have been used for precast concrete wall connections (McMullin et al. 2003; Pantelides et al. 2003, 2004; Volnyy and Pantelides 1999). Lamina were attached to the concrete by means of an epoxy-putty adhesive to provide a continuous length of reinforcement much like a connection replacement. A similar method was used by Tape et al. (2007) to connect the flanges of precast double tee precast concrete members using a CFRP flange-to-flange connection. Tests demonstrated the capability of CFRP connections to transfer necessary loads across a joint.

The use of FRP composite lamina along with FRP composite anchors has been used for flexural strengthening (Smith et al. 2011). The tensions side of a concrete beam was strengthened by the participation of FRP composite anchors when inserted into the member and splayed on the FRP lamina face. The contribution and performance of FRP composite anchors for a shear transfer application have not been evaluated. An objective of this research is to therefore evaluate the performance and shear transfer capacity of the connection between precast concrete wall panels using GFRP composite lamina and FRP composite anchors.

CHAPTER 3

PUSH-OFF TESTS FOR GFRP CONNECTIONS WITH VARIED CONCRETE SURFACE PREPARATION

3.1 Introduction

The push-off test is used to evaluate direct shear transfer capability of a GFRP connection between two elements of concrete. Each element of concrete is an L-shaped block having a surface preparation method performed on the connection area. Surface preparation methods change the surface of cured (or curing) concrete as to enhance the bonding between the concrete and another structure, in this case GFRP. Such methods were evaluated to determine which method best assists in shear transfer between concrete elements. The methods were either performed soon after casting or after the concrete had sufficiently cured. Concrete L-shaped elements were connected using two laminas of unidirectional GFRP (+45°, -45°) lamina on each face to form a specimen. Each specimen was axially loaded, forcing direct shear in the connection, until connection failure occurred. A total of six different surface preparation methods were used, with three specimens for each method, resulting in eighteen push-off tests. Vertical load and displacement were recorded up to connection failure. In this case, vertical load capacity indicates the surface preparation method participation in shear transfer capability.

3.2 Testing Program

3.2.1 Test Specimens

The setup for each specimen involves two 6-in. (152 mm) thick L-shaped concrete elements oriented to perform a push-off test. Figure 3.1 shows dimensions and orientation of the elements. Each L-shape had a total of four longitudinal #4 (13M) bars with #3 (10M) hoops at 2 ¼ in. (57 mm) on center, as shown in Figure 3.2. Thus, the expected failure of the specimen was at the GFRP connection. Specimens in the forms are shown in Figure 3.3.

The L-shapes were connected using a GFRP composite laminate system. This system includes the application of epoxy resin to the prepared concrete surface and a wet layup of two 12.5 in. (318 mm) x 9.5 in. (241 mm) unidirectional GFRP sheets (+45°, -45°) per side of the set-up as shown in Figure 3.1. Each test had a ½ in. (13 mm) gap, which was maintained using a ½ in. (13 mm) thick expanded polystyrene (EPS) sheet inserted in the seam prior to GFRP composite installation. The EPS remained in place during testing. Pressure was applied on each GFRP laminate by a ½ in. (13 mm) EPS sheet and a ½ in. (13 mm) steel plate on the front and back side of the set-up. A single ½ in. (13 mm) all thread passed through the seam between the L-shape elements to fasten the EPS sheets and steel plates on top of the GFRP. Washers, lock washers, and nuts were applied on each side of the all-thread and tightened firmly by hand. The resultant pressure on the GFRP was applied to reduce the thickness of the bond line and thus improve bonding of GFRP to concrete. Table 3.1 shows the test matrix.

Six groups of specimens varied based on the surface preparation method used in the connection area. Each group contained three specimens, resulting in eighteen total

push-off tests. The goal was to understand which surface preparation would best enhance shear transfer capability.

Group #1 specimens had an acid wash performed after 28 days of curing. Muriatic acid was used was in line with a pressure washer to remove the most superficial layer of the cured concrete paste, as shown in Figure 3.4.

Group #2 specimens had a media (garnet) blast performed after 28 days of curing. This was done to remove the most superficial layer of the cured concrete paste, as shown in Figure 3.4.

Group #3 specimens had a scrabbling method performed after 28 days of curing. Scrabbling was done with a pneumatic hand tool that contained three moving heads that impact the surface of the concrete to remove the most superficial layer of the cured concrete paste and expose large aggregates.

Group #4 specimens had a surface that was retarded from curing using Top Stop which was then washed with a 1,000 psi (6,895 kPa) pressure washer 18 hours after casting. A single pass with the pressure washer was performed to remove the most superficial layer of the cured concrete paste, as seen in Figure 3.5.

Group #5 specimens also had a surface that was retarded from curing using Top Stop which was then washed with a 1,000 psi (6,895 kPa) pressure washer. Multiple passes were performed with the pressure washer to remove the most superficial layer of the cured concrete paste and expose large aggregates, as seen in Figure 3.5.

Group #6 specimens had a surface that was washed with a 1,000 psi (6,895 kPa) pressure washer 18 hours after casting. Because no surface retarder was used, multiple passes were done with the pressure washer to remove the most superficial layer of the

cured concrete paste, as shown in Figure 3.5.

3.2.2 Material Properties

The #4 (13M) and #3 (10M) steel reinforcing bars were 60,000 psi (413,685 kPa) mild steel. The concrete was a structural mix with a design 28-day compressive strength of 10,000 psi (68,950 kPa). Table 3.2 shows the concrete mix design.

The GFRP composite used was SikaWrap Hex® 100G, a unidirectional fiber fabric. Using a two-part epoxy resin, a connection is formed by the following steps: (i) orient L-shape specimens (Figure 3.6), (ii) prime concrete surface and wet lay-up GFRP lamina (Figure 3.7), and (iii) apply pressure to the wet connection (Figure 3.8). The manufacturer's properties of the cured GFRP composite laminate are shown in Table 3.3.

3.2.3 Test Set-up

The test set-up included orientation of two precast concrete L-shape elements connected by the GFRP laminate system, as shown in Figure 3.1. The GFRP composite was applied on both faces of the set-up. Elastomeric bearing pads were in-between the loading apparatus and concrete specimen. The load was applied axially to the set-up, causing the connection to undergo shear, as shown in Figure 3.9.

3.2.4 Instrumentation

Displacement was measured in the experiments using linear variable differential transducers (LVDTs). Two LVDTs were externally mounted to one side of the setup to measure vertical displacements, as shown in Figure 3.9. Strain gauges were applied in the horizontal direction to the outermost lamina of GFRP near the middle of each

connection, as shown in Figure 3.9. The first three groups revealed little difference between front and back GFRP composite laminates, then interest was taken in understanding the strain along the seam for the remaining three groups. These two different strain gauge layouts are shown in Figure 3.10. The load cell located within the testing apparatus measured the axial force.

3.2.5 Loading Protocol

A cyclic quasi-static axial load was applied to the specimen using displacement control, and the displacement was increased at a rate of 0.125 in./min., as shown in Figure 3.11.

3.3 Test Results

3.3.1 Introduction

For each specimen test within surface preparation method groups, the vertical load versus vertical slip is presented. To better compare surface preparation methods, an average of vertical load is indicated. These results and a comparison of the GFRP composite connection failure mode are presented as well. An average of vertical slip is not indicated because of the variability that exists in the concrete surface affects vertical slip in magnitudes similar to that of the displacements measured. Strain data are presented but are inherently unpredictable because of the indistinctness when attempting to measure the strain of the whole GFRP composite laminate, composed of multiple unidirectional laminas, by gauging only one local area. The horizontal strain range in both laminates of the connection for all tests was 3,140 to 13,600 microstrain.

3.3.2 Results

Surface preparation method groups along with corresponding test results and failure mode (progressive delamination, fiber failure, or both) are presented for each specimen in Table 3.4. Progressive delamination failure is when the GFRP peeled a thin layer of concrete away from the concrete elements as vertical displacements increased, ultimately losing connectivity between concrete elements. Fiber failure is when the GFRP composite remained bonded to the concrete but the fibers bridging the concrete elements began to tear as vertical displacements increased, ultimately splitting the GFRP composite connection. The load slip curves were similar within each group, and therefore the best representation of load slip behavior will be presented for each surface preparation method.

Acid washed and media blasted specimens had load slip behavior as shown in Figure 3.12 and Figure 3.13, respectively. Media blasted specimens displayed a more abrupt slippage than the acid washed specimens. Both methods had a failure mode of progressive delamination in which the failed GFRP composite laminate section removed areas of concrete during failure. The acid washed and media blasted specimen GFRP displaying concrete removed is shown in Figure 3.14a and Figure 3.14b, respectively. Acid washed specimens showed slightly more area of concrete removal than media blasted specimens. The acid washed specimen GFRP horizontal strain had a range of 3,140 to 7,580 microstrain and media blasted specimen GFRP horizontal strain had a range of 4,220 to 10,640 microstrain. Typical strain behavior for acid washed and media blasted specimens during testing is shown in Figure 3.15 and Figure 3.16, respectively.

Scrabbled specimens had load slip behavior shown in Figure 3.17. With the

failure mode being fiber failure, the load slip curve shows a more gradual decrease in load where other forms of failure showed jagged decreases in load. The GFRP composite did not delaminate in scrabbled specimens as shown in Figure 3.18, therefore, no comparison of concrete removal is made. Typical scrabbled specimens GFRP horizontal strain had a range of 4,700 to 9,920 microstrain and is shown in Figure 3.19.

Specimens using a surface retarder with single-pass and surface retarder with multiple-pass wash had load slip behavior shown in Figure 3.20 and Figure 3.21, respectively. Both methods showed similar behavior in load slip. Single-pass and multiple-pass methods had a similar failure mode of both progressive delamination and fiber failure as shown in Figure 3.22a and Figure 3.22b, respectively. Typical single-pass and multiple-pass specimens GFRP displaying concrete removal is shown in Figure 3.23a and Figure 3.23b, respectively. Single-pass specimens showed slightly more area of concrete removal than multiple-pass specimens. Single-pass specimen GFRP experienced a horizontal strain range of 3,500 to 4,430 microstrain and multiple-pass specimen GFRP experienced a horizontal strain range of 3,780 to 13,600 microstrain. Typical single-pass and multiple-pass specimens GFRP horizontal strain is shown in Figure 3.24 and Figure 3.25, respectively.

Multiple-pass washed specimens had load slip behavior shown in Figure 3.26. The load slip behavior and failure mode is similar to that of acid washed specimens. The typical multiple-pass washed specimen GFRP displaying concrete removed is shown in Figure 3.27. Multiple-pass washed specimens showed slightly more area of concrete removal than both acid washed and media blasted specimens. The typical multiple-pass washed specimen GFRP horizontal strain, upwards of 6,200 microstrain, is shown in

Figure 3.28.

3.3.3 Test Summary

For applications where a surface preparation method was performed over 28 days after concrete casting, the use of an acid wash was most beneficial for a GFRP connection in direct shear. The 7.7 kip (34 kN) average load required to fail acid washed specimens was 1.5 times higher than the 5.2 kip (23 kN) average load for media blasted specimens and 1.1 times higher than the 7.0 kip (31 kN) average load for scrabbled specimens.

For applications where surface preparation was performed 18 hours after concrete casting, the use of a multiple-pass wash was most beneficial for a GFRP connection in direct shear. The 11.2 kip (50 kN) average load required to fail multiple-pass washed specimens was 1.2 times higher than the 9.2 kip (41 kN) average load for surface retarder with single-pass washed specimens and also 1.5 times higher than the 7.7 kip (34 kN) average load for surface retarder with multiple-pass washed specimens.

Higher load capacity was seen in surface preparation methods where pressured water washing was involved.

3.4 Summary and Conclusions

3.4.1 Summary

Shear transfer tests were carried out to determine the most beneficial surface preparation for shear transfer between concrete elements using a GFRP composite connection. The surface preparation methods of acid wash, surface retarder with multiple-pass wash, and multiple-pass wash were determined to be the most beneficial.

3.4.2 Conclusions

The only surface preparation technique resulting in sole fiber failure was the scrabble method. All other methods resulted in progressive delamination or a combination of both delamination and fiber failure. However, scrabbled specimens achieved some of the lowest load capacity. This indicates that the bond between the GFRP connection and the concrete was likely better than other specimens and resisted early delamination, which immediately propagates with slip. A more thorough investigation is required to determine the effects of the scrabble method on GFRP bond in shear transfer.

Pressure washing of the concrete 18 hours after casting proved to increase the load capacity. High-pressure washing has been observed to improve bond strength in fully cured concrete with other wall experiments (Pantelides et al 2003). However, this technique is likely dependent on concrete strength at the particular time during curing. The early strength in concrete curing is affected by several factors including ambient temperature, ambient moisture, and small alterations in mix design. The washing of concrete surfaces at different times during curing and how that method affects GFRP bond in shear transfer should be more thoroughly investigated.

Table 3.1 – Test matrix

Test Group	Surface Preparation
1	Muriatic Acid Wash
2	Garnet Media Blast
3	Scrabble (Pneumatic Impact Tool)
4	Retarder with Single-Pass Wash
5	Retarder with Multiple-Pass Wash
6	Multiple-Pass Wash

Table 3.2 – Concrete mix design

Concrete Materials	Density, lbs/ft^3 (kg/m^3)
Grey Cement	24.07 (385.63)
Flyash Class F	6.04 (96.70)
Fine Aggregate	41.41 (663.28)
Coarse Aggregate	56.48 (904.75)
Water	9.63 (154.25)
High Range Water Reducer	0.25 (4)
Air Entrainment	0.009 (0.148)

Table 3.3 – Manufacturers cured GFRP laminate properties

Cured Laminate Properties	Average Values
Tensile Strength	83,400 psi (575 MPa)
Tensile Modulus	3.672 x 10^6 psi (25,300 MPa)
Tensile Elongation	2.31%
Thickness	0.040 in. (1.016 mm)

Table 3.4 – Test results

Test Group	Specimen	Surface Prep-aration Method	Max Load, kip (kN)	Avg. Max. Load, kip (kN)	Slip at Failure, in. (mm)	* Failure Mode	Max Horizontal Microstrain
1	1	Acid Wash	8.5 (38)	7.7 (34)	-	PD	3,140
	2		8.2 (36)		0.021 (0.53)		3,860
	3		6.4 (28)		0.045 (1.14)		7,580
2	4	Media Blast	+12.0 (53)	5.2 (23)	0.012 (0.30)	PD	10,640
	5		5.2 (23)		0.015 (0.38)		6,850
	6		5.1 (23)		0.026 (0.66)		4,220
3	7	Scrabbl-ing	6.5 (29)	7.0 (31)	0.014 (0.36)	FF	9,920
	8		6.7 (30)		0.053 (1.35)		7,830
	9		7.8 (35)		0.009 (0.22)		4,700
4	10	Retarder Single-Pass Wash	10.0 (44)	9.2 (41)	0.023 (0.58)	PD; FF	-
	11		8.4 (37)		0.016 (0.41)		3,500
	12		+4.6 (20)		0.021 (0.53)		4,430
5	13	Retarder Multiple -Pass Wash	5.7 (25)	7.7 (34)	0.033 (0.84)	PD; FF	13,600
	14		9.5 (42)		0.037 (0.94)		8,350
	15		8.0 (36)		0.026 (0.66)		3,780
6	16	Multiple -Pass Wash	12.2 (54)	11.2 (50)	0.070 (1.78)	PD	-
	17		10.5 (47)		0.032 (0.81)		-
	18		11.0 (49)		0.029 (0.74)		6,200

* Failure Mode Types:
PD – Progressive Delamination
FF – Fiber Failure

\+ Extreme outlier values omitted in calculating the average value

\- Unreliable test data

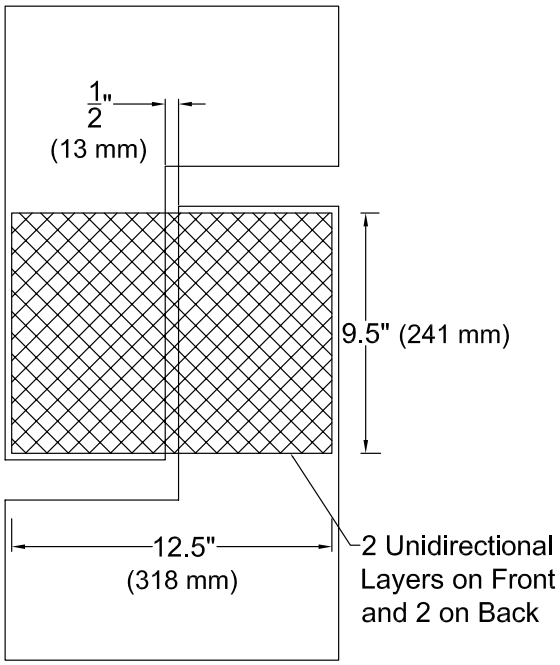

Figure 3.1 – Specimen details.

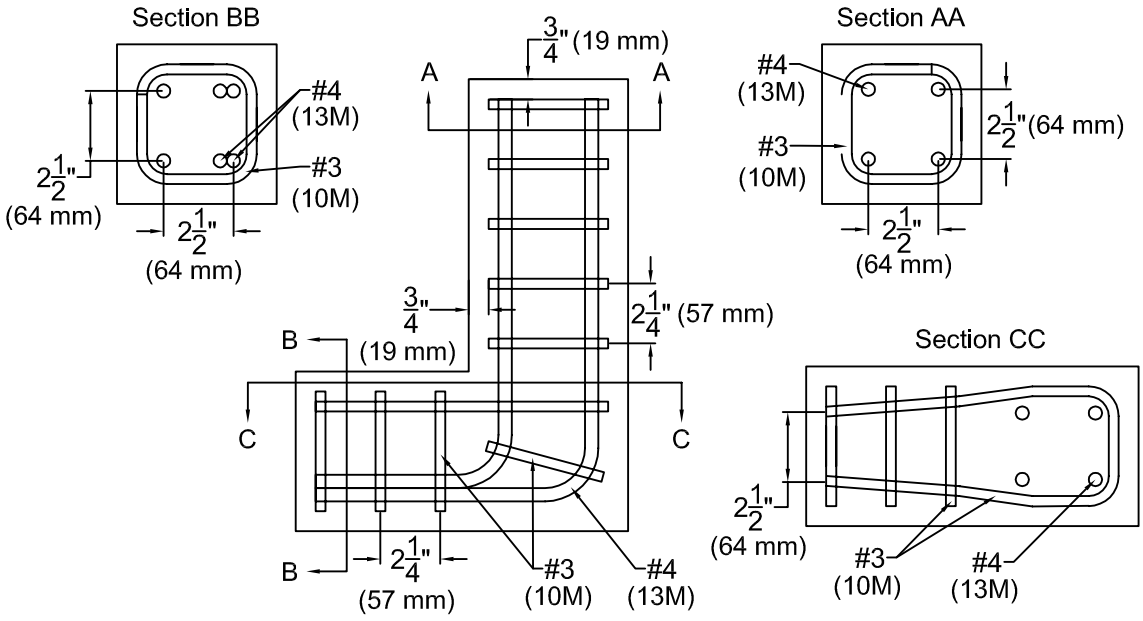

Figure 3.2 – Individual concrete L-shape element steel reinforcement.

Figure 3.3 – L-shape forms during rebar tying.

Figure 3.4 – Acid washed and media blasted specimens.

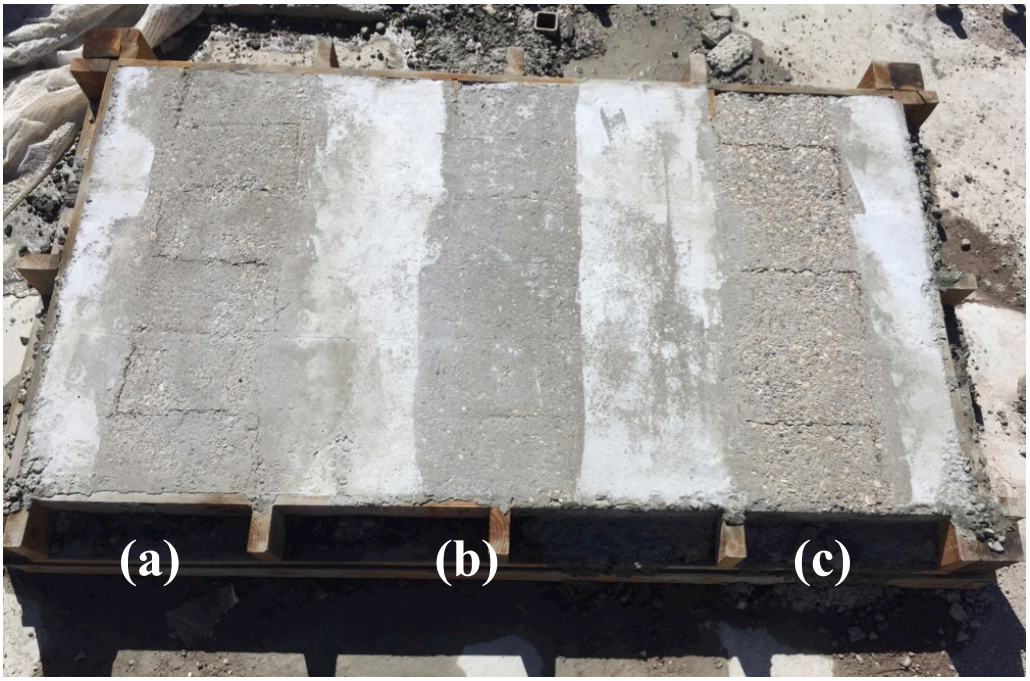

Figure 3.5 – Surface preparation on poured concrete L-shapes: (a) surface retarder with single-pass wash; (b) multiple-pass wash; (c) surface retarder with multiple-pass wash.

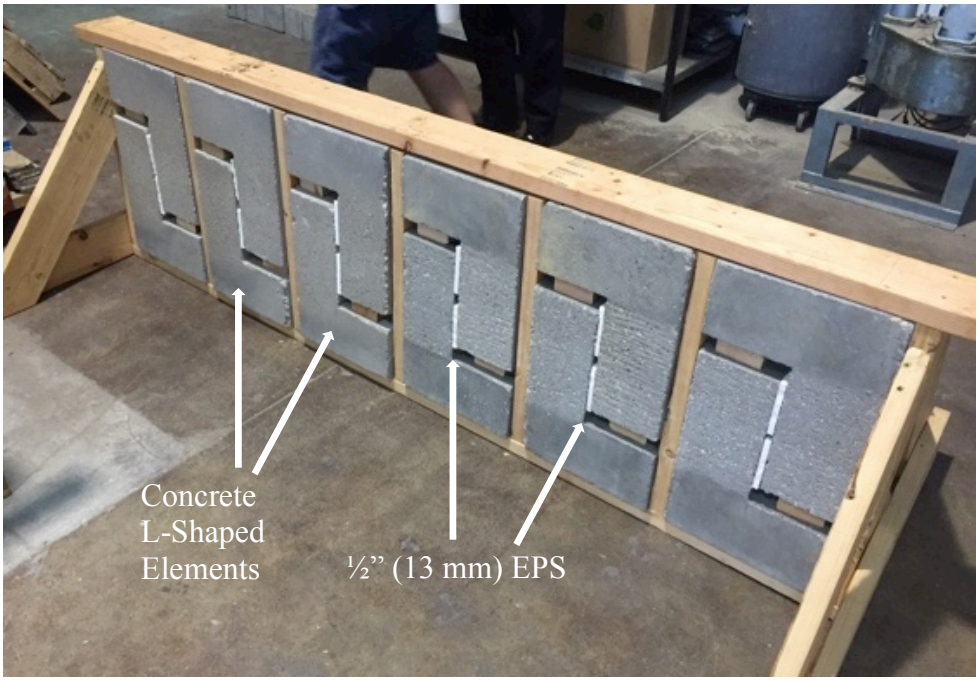

Figure 3.6 – Step 1: Orient concrete L-Shape elements.

Figure 3.7 – Step 2: Prime surface with epoxy resin and perform GFRP wet layup.

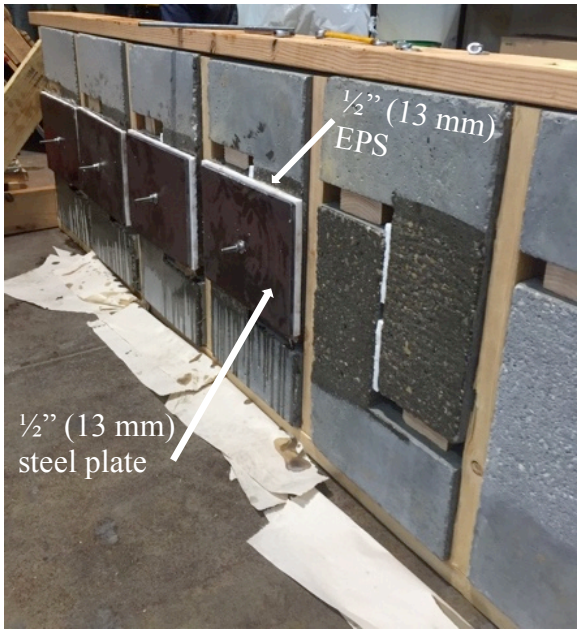

Figure 3.8 – Step 3: Apply pressure on both sides of specimen.

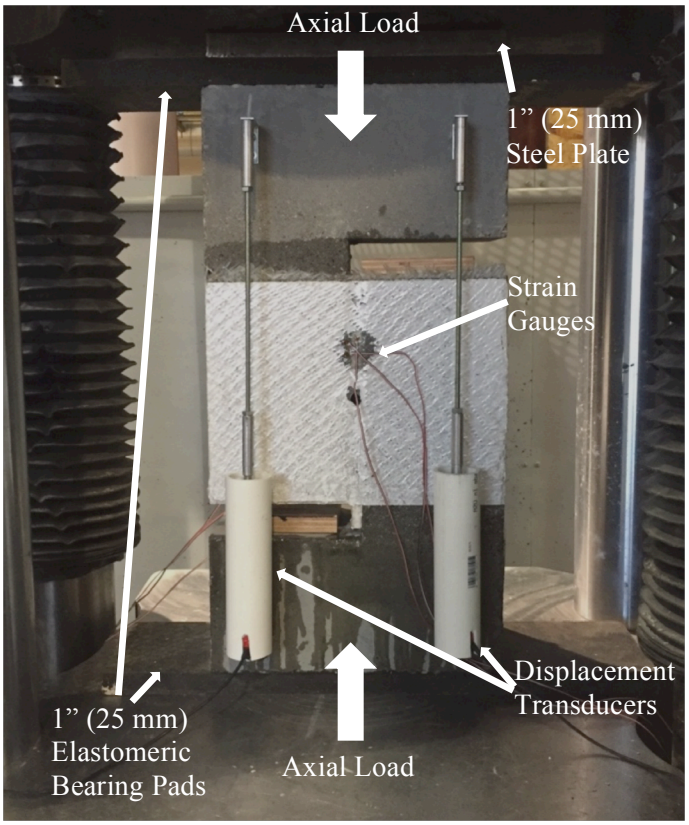

Figure 3.9 – Typical test set-up.

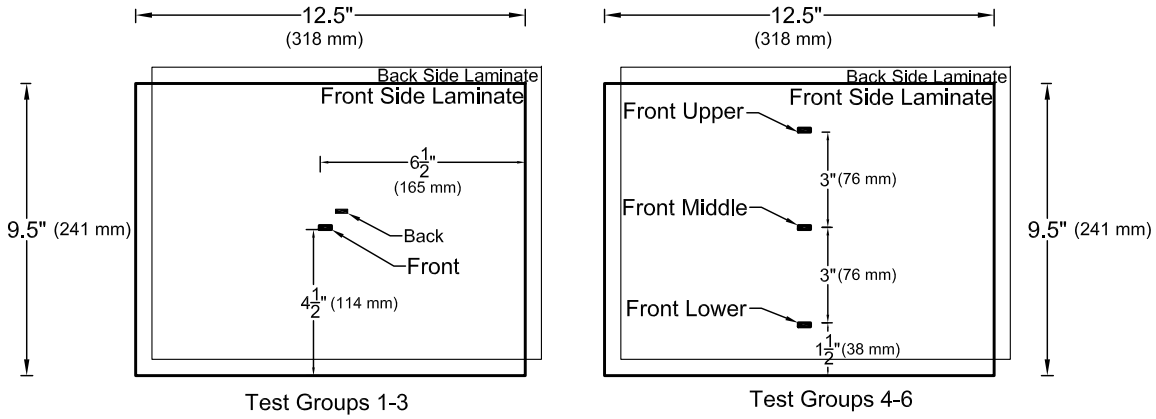

Figure 3.10 – Strain gauge layouts on the GFRP laminates.

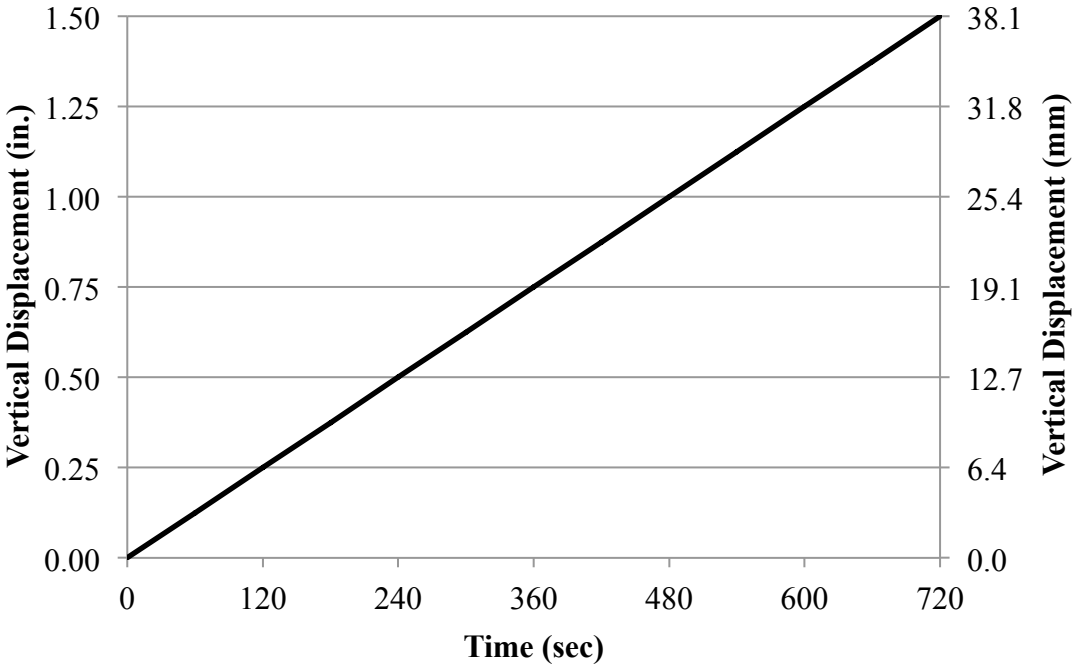

Figure 3.11 – Loading protocol.

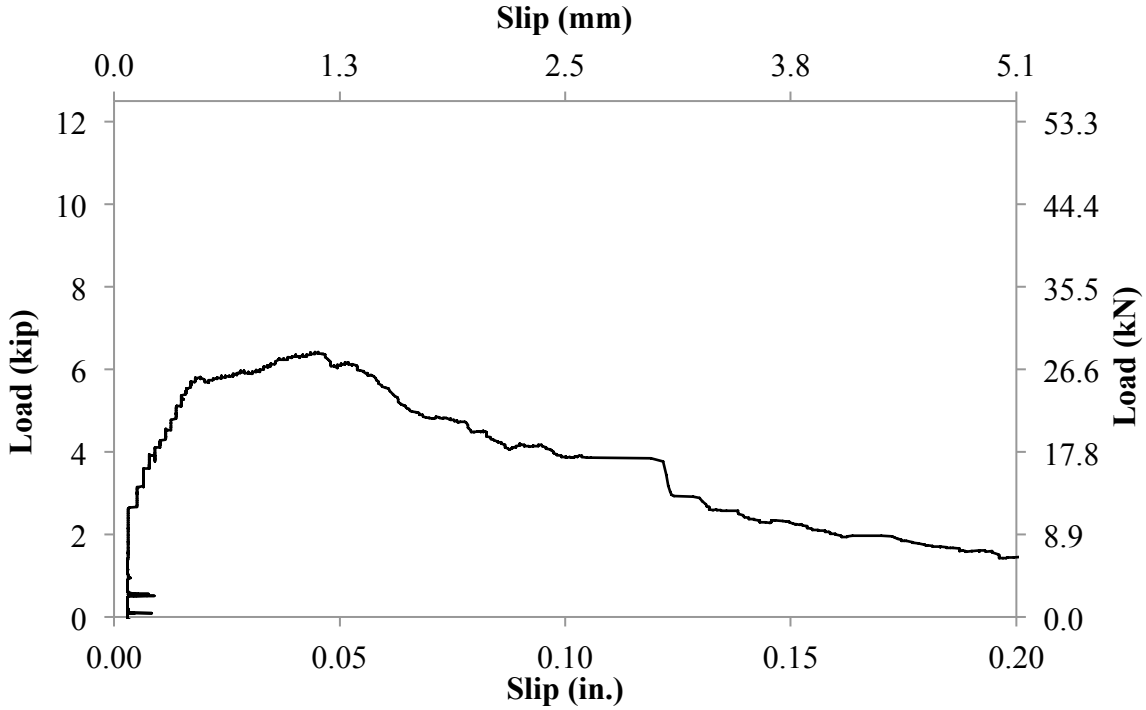

Figure 3.12 – Typical acid wash load slip curve.

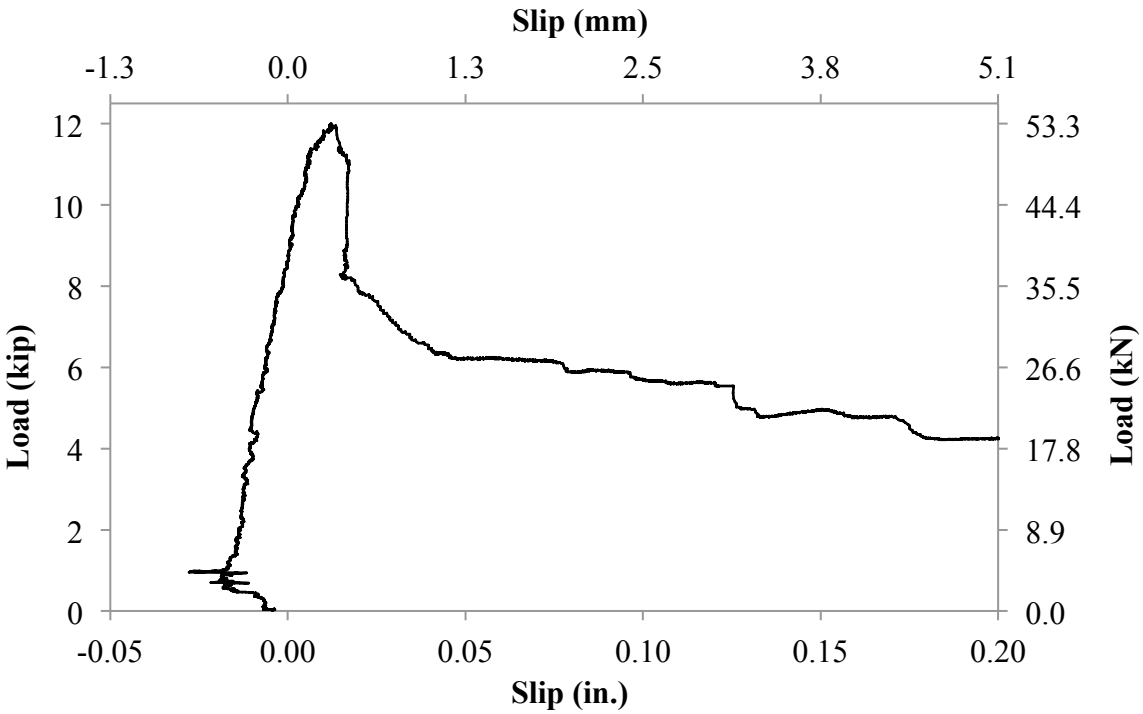

Figure 3.13 – Typical media blast load-slip curve.

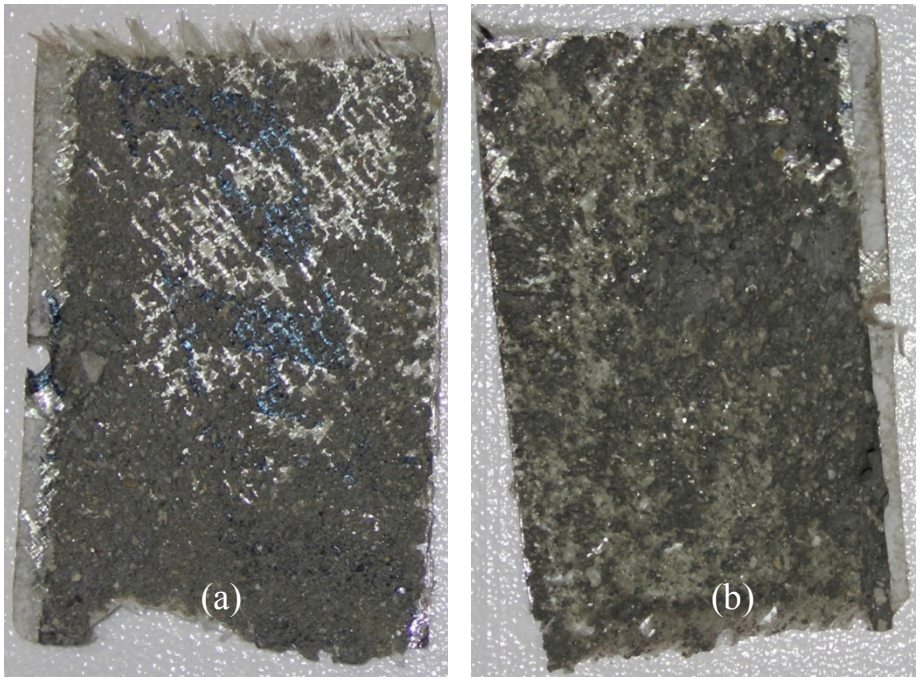

Figure 3.14 – Typical delaminated GFRP concrete removal: (a) acid washed specimen; (b) media blasted specimen.

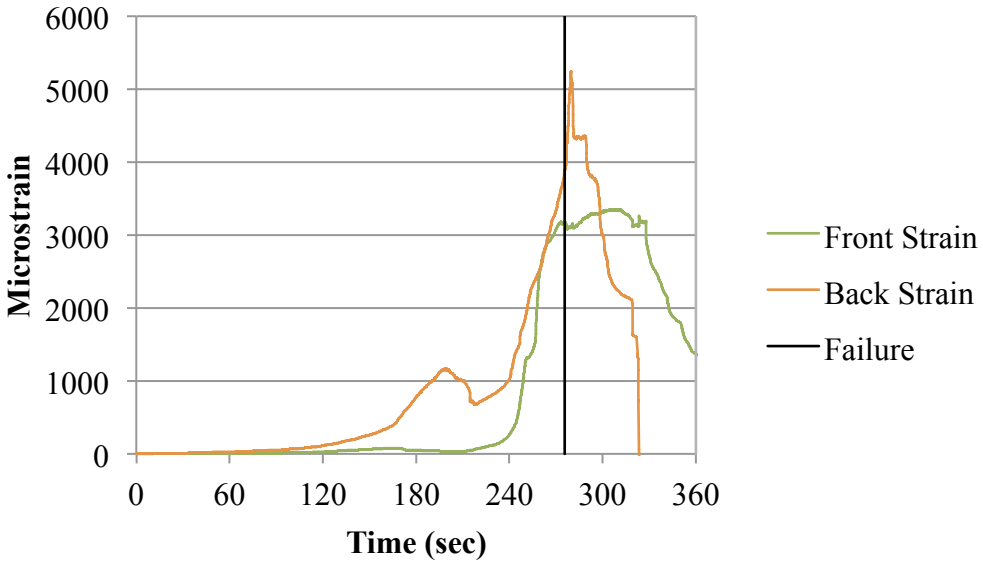

Figure 3.15 – Horizontal GFRP strains on an acid washed specimen.

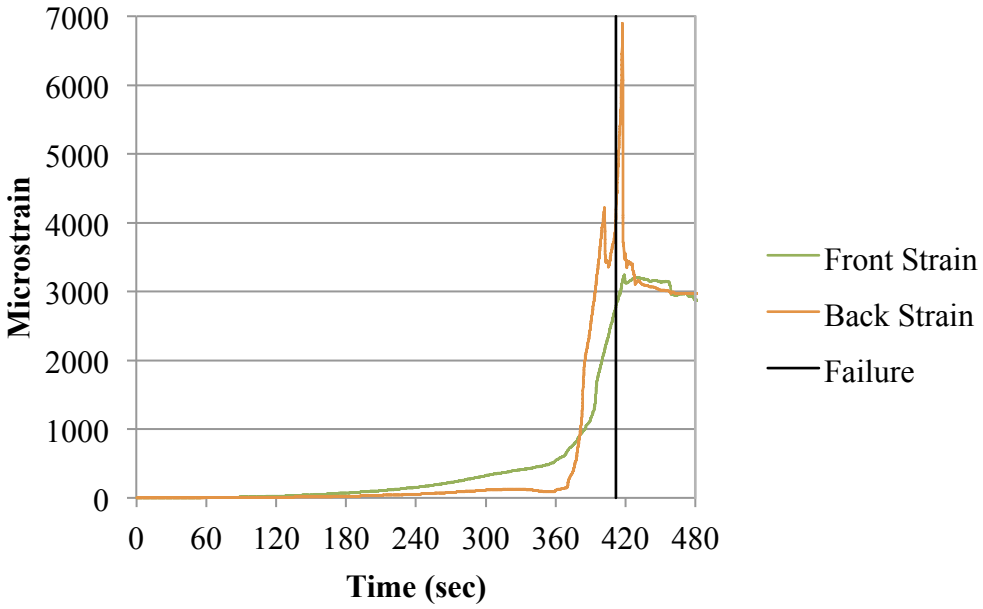

Figure 3.16 – Horizontal GFRP strains on a media blasted specimen.

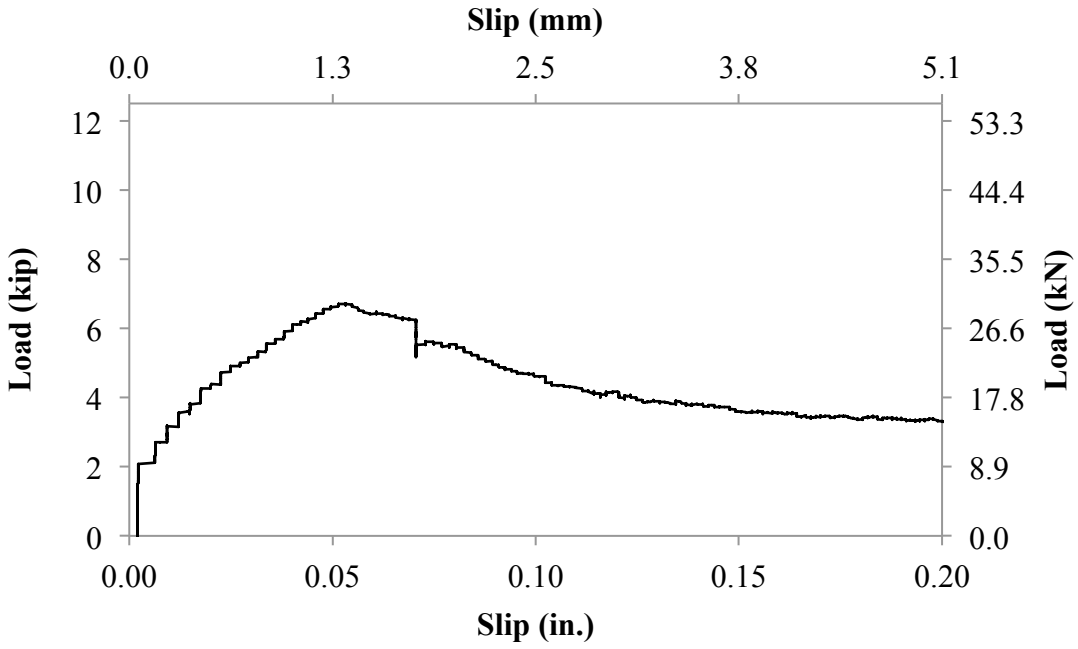

Figure 3.17 – Typical scrabble load-slip curve.

Figure 3.18 – Typical failure with scrabble method specimens.

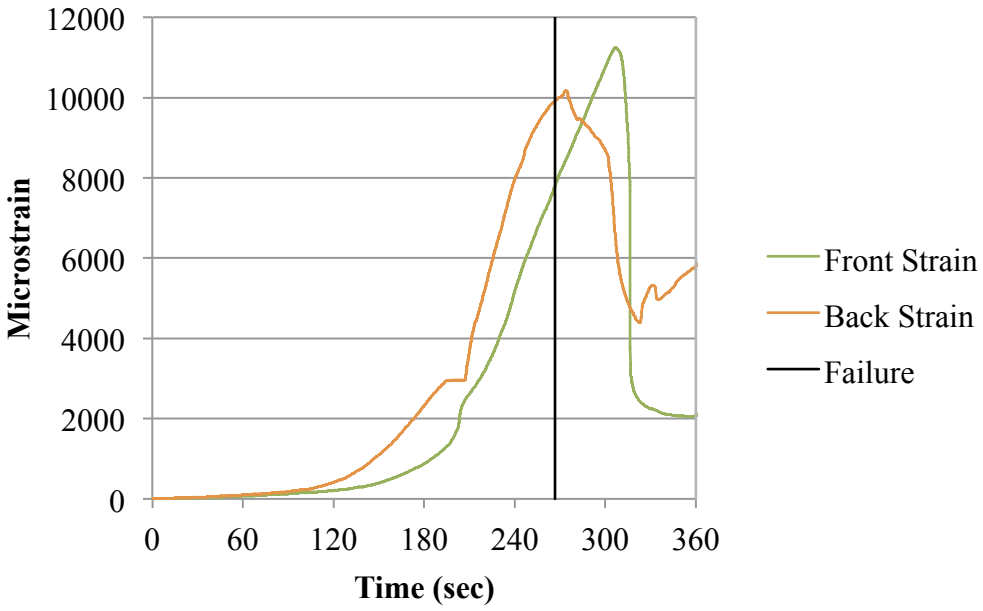

Figure 3.19 – Horizontal GFRP strains on a scrabbled specimen.

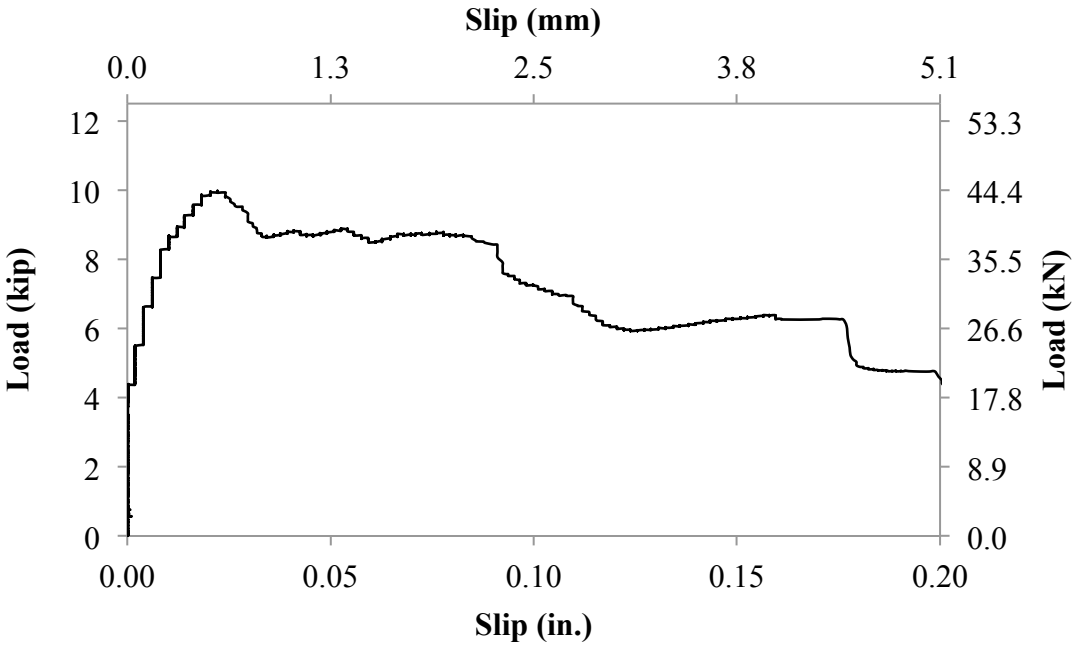

Figure 3.20 – Typical surface retarder with single-pass wash load-slip curve.

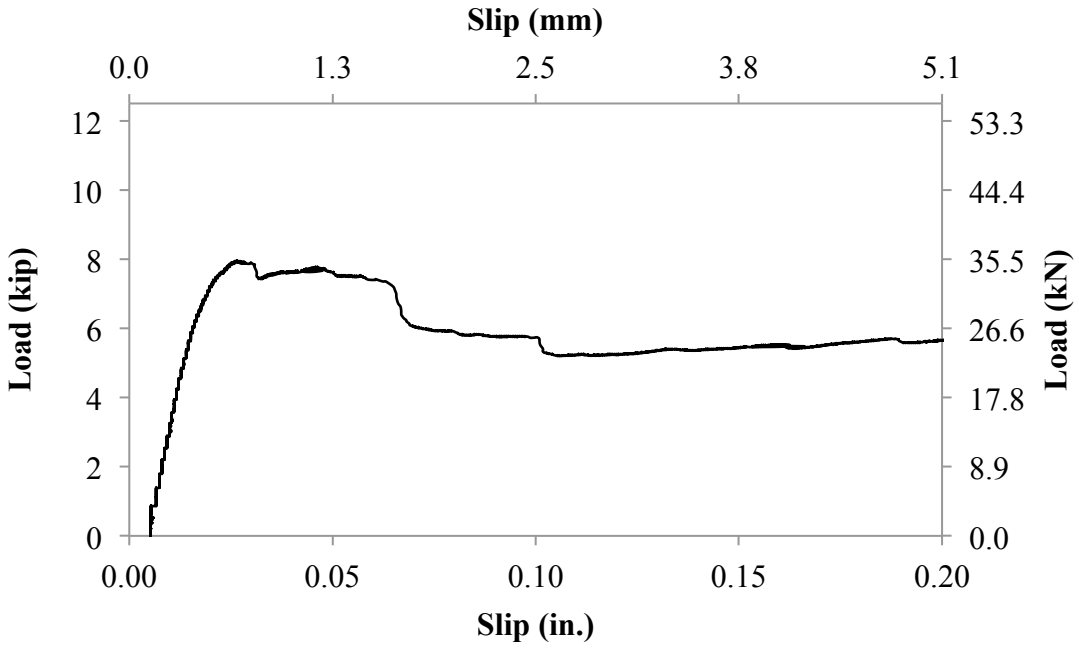

Figure 3.21 – Typical surface retarder with multiple-pass wash load-slip curve.

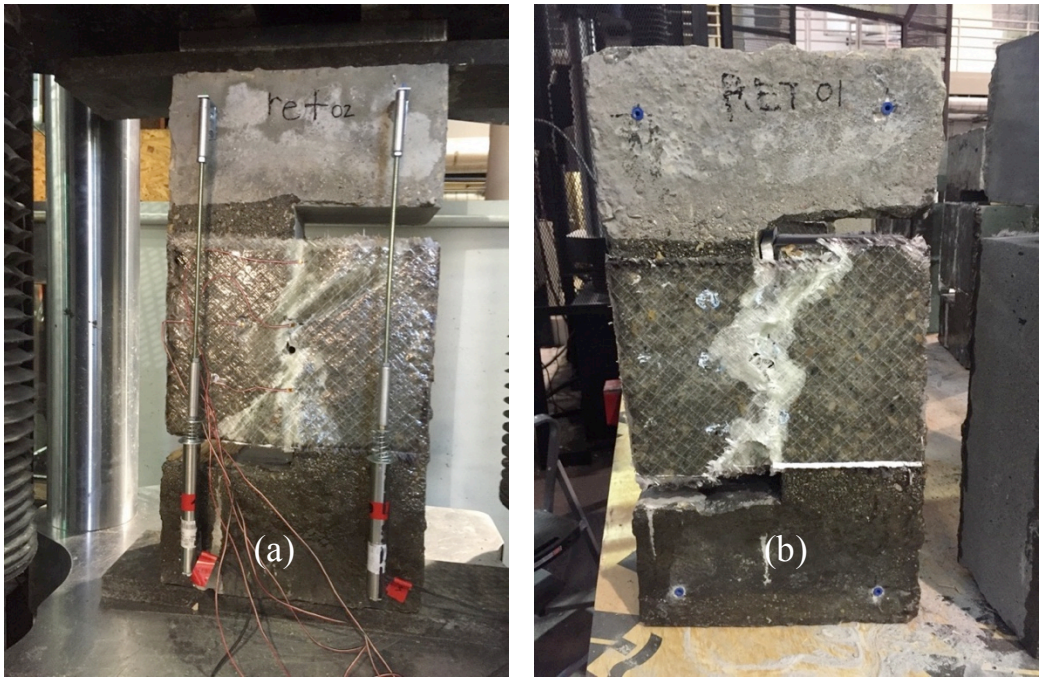

Figure 3.22 – Typical failure: (a) surface retarder with single-pass wash specimen; (b) surface retarder with multiple-pass wash specimen.

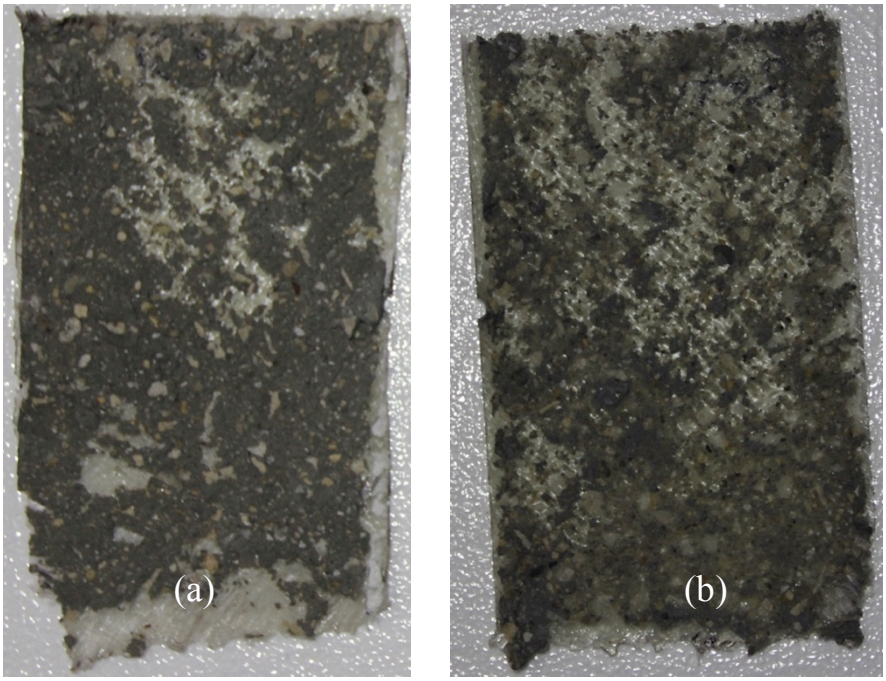

Figure 3.23 – Typical delaminated GFRP concrete removal: (a) surface retarder with single-pass wash specimen; (b) surface retarder with multiple-pass wash specimen.

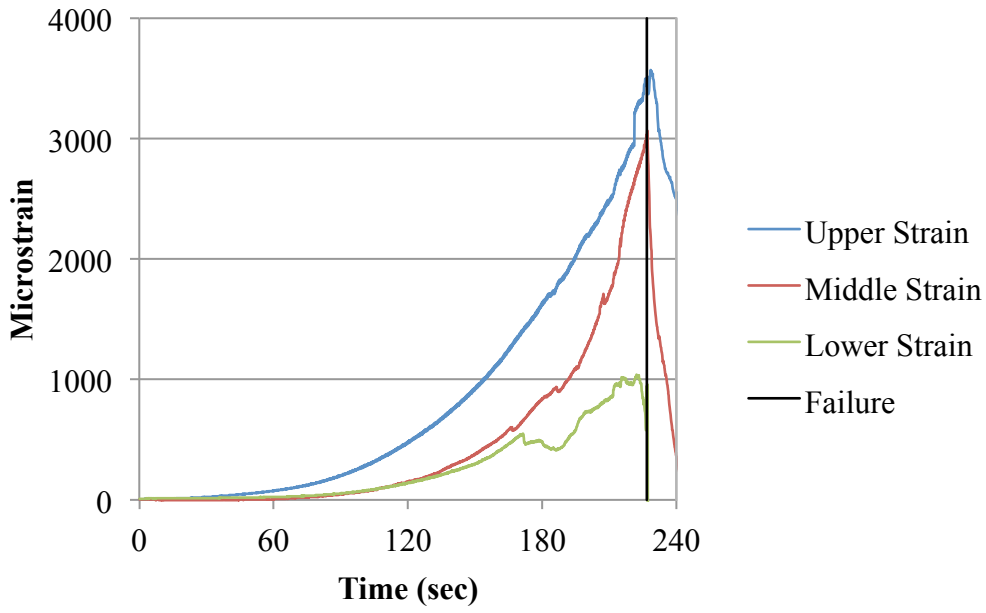

Figure 3.24 – Horizontal GFRP strains on a surface retarder with single-pass washed specimen.

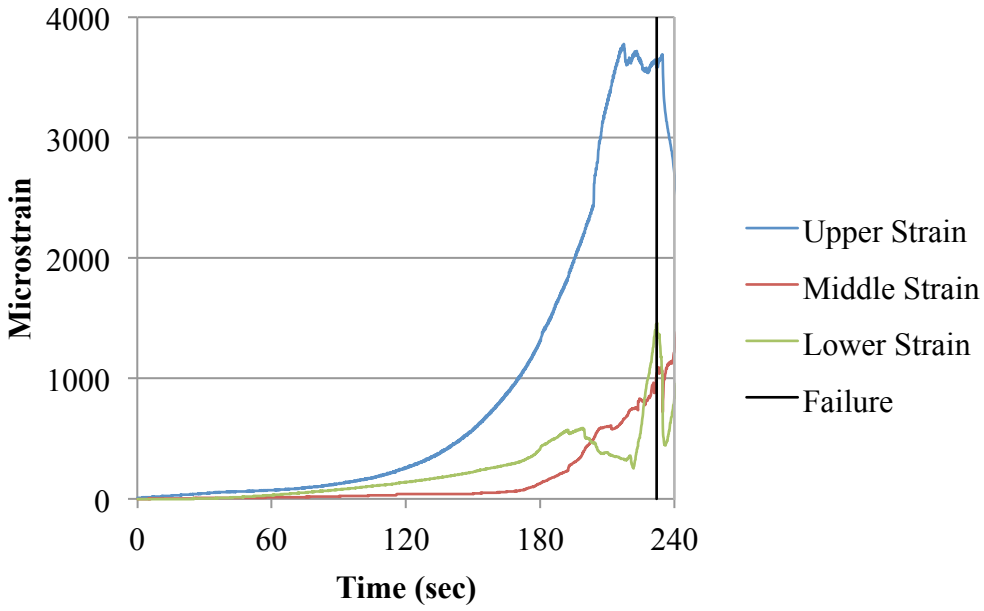

Figure 3.25 – Horizontal GFRP strains on a surface retarder with multiple-pass washed specimen.

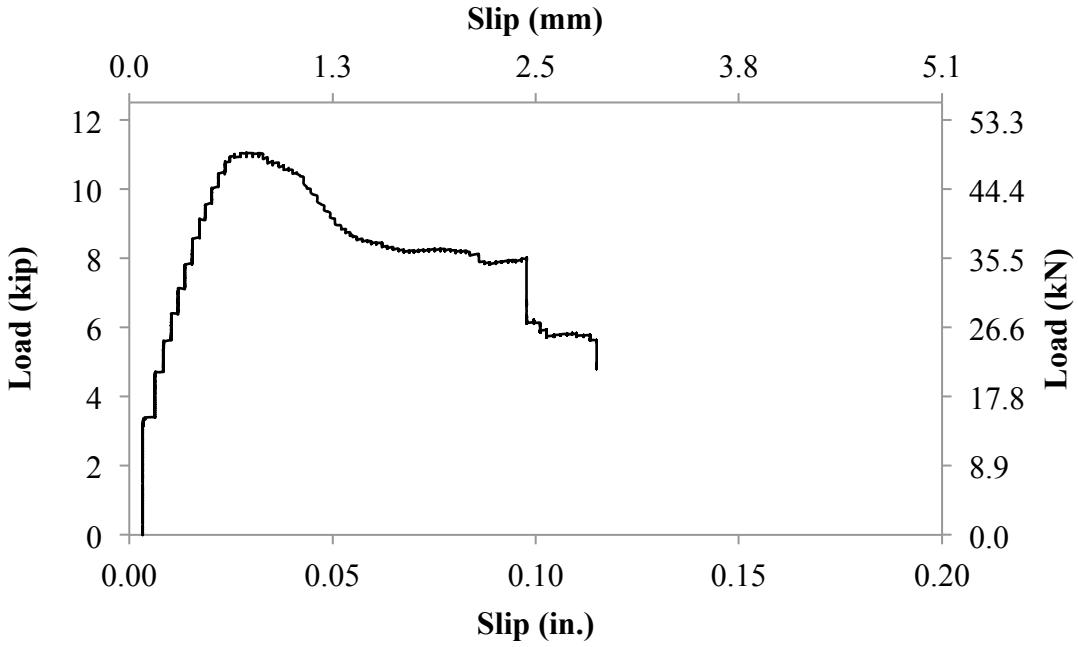

Figure 3.26 – Typical multiple-pass wash load-slip curve.

Figure 3.27 – Typical delaminated GFRP concrete removal for multiple-pass washed specimen.

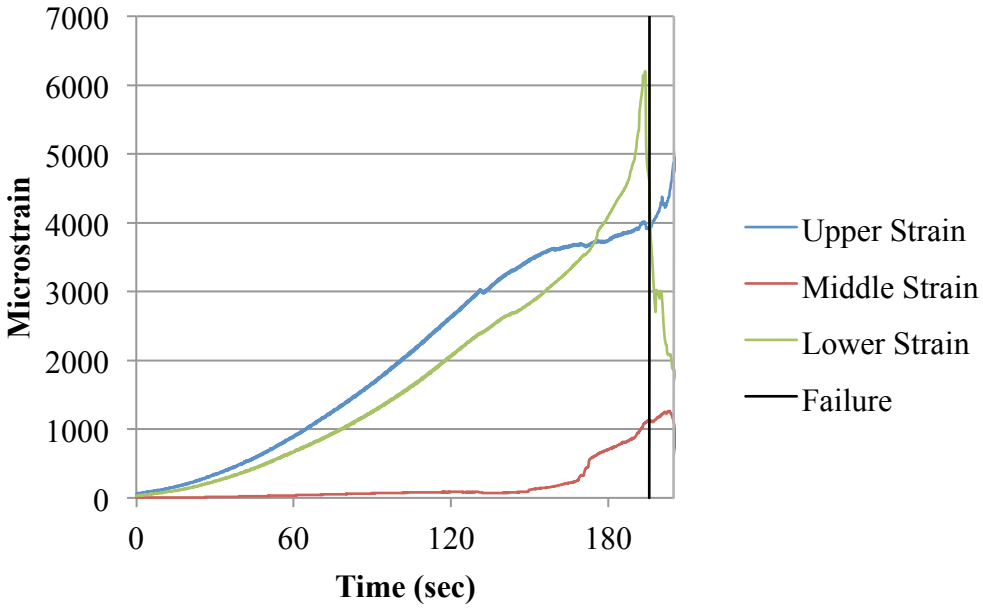

Figure 3.28 – Horizontal GFRP strains on a multiple-pass washed specimen.

CHAPTER 4

PERFORMANCE OF UNIDIRECTIONAL GFRP CONNECTIONS BETWEEN CONCRETE WALL PANELS UNDER CYCLIC SHEAR

4.1 Introduction

Test specimens were comprised of two erect precast concrete panels side by side connected with two or four laminas of unidirectional GFRP composite as the only connection between the two walls. The connection area on each concrete wall was surface prepared in order to ensure a better GFRP to concrete bond. Applying a simulated seismic lateral load at the top of the specimen, and restraining the horizontal and vertical directions, induced cyclic shear in the connection. Eight specimens were tested to explore the effects of concrete surface preparation, GFRP application pressure, number of unidirectional GFRP laminas, and use of carbon fiber reinforced polymer (CFRP) anchors. The GFRP composite connection was tested with the purpose of exploring an alternative to the welded steel plate connectors. Performance of the GFRP connection is determined by the load, displacement, energy dissipation, and shear transfer capacity.

4.2 Testing Program

4.2.1 Test Specimens

One concrete wall panel has dimensions 4 ft x 8 ft x 8 in. (1.2 m x 2.4 m x 203 mm) as shown in Figure 4.1. Each wall had two 4x4 W4xW4 (102x102

MW25.8xMW25.8) curtains of steel reinforcement, as shown in Figure 4.1, and corner reinforcement consisting of an 8 x 8 x ½ in. (203 x 203 x 13 mm) steel plate with four welded 12-in. (305 mm) long No. 4 (13M) deformed bar anchor (DBA), as shown in Figure 4.1. Thus, any failure of the specimen was at the GFRP connection.

In each test, a ½ in. (13 mm) gap was created between the two erect walls and maintained using a ½ in. (13 mm) thick high-density polyethylene (HDPE) shim at the top and bottom of the wall seam. The HDPE shims remained in place after application of the GFRP composite and during testing.

The condition of the concrete wall panels varied based on the surface preparation used in the connection area. The GFRP composite connections varied based on GFRP application pressure during curing, number of GFRP laminas, and the presence of CFRP anchors. Table 4.1 shows the test matrix. Surface preparation methods included a garnet media blast, muriatic acid wash, and a surface retarder (Top Stop) with multiple-pass 1,000 psi (6,895 kPa) wash. Acid wash and media blast was performed 28 days after casting; surface retarder with multiple-pass wash was performed 18 hours after casting. Surface preparation methods were performed as to remove the outermost cement paste layer of the curing concrete and expose aggregates. Application pressure was implemented using a ¾ in. (19 mm) stiff form-ply fastened to the connection area on the front side of the walls with eight ½ in. (13 mm) all-thread rods that passed through the gap between the walls. The all thread rods were fastened to 6 in. x 6 in. x ½ in. (152 x 152 x 13 mm) steel plates on the backside, as seen in Figure 4.2. In between the wood panel and GFRP composite, there was a ½ in. (13 mm) sheet of expanded polystyrene (EPS). A pneumatic 380 ft-lbs (0.5 kN-m) impact wrench was used to tighten

the eight ½ in. (13 mm) all-threads that were evenly spaced along the full height of the wall seam. Each all-thread was fastened with steel nuts and several washers as to ensure a uniform dispersion of force over the wood panel. The force exerted by each all-thread, *F*, is given as:

$$F = \frac{T}{\mu D} \tag{4.1}$$

where *T* is the torque from the pneumatic impact wrench in *in.-lbs*, μ is the coefficient of friction between the steel nuts and washers, given as *0.8*, and *D* is the all-thread diameter in *in.* Using this equation an application pressure of 20 psi (276 kPa) was achieved.

Test #1 had a garnet media blast performed in the connection area. The connection was applied after erection and consisted of two laminas of unidirectional GFRP composite (+45°, -45°) applied for the total 8 ft (2.4 m) height of the wall and a total width connecting the two walls of 1.5 ft (0.5 m). No pressure was applied during the curing process of the GFRP composite. Figure 4.3 shows the GFRP composite connection details and Figure 4.4 shows the finished GFRP connection.

Test #2 had a muriatic acid wash performed in the connection area. The connection was similar to that of Test #1, differing in that pressure was applied during the curing process of the GFRP composite connection.

Test #3 had a surface retarder with multiple-pass wash performed in the connection area. The connection was similar to that of Test #2. Figure 4.5 shows the finished GFRP composite connection.

Test #4 had a garnet media blast performed in the connection area. The connection was similar to that of Test #1, differing in that eighteen 3/8 in. (9.5 mm) diameter CFRP anchors, spaced on each wall at 10 7/8 in. (276 mm), were inserted into

the wall face to a depth of 3 in. (76 mm) and splayed with a diameter of 9 in. (229 mm) above the second lamina of GFRP composite on both sides of the seam. Figure 4.6 shows the detailed GFRP composite connection with the CFRP anchors and Figure 4.7 shows the finished connection.

Test #5 had a muriatic acid wash performed in the connection area. The connection consisted of four laminas of unidirectional GFRP (+45°, -45°, 90°, 0°) for the total 8 ft (2.4 m) height of the wall and a total width connecting the two walls of 1.5 ft (0.5 m). Figure 4.8 shows the GFRP composite connection details. Pressure was applied during the curing process of the GFRP composite connection.

Test #6 had a surface retarder with multiple-pass wash performed in the connection area. The connection was similar to that of Test #5. Figure 4.9 shows the finished GFRP composite connection.

Test #7 had a muriatic acid wash performed in the connection area. The connection was similar to that of Test #5, differing in that eighteen 3/8 in. (9.5 mm) diameter CFRP anchors, spaced at 10 7/8 in. (276 mm), were inserted to a depth of 3 in. (76 mm) and splayed at a diameter of 9 in. (229 mm) above the outermost lamina of the GFRP composite laminate on both sides of the seam. Figure 4.10 shows the detailed GFRP composite connection with CFRP anchors and Figure 4.11 shows the finished GFRP composite connection.

Test #8 had a surface retarder with multiple-pass wash performed in the connection area. The connection was similar to that of Test #7.

4.2.2 Material Properties

The welded wire mesh (WWM) curtains and four steel plates with welded DBA were 60,000 psi (413,685 kPa) mile steel. The concrete was a structural mix with a design 28-day compressive strength of 10,000 psi (68,950 kPa). Table 4.2 shows the concrete mix design.

The GFRP composite used was SikaWrap Hex® 100G unidirectional fiber fabric. Using a two-part epoxy resin, a connection is formed using the following steps: (i) prime the concrete surface with epoxy resin (Figure 4.12), (ii) wet lay-up GFRP laminas (Figure 4.13), and (iii) when applicable, apply pressure to the wet connection (Figure 4.14). The manufacturer's properties of the cured GFRP composite laminate are shown in Table 4.3. The manufacturer's properties of the cured CFRP composite laminate, SikaWrap Hex® 103C, are shown in Table 4.4. Using the same two-part epoxy resin and a segment of CFRP lamina, anchors are applied using the following steps: (i) cut strips into a 7.5 in. (191 mm) long by 6.25 in (159 mm) wide segment of CFRP (Figure 4.15), (ii) saturate segment with resin and roll into applicable anchor shape (Figure 4.16), and (iii) insert the rolled-anchor through the sheets of GFRP into a previously drilled hole and splay the strips (Figure 4.17).

4.2.3 Test Set-up

Specimens consisting of two erect concrete wall panels joined with a GFRP composite connection were subject to simulated seismic loads. The seismic, or cyclic, load was applied using a 150 kip (222 kN) hydraulic actuator near the top of the two walls through two W8x31 (W200x46) steel beams connected with two HSS 4x8x3/8 in. (HSS 102x20x9.5 mm) steel tubes, serving as a yoke; this allowed specimens to undergo

horizontal cyclic motion. The system was constrained horizontally by steel blocking, near the base, constructed out of W10x100 (W250x149) steel sections, 1 in. (25 mm) thick steel plates, and ½ in. (13 mm) thick triangular-shaped steel plates. Vertical constraint was introduced using W10x100 (W250x149) steel box sections and four vertical 1 in. (25 mm) diameter steel all thread rods located near the outside extremity of each wall; when these constraints are engaged, a shear force is introduced in the GFRP composite connection. The test set-up is shown in Figure 4.18.

4.2.4 Loading Protocol

A cyclic quasi-static horizontal load was applied to the wall system using displacement control. The displacement was increased by 0.25 in. (6.4 mm) after two cycles of motion, as shown in Figure 4.19. The rate at which the cyclic force was applied was 1.2 in./min. (30 mm/min.). After two cycles, a pause was programmed into the loading protocol in order to evaluate damage to the GFRP composite connection.

4.2.5 Instrumentation

Displacement was measured with linear variable differential transducers (LVDTs) and string pots. Two LVDTs were externally mounted to the lower west and lower east external sides of the wall setup to measure horizontal displacements. Two string pots were mounted horizontally to the upper west and upper east external sides of the wall setup to measure horizontal displacements. Two string pots were mounted vertically to the upper west and upper east interior sides of the wall setup to measure vertical displacements. Three LVDTs were internally mounted between the walls across the seam at 18 in. (0.5 m), 48 in. (1.2 m) and 78 in. (2 m). Five horizontally oriented strain gauges were applied to the outermost lamina of GFRP composite laminate near the middle of

each connection. Three gauges were placed along the seam at 45 in. (1.14 m), 51 in. (1.30 m) and 57 in. (1.45 m). Two gauges were spaced horizontally 3 in. (76 mm) from the center gauge. The force was measured by a load cell that was in-line with the hydraulic actuator at the upper west external side of the test set-up. Specimen instrumentation is shown in Figure 4.20.

4.3 Test Results

4.3.1 Introduction

For each tested specimen, the horizontal force versus horizontal displacement hysteresis is presented. A comparison of the hysteretic behavior and energy dissipation are compared among the tests. Static analysis to determine shear in the connection is presented. String pots above and LVDTs on the face of each specimen and measured negligible displacements before failure and are not reported herein. Strain data are inherently unpredictable because of the indistinctness when attempting to measure the strain of the whole GFRP composite laminate, composed of multiple unidirectional laminas, by gauging only one local area; and therefore is not reported for each specimen herein. The horizontal strain range in the GFRP laminate connections for all tests was 7,700 to 19,900 microstrain.

4.3.2 Results

The connection performance in terms of horizontal load, horizontal deflection, horizontal drift, and failure mode are presented for each specimen in Table 4.5. Modes of failure included immediate delamination, progressive delamination, and progressive delamination with GFRP fiber failure or CFRP anchor failure.

Test #1 had a media blasted surface preparation of the concrete and a connection

laminate comprised of two unidirectional laminas of continuous GFRP composite (+45°, -45°) applied without pressure. The connection had a horizontal load capacity of 40 kips (179 kN) and a horizontal deflection capacity of 0.60 in. (15 mm). Failure occurred by immediate delamination of the GFRP composite laminate connection from the west concrete wall panel (east/west shown in Figure 4.20). Figure 4.21 shows the 45° shear bands just before the complete delamination failure, shown in Figure 4.22. The hysteretic behavior *Test #1* is shown in the curve of Figure 4.23.

Test #2 had an acid washed surface preparation of the concrete and a connection similar to Test #1 but applied with pressure. Initial GFRP delamination from concrete, shown in Figure 4.24, occurred at a horizontal load of 53 kips (237 kN) and a horizontal deflection of 0.70 in. (18 mm). During progressive delamination, the GFRP composite fibers failed. Connection failure, shown in Figure 4.25, occurred on both concrete wall panels at a horizontal load capacity of 34 kips (151 kN) and a horizontal deflection capacity of 0.85 in. (22 mm). The hysteretic behavior of *Test #2* is shown in Figure 4.26.

Test #3 had a surface retarder with multiple-pass washed surface preparation of the concrete and a connection similar to that of Test #2. Initial GFRP delamination from concrete, shown in Figure 4.27, occurred at a horizontal load of 42 kips (186 kN) and a horizontal deflection of 0.47 in. (12 mm). Connection failure, shown in Figure 4.28, occurred on the east concrete wall panel at a horizontal load capacity of 59 kips (263 kN) and a horizontal deflection capacity of 0.89 in. (23 mm). The hysteretic behavior of *Test #3* is shown in Figure 4.29.

Test #4 had a surface preparation of the concrete and a connection similar to that of Test #1 but with eighteen CFRP anchors spaced at 10-7/8 in. (276 mm). The 45° shear

bands developed in the GFRP before leading up to failure, shown in Figure 4.30. The bands are held down with the development of the CFRP anchors, as opposed to the bands developed in a connection without anchors, shown in Figure 4.22. Connection failure, shown in Figure 4.31, occurred on the west concrete wall panel at a horizontal load capacity of 77 kips (344 kN) and a horizontal deflection capacity of 1.04 in. (26 mm). The hysteretic behavior of *Test #4* is shown in Figure 4.32. Various CFRP anchors failed near the surface of the concrete due to shear forces imposed by the GFRP laminate, as shown in Figure 4.33.

Test #5 had a surface preparation of the concrete similar to that of Test #2 and a connection laminate comprised of four unidirectional laminas of continuous GFRP composite (+45°, -45°, 90°, 0°) applied with pressure. The connection had a horizontal load capacity of 62 kips (274 kN) and a horizontal deflection capacity of 0.59 in. (15 mm). Failure was an immediate delamination of the GFRP connection from the west concrete wall panel, shown in Figure 4.34. The hysteretic behavior of *Test #5* is shown in Figure 4.35.

Test #6 had a surface preparation of the concrete similar to that of Test #3 and a connection similar to Test #5. The connection had a horizontal load capacity of 57 kips (255 kN) and a horizontal deflection capacity of 0.63 in. (16 mm). Failure was similar to that of Test #5, shown in Figure 4.36. The hysteretic behavior of *Test #6* is shown in Figure 4.37.

Test #7 had a surface preparation of the concrete and a connection similar to that of Test #5 but with eighteen CFRP anchors spaced at 10-7/8 in. (276 mm). Progressive GFRP delamination assisted with connection failure. The connection had a horizontal

load capacity of 82 kips (363 kN) and a horizontal deflection capacity of 0.92 in. (23 mm). Failure was due to CFRP anchor failure and GFRP delamination from the east concrete wall panel, shown in Figure 4.38. The hysteretic behavior of *Test #7* is shown in Figure 4.39. Various CFRP anchors failed near the concrete surface due to shear forces imposed by the GFRP laminate, as shown in Figure 4.33.

Test #8 had a surface preparation of the concrete similar to that of Test #6 and a connection similar to that of Test #7. The connection had a horizontal load capacity of 89 kips (395 kN) and a horizontal deflection capacity of 1.11 in. (28 mm). Failure was similar to that of Test #7 but failure occurred from the west concrete wall panel. The hysteretic behavior of *Test #8* is shown in Figure 4.40. Various CFRP anchors failed near the surface of the concrete similar to the occurrence in Test #7.

4.3.3 Hysteresis Summary Curves

The hysteretic envelope shows the horizontal load and horizontal displacement for each cycle. These curves are significant in determining the capacity of each connection. The following connection comparisons are presented: (i) application pressure, (ii) number of unidirectional GFRP laminas, (iii) concrete surface preparation, and (iv) CFRP anchors.

The use of application pressure moderately increased horizontal load and horizontal displacement capacity as seen by comparing Test #1 (no pressure) with Tests #2 and #3 (pressure) in Figure 4.41. The use of application pressure reduced the amount of epoxy resin at the bond line and ensures a better fiber-aggregate interaction, both forming a superior bond.

Using more GFRP laminas modestly increased the horizontal load capacity, as

seen in Figure 4.42 by comparing Test #2 (two laminas) with Test #5 (four laminas). The slightly higher horizontal load capacity was also seen in Figure 4.43 by comparing Tests #4 (two laminas with anchors) with Tests #7 and #8 (four laminas with anchors). A moderately smaller horizontal displacement capacity was observed for Test #7 with four laminas because the stiffness of the connection increases with more laminas. Slightly larger horizontal displacement capacities were obtained for connections with fewer GFRP laminas as seen in Figure 4.42 by comparing Test #2 with #5. This behavior was also observed in Figure 4.44 when comparing Test #3 (two laminas) with Test #6 (four laminas). However, this displacement trend was not observed in tests with CFRP anchors, as seen in Figure 4.43 by comparing Tests #4 (two laminas with anchors) with Tests #7 and #8 (four laminas with anchors).

A surface retarder concrete preparation modestly increased the horizontal load and horizontal displacement capacity of the connections more than a media blasted or acid wash surface preparation, as seen from Test #3 (surface retarder) compared to Test #2 (acid wash) in Figure 4.41. The same was true when comparing Test #8 (surface retarder) with Test #7 (acid wash) in Figure 4.43.

Independent of other variables, tests with CFRP anchors significantly increased horizontal load and horizontal displacement capacity by adding more strength to the laminate and providing anchorage into the concrete. This seen by comparing Test #4 and Test #2 in Figure 4.45, and also by comparing Tests #7 and #8 to Test #5 and #6 in Figure 4.46.

4.3.4 Energy Dissipation Curves

Energy dissipated versus horizontal displacement for each cycle is plotted to show a summary of seismic energy dissipation for each connection. Energy dissipation is also significant in determining the capacity of each connection for seismic applications – a higher dissipation of energy implies an overall better seismic performance. The following connection comparisons are presented: (i) application pressure, (ii) number of unidirectional GFRP laminas, (iii) concrete surface preparation, and (iv) CFRP anchors.

Application pressure on the GFRP connection significantly increased energy dissipation as seen in Figure 4.47 by comparing Test #1 (no pressure) with Tests #2 and #3 (with pressure). However, an increase in energy dissipation was not exhibited when applying pressure when CFRP anchors are in use, as seen by comparing Test #4 (no pressure) with Tests #7 and #8 (with pressure) in Figure 4.48. This is potentially due to the application pressure damaging the CFRP anchors where the carbon strands exit the drilled hole in the wall panel and bend to flatten (or splay) on the face of the outermost GFRP laminate, as seen in Figure 4.49. This occurrence lowered energy dissipation in the connections.

A connection with two GFRP laminas dissipated significantly more energy than a connection with four laminas, as seen in Figure 4.50 when comparing Tests #2 and #3 (two laminas) with Tests #5 and #6 (four laminas).

Independent of other variables, tests with CFRP anchors significantly increased energy dissipation by comparing Tests #1 (no anchors) to Test #4 (with anchors) in Figure 4.51 and also by comparing Tests #5 and #6 (no anchors) to Test #7 and #8 (with anchors) in Figure 4.52.

4.3.5 Shear Transfer

The shear transferred between the two walls was determined for each specimen. Figure 4.53 shows an idealization of a specimen, with the applied lateral load denoted as *P*. The vertical constraint provided by the all-thread rods is denoted as *R*; this force was measured during the tests using strain gauges. Under this system of loads and constraints, the reactions are shown as F_x and F_y on the west wall panel at corner *F* and H_x and H_y on the east wall at corner *H*. Equilibrium of the wall system in Figure 4.53(a) results in the following:

$$F_y = 2(R + W) - P\left(\frac{h}{s}\right) \tag{4.2}$$

$$H_y = P\left(\frac{h}{s}\right) - R \tag{4.3}$$

$$H_x + F_x = P \tag{4.4}$$

where *W* is the weight of one wall panel (3.2 kip (14 kN)), *h* is the height of the panels (8 ft (2.4 m)) and *s* is the width of one wall panel (4 ft (1.2 m)). Equilibrium in the free-body diagram of the east wall in Figure 4.53(b) results in the value of shear resisted by the GFRP composite connection as:

$$V = P\left(\frac{h}{s}\right) - (R + W) \tag{4.5}$$

$$N = H_x \tag{4.6}$$

where *V* is the total shear in the GFRP composite connections and *N* is the total horizontal reaction. The unit shear, in force per length, at the GFRP composite connection, *v*, is given as:

$$v = \frac{V}{h} \tag{4.7}$$

Using these equations, the unit shears at failure in the GFRP connections are

obtained, as shown in Table 4.6. The following connection comparisons are presented: (i) application pressure, (ii) number of unidirectional GFRP laminas, (iii) concrete surface preparation, and (iv) CFRP anchors.

Application pressure moderately increased the GFRP connection ability to transfer shear as seen when comparing Test #1 (no pressure) with Test #2 (with pressure). When CFRP anchors are present a similar damaging effect like observed with energy dissipation is seen when application pressure is used as seen when comparing Test #4 (no pressure) with Test #7 and Test #8 (with pressure).

The number of unidirectional GFRP laminas did not have an obvious affect on shear transfer as seen when comparing Test #2 and #3 (two laminas) with Test #5 and #6 (four laminas). Concrete surface preparation had similar comparisons to that of number of unidirectional GFRP laminas.

CFRP anchors modestly increased the GFRP connection ability to transfer shear as seen when comparing Test #1 (no anchors) with Test #4 (with anchors); also by comparing Test #5 and #6 (no anchors) with Test #7 and #8 (with anchors).

4.4 Summary and Conclusions

4.4.1 Summary

An increase of both load and drift was observed when pressure was applied during curing of the GFRP composite connection. Load increased by 1.4 times, displacement increased by 1.2 times, energy dissipation doubled, and shear transfer increased by 1.4 times from using application pressure.

A 1.2 times increase in load was observed when four GFRP laminas were used in the connection instead of two GFRP laminas. However, a 1.4 times higher displacement

and 1.8 times higher energy dissipation was observed when two GFRP laminas were used in the connection instead of four GFRP laminas. Fewer laminas caused the connection to be less stiff.

An increase in load and displacement was observed when the concrete surface was prepared using a surface retarder with multiple-pass wash. The load was increased by 1.1 times and the displacement was increased by 1.2 times. The surface retarder with multiple-pass wash method exposed more large aggregate at the concrete surface and therefore strengthened the bond. However, muriatic acid washed surface increased energy dissipation by 1.3 times.

The use of CFRP anchors increased the load and displacement capacity of the connection. A GFRP composite connection with CFRP anchors and without applying pressure resisted 1.4 times the load of a similar connection without anchors and with applying pressure. A GFRP composite connection with CFRP anchors and without applying pressure resisted 1.9 times the load of a similar connection without anchors and without applying pressure. A GFRP composite connection with CFRP anchors and with applying pressure resisted 1.5 times the load of similar connections without anchors. Tests with CFRP anchors had the highest displacement capacity of all tests by 1.6 times and the highest energy dissipation of all tests by 2.8 times.

The test with two laminas of unidirectional GFRP laminate and eighteen CFRP composite anchors resisted 2.5 times the unit shear resisted by a similar composite connection without anchors. Tests with four laminas of unidirectional GFRP laminate and eighteen CFRP composite anchors applied with pressure resisted 1.2 times the unit shear resisted by a similar composite connection without anchors.

4.4.2 Conclusions

Application pressure improved the GFRP composite connection horizontal load, horizontal displacement, and energy dissipation capacity. Using a stiff material (in this case ¾ in. (19 mm) formply) to apply pressure allows for a more uniform bond. The use of a soft material (in this case ½" (13 mm) EPS) between the stiff material and the wet GFRP laminate allows the fibers to follow the contours of the concrete surface. Application of pressure also reduces the bond line thickness and creates a superior bond between the GFRP laminate and concrete. However, the applied pressure is potentially damaging to splayed fibers of the CFRP anchors on the outermost lamina. This is likely due to forcing the fibers of the CFRP anchors to splay at a sharp 90° turn. Although a slight chamfer is made when drilling the holes, a more drastic chamfering of each hole may eliminate this issue.

Four GFRP laminas created a stiffer laminate and a failure mechanism more likely to propagate after initial delamination. CFRP anchors help improve and preserve the bond of the GFRP laminate to concrete and prevent occurrence of a sudden delamination or total loss of connectivity between concrete panels. Two GFRP laminas are not able to resist as much load as four laminas, but create a more flexible connection by way of displacement and energy dissipation capacity.

Larger aggregates were exposed when using a surface retarder with multiple-pass wash. More large aggregates were engaged in the composite connection and contributed to a moderate increase in horizontal load and horizontal displacement capacity.

The use of approximately one CFRP anchor per 1 ft. (0.3 m) of wall height demonstrated that anchorage of the GFRP laminate to the concrete increased the load,

displacement, energy dissipation, and shear transfer capacity. As drift and cyclic shear between the panels increases, the GFRP laminate distributes forces throughout the connection in orthogonal directions. This distribution of forces through the connection causes the forces in the fibers to change direction and a 360° splay is beneficial to counteract these changing directional forces. Once delamination starts at the seam, the anchors engage and counteract propagating delamination in all directions.

It is recommended that in future research GFRP anchors should be considered since they have a higher strain capacity than CFRP anchors. However, because of lower ultimate strength more research is required to determine their applicability.

It is also recommended that in future research, splaying of GFRP or CFRP anchors should be performed in-between GFRP laminas to create a more integrated anchorage system; this could reduce damage to splayed anchor fibers from application of pressure during curing and delay delamination during simulated seismic motion.

The application of bidirectional lamina (±45º) would likely achieve similar results and decrease installation efforts. However, further research is recommended to observe if similar results would be obtained with less installation effort.

Table 4.1 – Test matrix

Test	Application Pressure	GFRP Lamina Configuration	Surface Preparation	*Number of Laminas	CFRP Anchors
1	No	(-45°, +45°)	Media Blast	2	No
2	Yes	(-45°, +45°)	Acid Wash	2	No
3	Yes	(-45°, +45°)	Retarder, Multiple-Pass Wash	2	No
4	No	(-45°, +45°)	Media Blast	2	Yes
5	Yes	(-45°, +45°, 90°, 0°)	Acid Wash	4	No
6	Yes	(-45°, +45°, 90°, 0°)	Retarder, Multiple-Pass Wash	4	No
7	Yes	(-45°, +45°, 90°, 0°)	Acid Wash	4	Yes
8	Yes	(-45°, +45°, 90°, 0°)	Retarder, Multiple-Pass Wash	4	Yes

* Thickness of 1 Lamina = 0.04 in. (1.016 mm)

Table 4.2 – Concrete mix design

Concrete Materials	Density, lbs/ft^3 (kg/m^3)
Grey Cement	24.07 (385.63)
Flyash Class F	6.04 (96.70)
Fine Aggregate	41.41 (663.28)
Coarse Aggregate	56.48 (904.75)
Water	9.63 (154.25)
High Range Water Reducer	0.25 (4)
Air Entrainment	0.009 (0.148)

Table 4.3 – Cured GFRP lamina properties

Cured Laminate Properties	Average Values
Tensile Strength	83,400 psi (575 MPa)
Tensile Modulus	3.672 x 10 ^{6} psi (25,300 MPa)
Tensile Elongation	2.31%
Thickness	0.040 in. (1.016 mm)

Table 4.4 – Cured CFRP lamina properties

Cured Laminate Properties	Average Values
Tensile Strength	180,000 psi (1,241 MPa)
Tensile Modulus	9.4 x 10^{6} psi (64,828 MPa)
Tensile Elongation	1.60%
Thickness	0.040 in. (1.016 mm)
Tensile Strength per Unit Width	7,200 lbs/in (0.81 kN/m)

Table 4.5 – Test results

Test	Horizontal Load, kip (kN)	Horizontal Deflection, in. (mm)	Horizontal Drift (%)	*Failure Mode	Energy Dissipated kip-in. (kN-mm)
1	40.1 (179)	0.71 (15)	0.74	ID	18 (2.0)
2	53.4 (237)	0.85 (22)	0.92	PD; FF	39 (4.4)
3	59.1 (263)	0.89 (23)	0.93	PD	34 (3.9)
4	77.3 (344)	1.04 (26)	1.15	PD; AF	75 (8.4)
5	61.5 (274)	0.59 (15)	0.52	ID	25 (2.9)
6	57.3 (255)	0.63 (16)	0.62	ID	16 (1.8)
7	81.6 (363)	0.92 (23)	0.93	PD; AF	45 (5.1)
8	88.7 (395)	1.11 (28)	0.98	PD; AF	41 (4.6)

* Failure Mode Types:
ID – Immediate Delamination
PD – Progressive Delamination
FF – Fiber Failure
AF – Anchor Failure

Table 4.6 – Shear transfer values

Test	Applied Lateral Load *P*, kip (kN)	Restraining Vertical Force *R*, kip (kN)	Shear *V*, kip (kN)	Unit Shear *v*, kip/ft (kN/m)
1	40 (178)	40 (178)	37 (162)	4.6 (67)
2	53 (236)	59 (265)	43 (193)	5.4 (79)
3	59 (262)	57 (253)	58 (258)	7.2 (106)
4	77 (343)	57 (253)	94 (416)	11.7 (171)
5	62 (276)	56 (249)	63 (279)	7.9 (115)
6	57 (254)	55 (246)	56 (247)	7.0 (101)
7	82 (365)	86 (383)	75 (333)	9.3 (136)
8	89 (396)	106 (471)	69 (307)	8.6 (126)

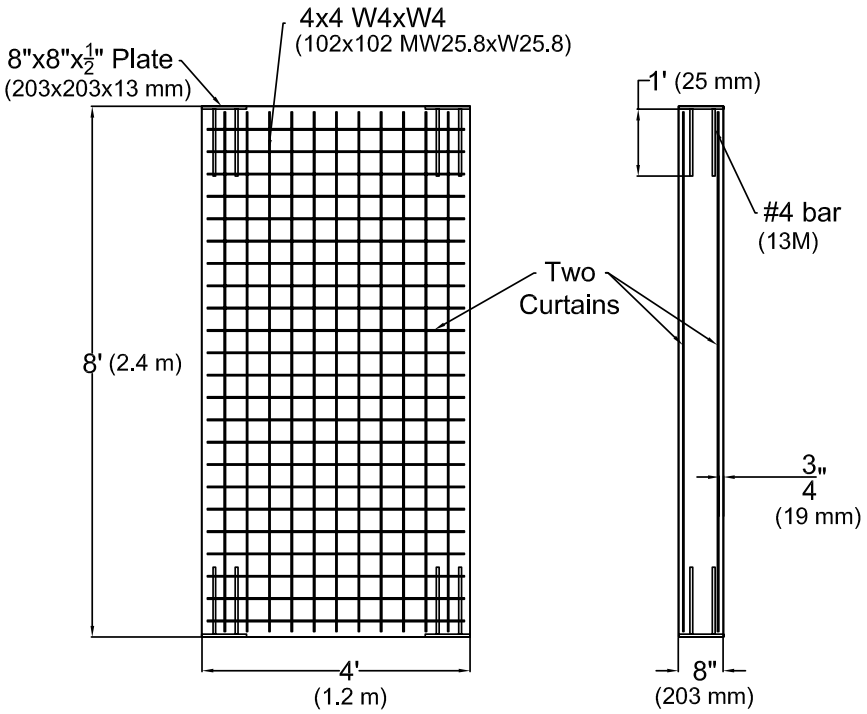

Figure 4.1 – Individual concrete wall panel dimensions and reinforcement details.

Figure 4.2 – Method of applying pressure during curing to GFRP composite connection.

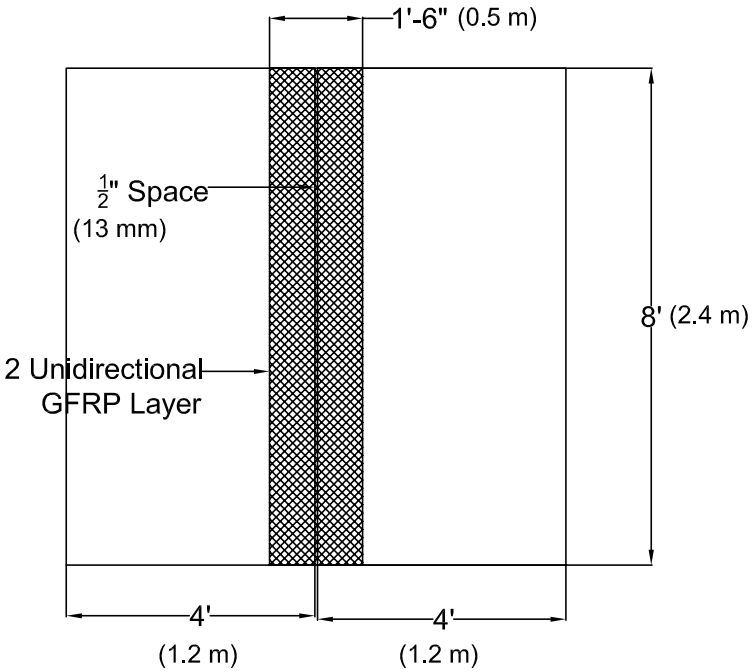

Figure 4.3 – Test #1, #2, and #3 specimen details.

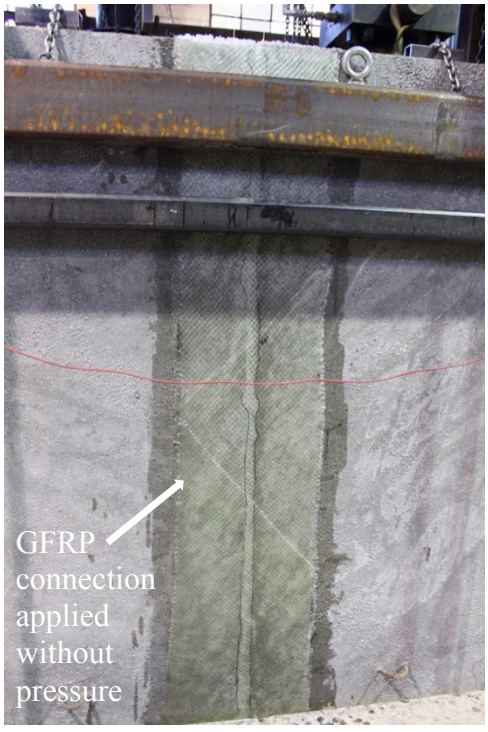

Figure 4.4 –Test #1 specimen.

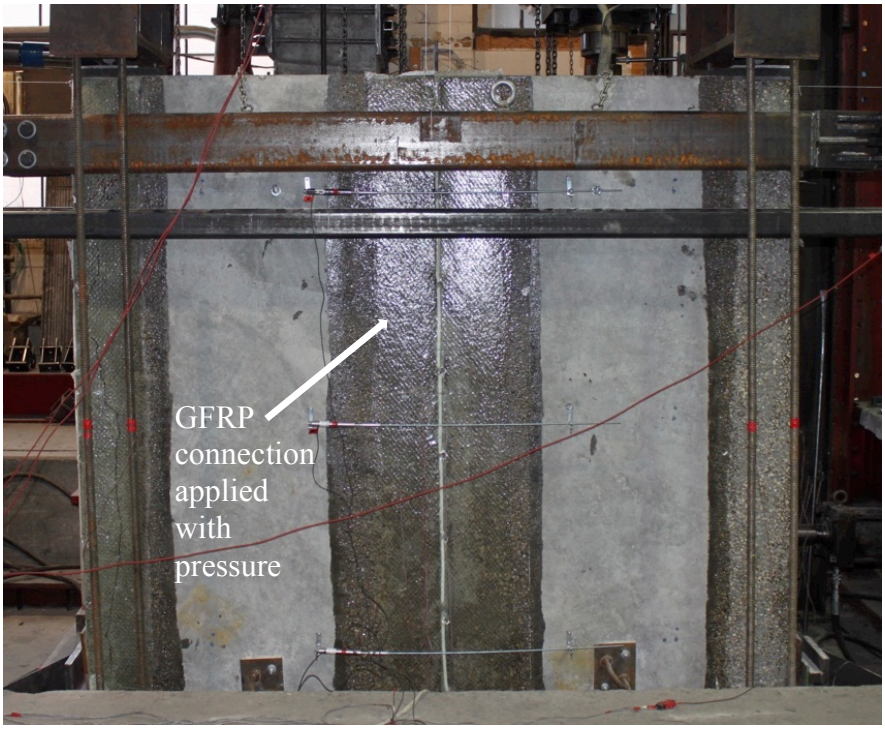

Figure 4.5 –Test #3 specimen.

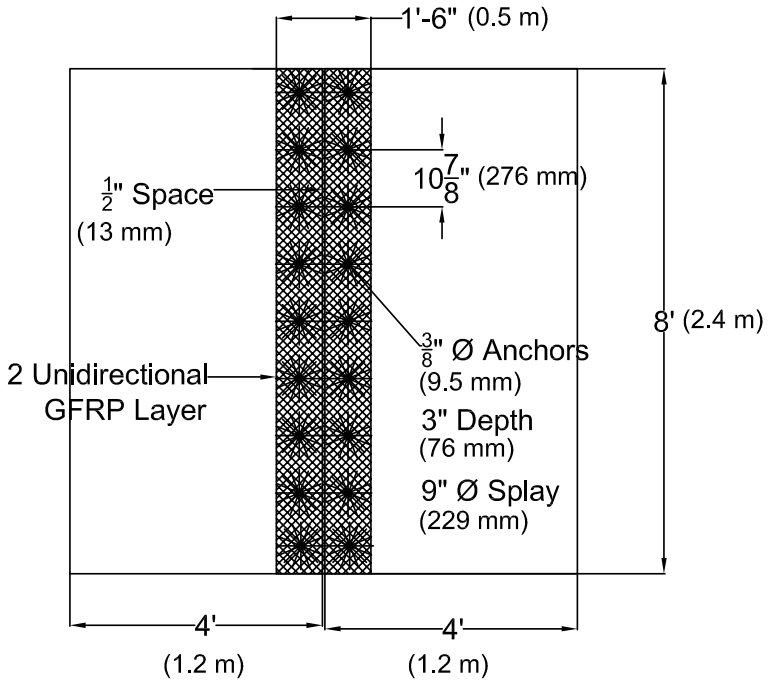

Figure 4.6 – Test #4 specimen details.

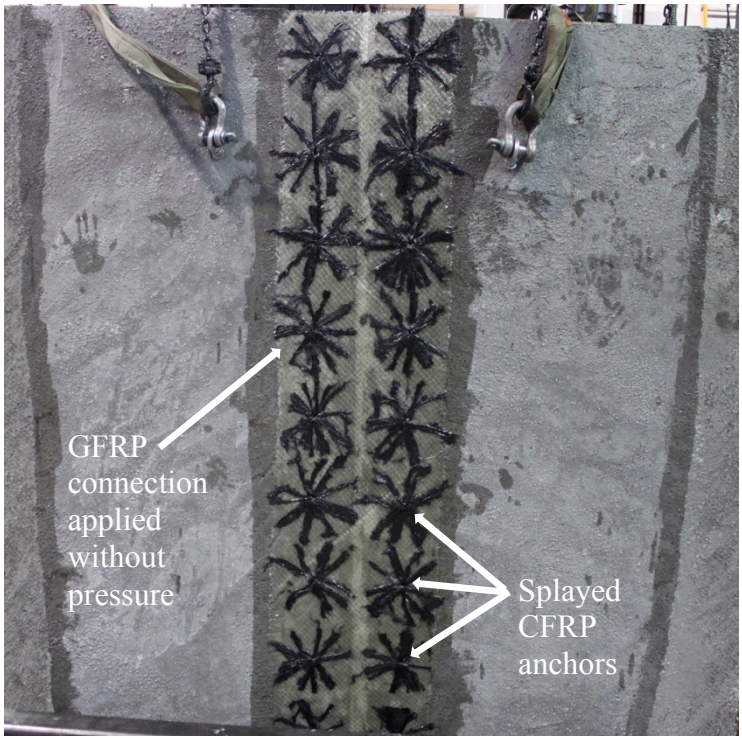

Figure 4.7 – Test #4 specimen.

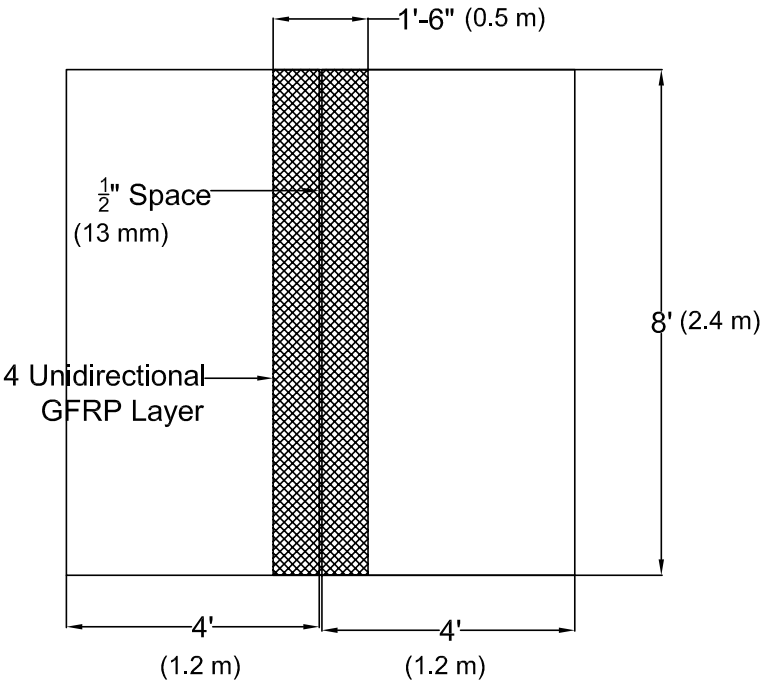

Figure 4.8 – Test #5 and #6 specimen details.

Figure 4.9 –Test #6 specimen.

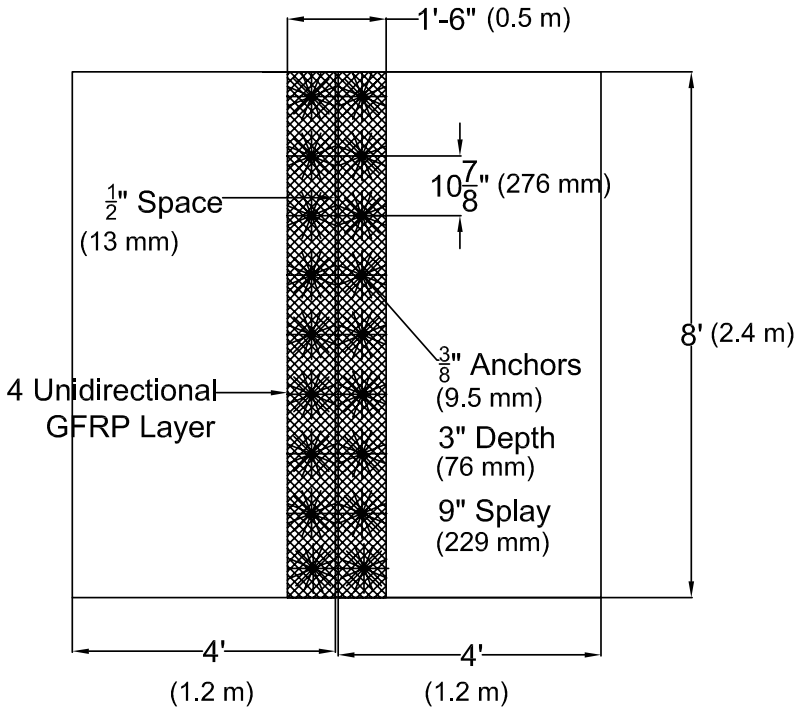

Figure 4.10 –Test #7 and Test #8 details.

Figure 4.11 –Test #7.

Figure 4.12 – Connection step 1: Prime concrete surface with epoxy resin.

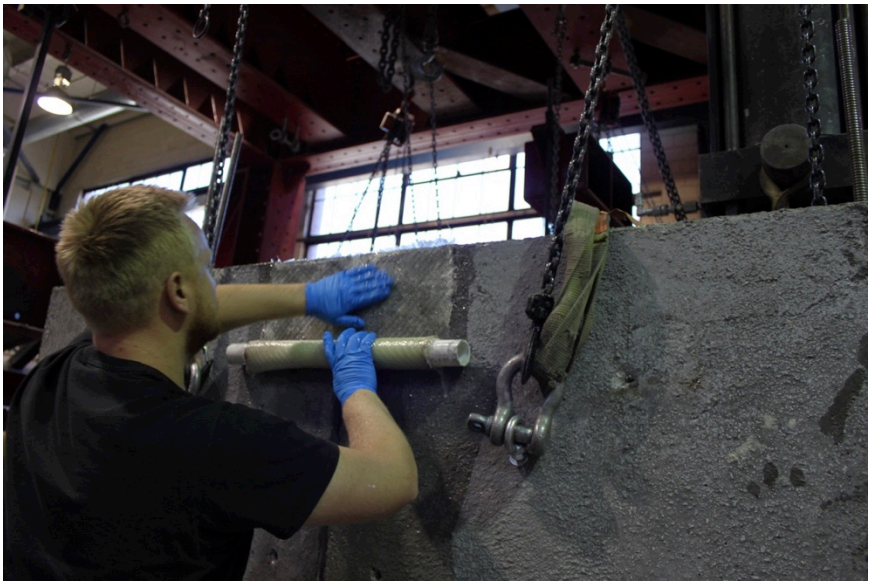

Figure 4.13 – Connection step 2: Lay-up wet GFRP laminas.

Figure 4.14 – Laminate step 3: Apply pressure with formply, EPS, and all-thread connectors through the seam.

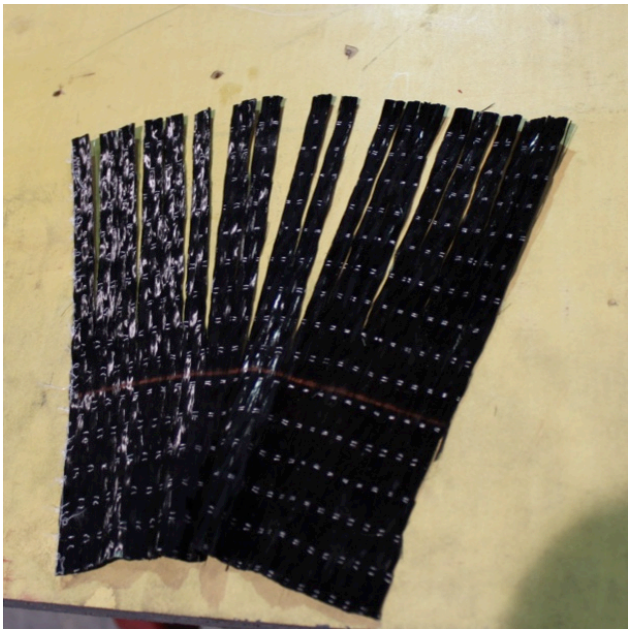

Figure 4.15 – Anchor step 1: Cut strips into a small sheet of CFRP.

Figure 4.16 – Anchor step 2: Saturate with resin and roll into applicable anchor shape.

Figure 4.17 – Anchor step 3: Insert into drilled hole and splay the saturated strips.

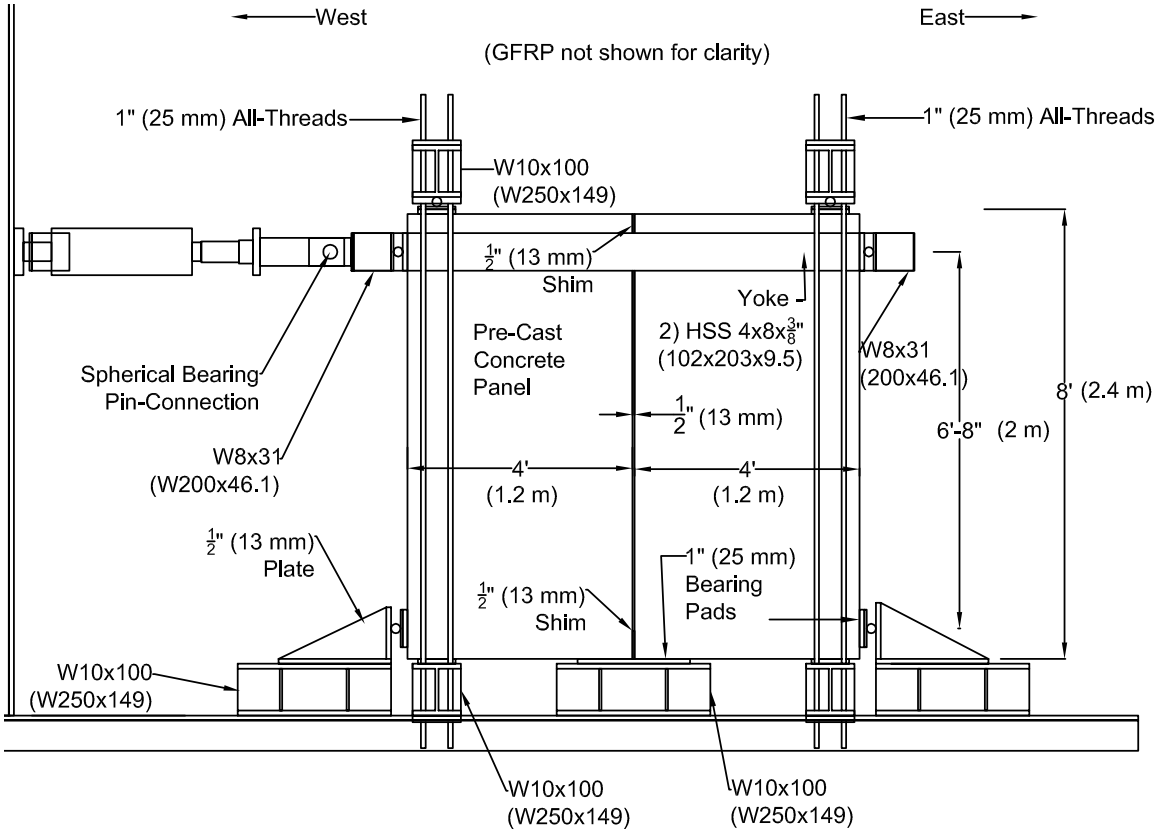

Figure 4.18 – Test set-up.

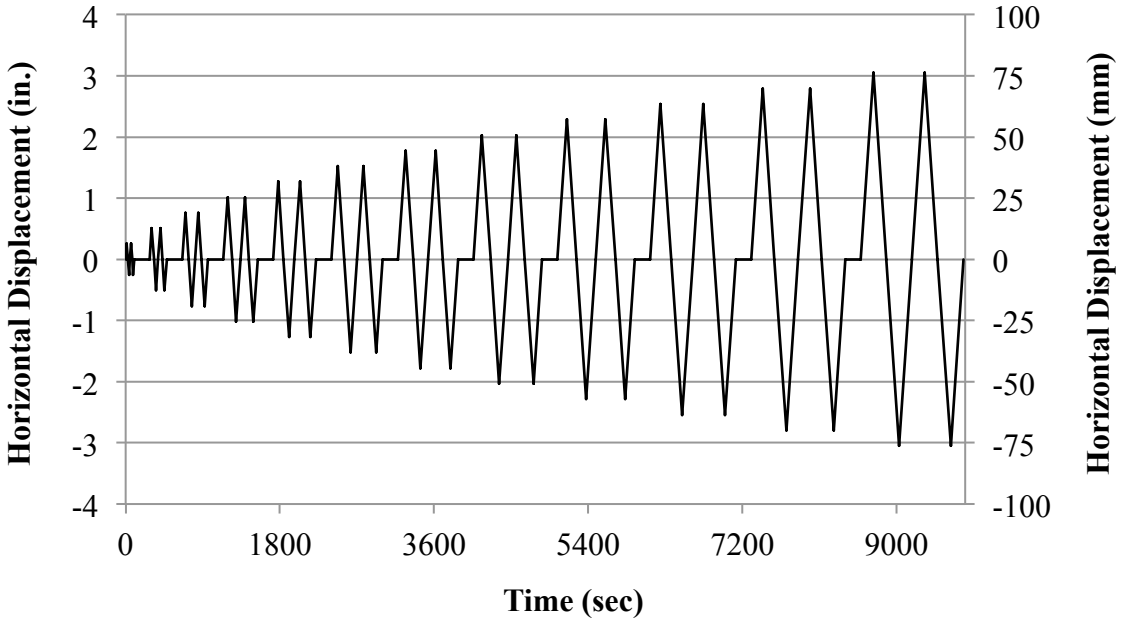

Figure 4.19 – Loading protocol.

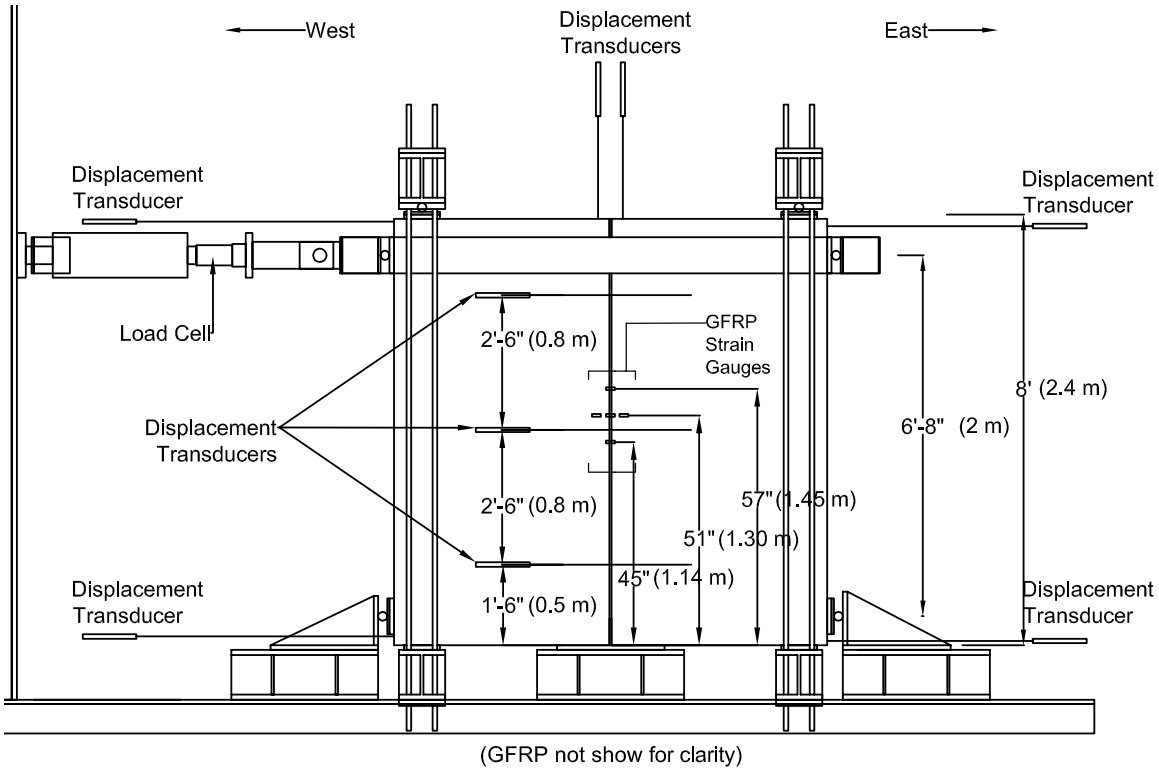

Figure 4.20 – Instrumentation set-up.

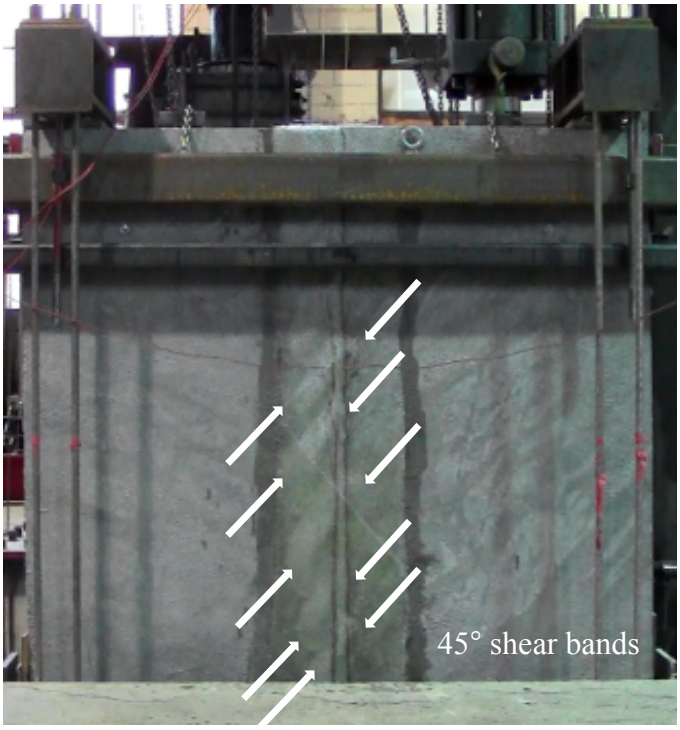

Figure 4.21 – Test #1 connection during failure.

Figure 4.22 – Test #1 connection at failure.

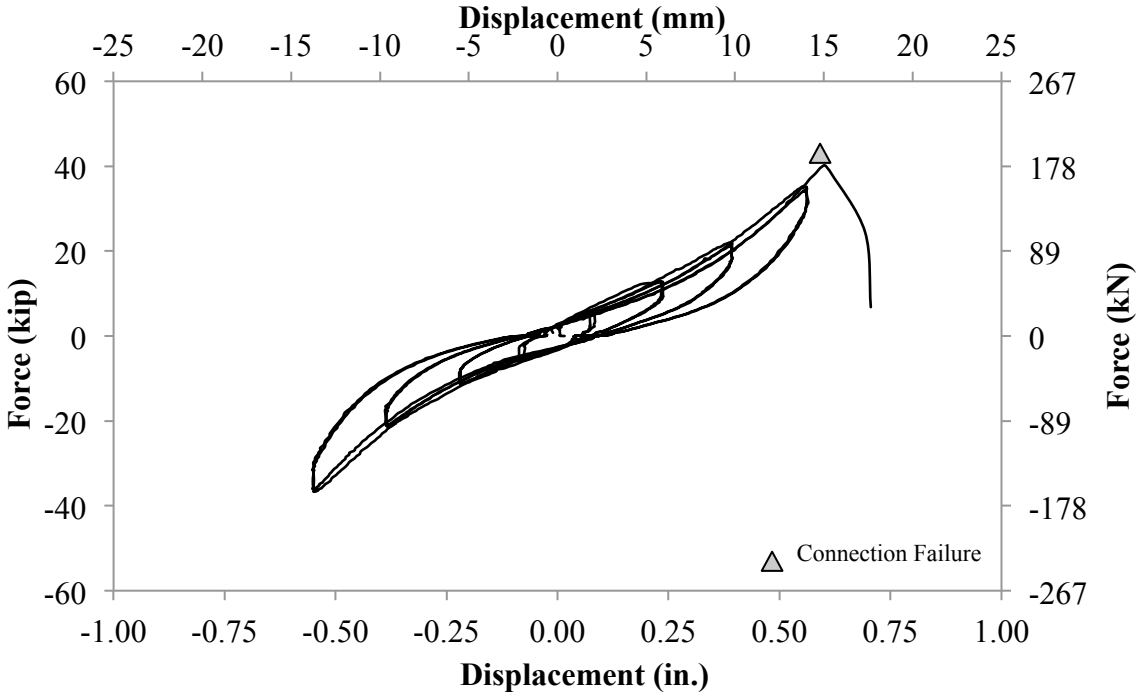

Figure 4.23 – Test #1 hysteresis.

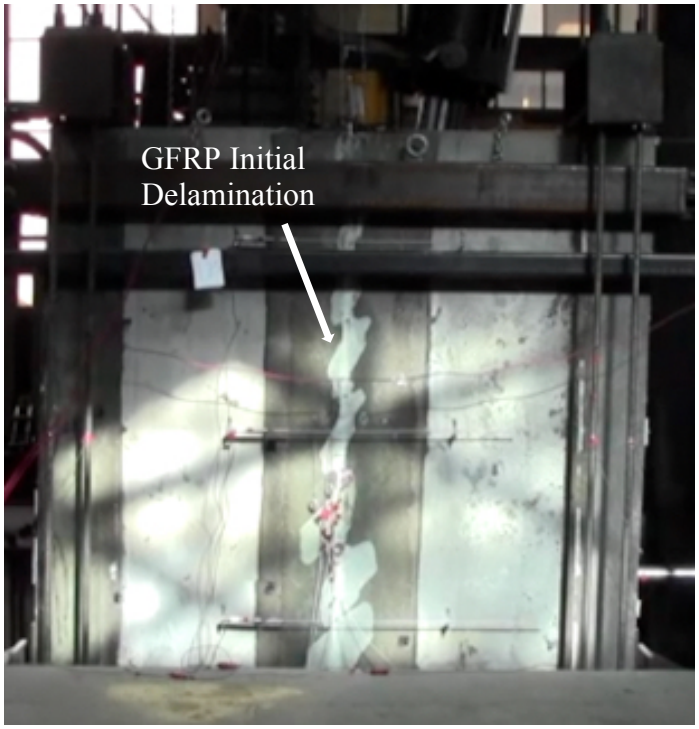

Figure 4.24 – Test #2 initial delamination.

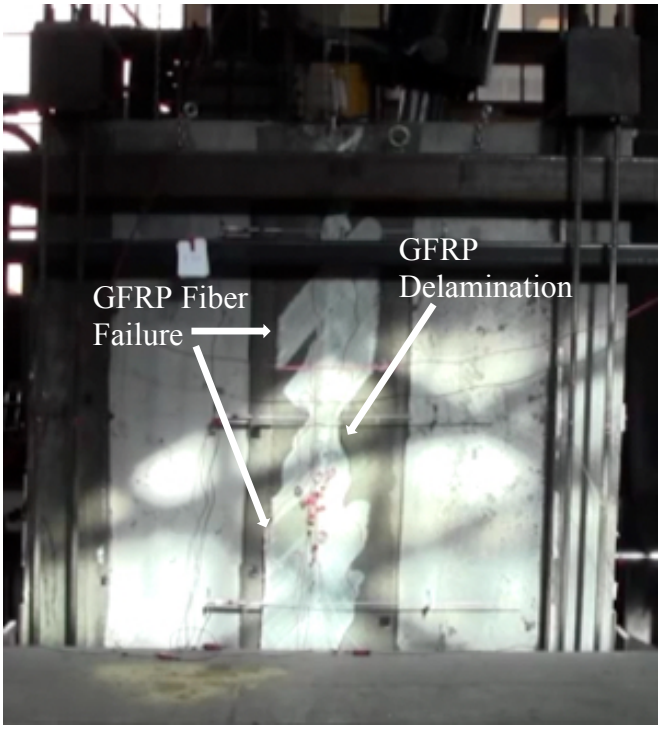

Figure 4.25 – Test #2 connection failure.

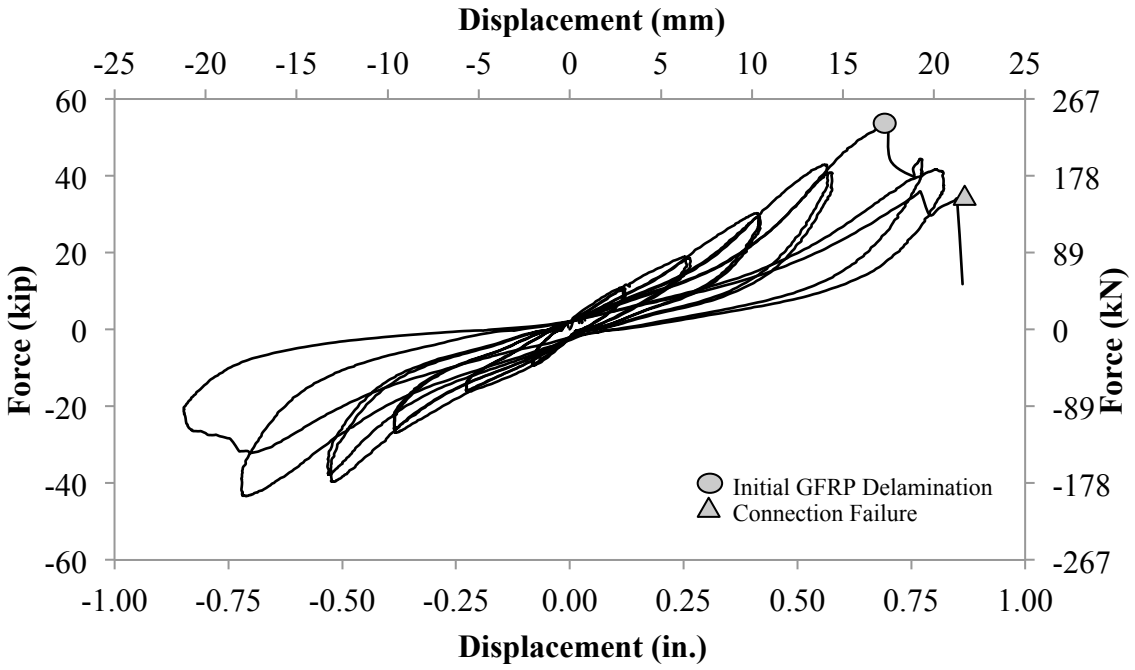

Figure 4.26 – Test #2 hysteresis.

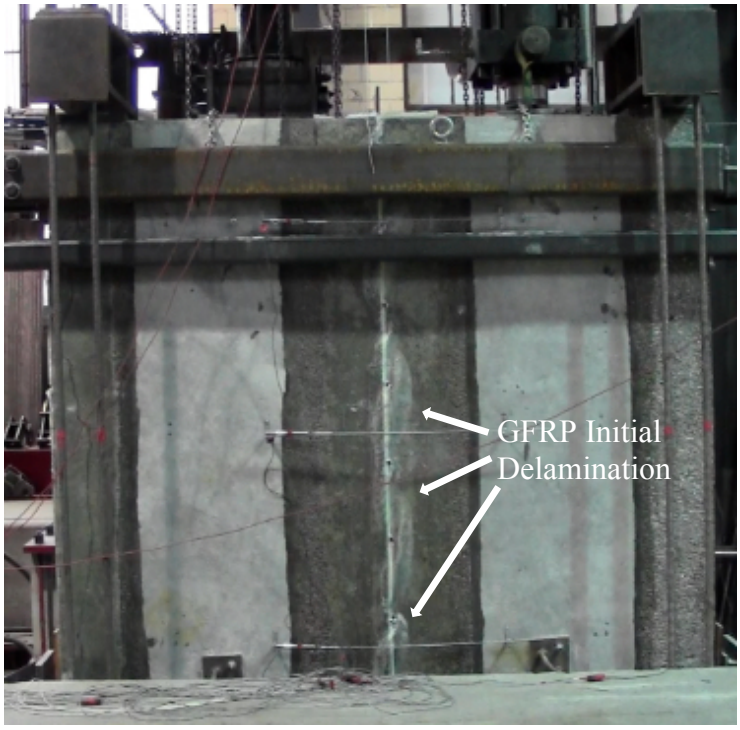

Figure 4.27 – Test #3 initial delamination.

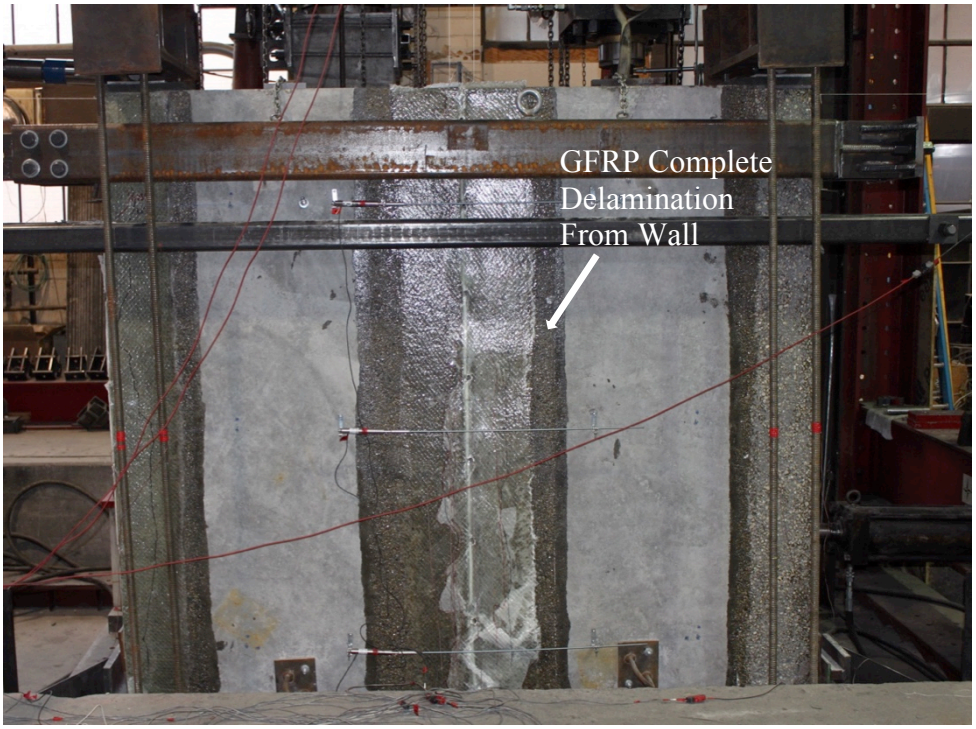

Figure 4.28 – Test #3 connection failure

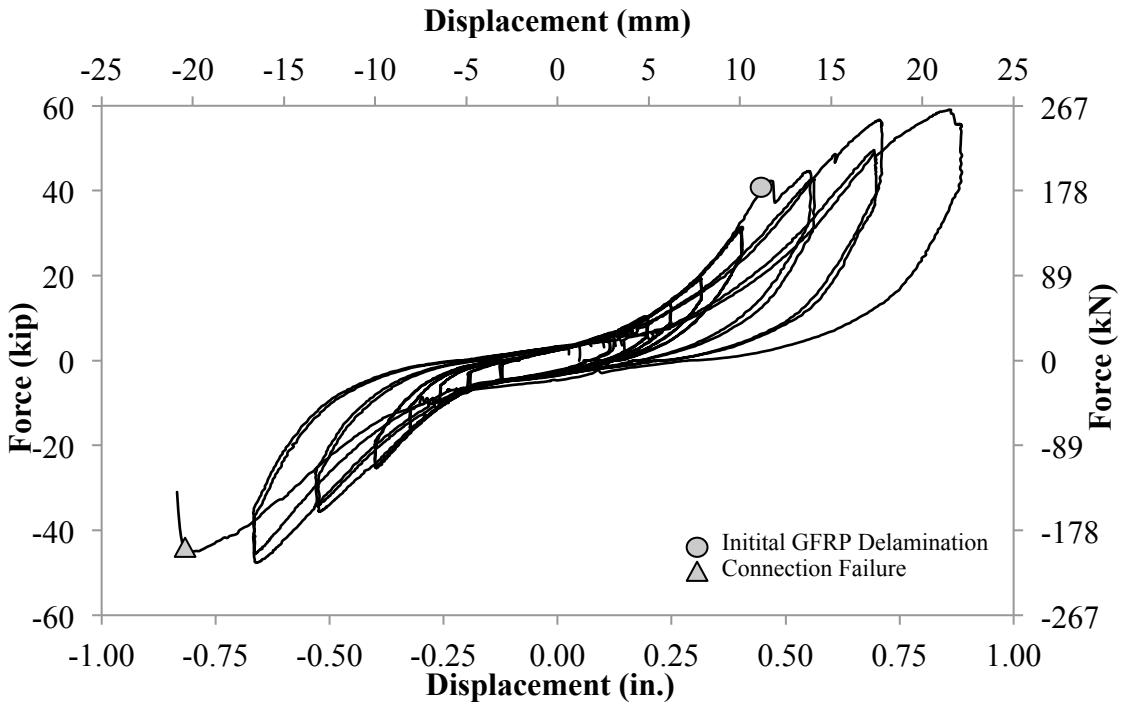

Figure 4.29 – Test #3 hysteresis.

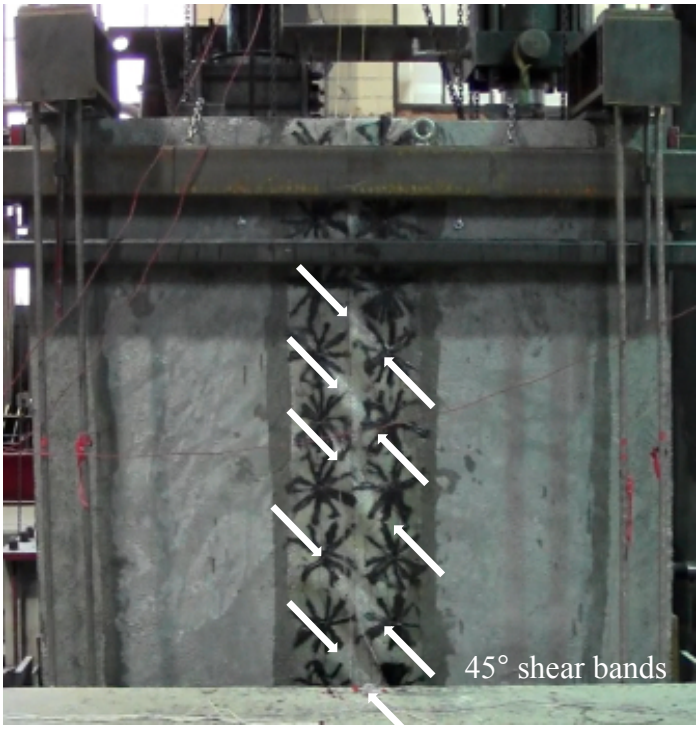

Figure 4.30 – Test #4 connection during failure.

Figure 4.31 – Test #4 connection failure.

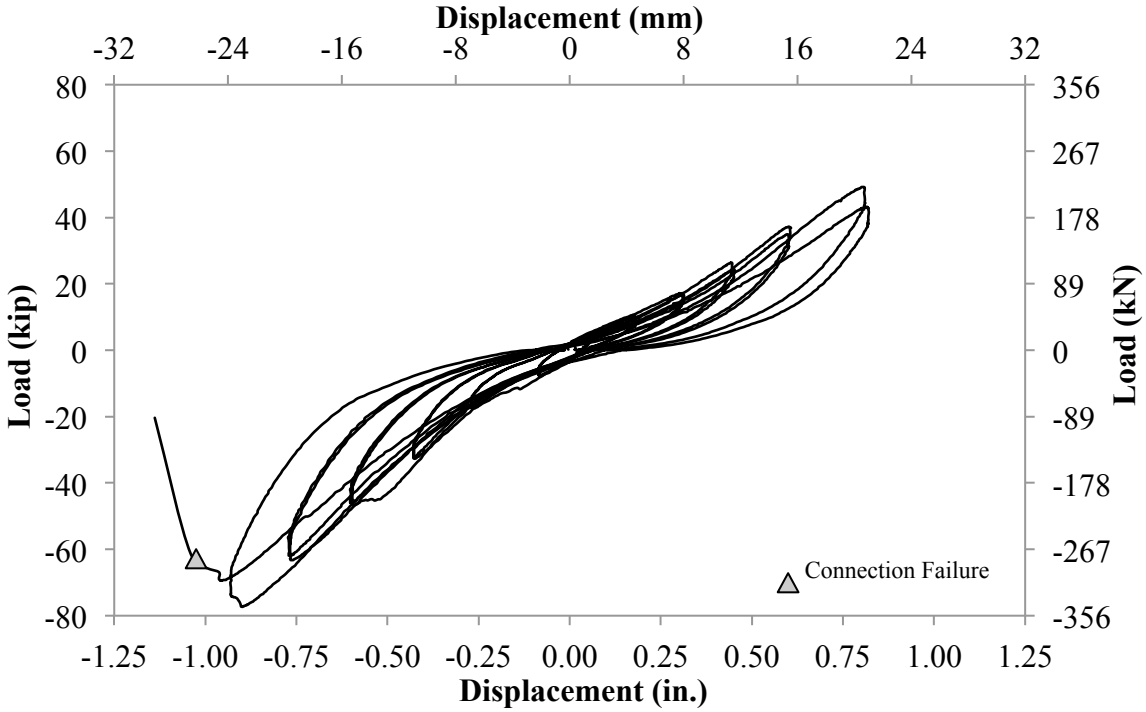

Figure 4.32 – Test #4 hysteresis.

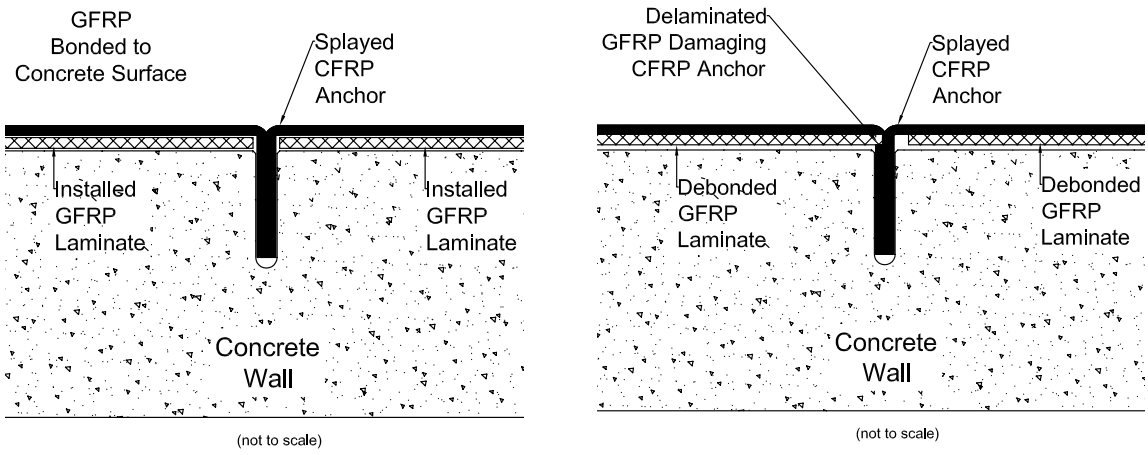

(a) (b)

Figure 4.33 – Schematic of potential shearing of CFRP anchors: (a) bonded GFRP; (b) debonded GFRP

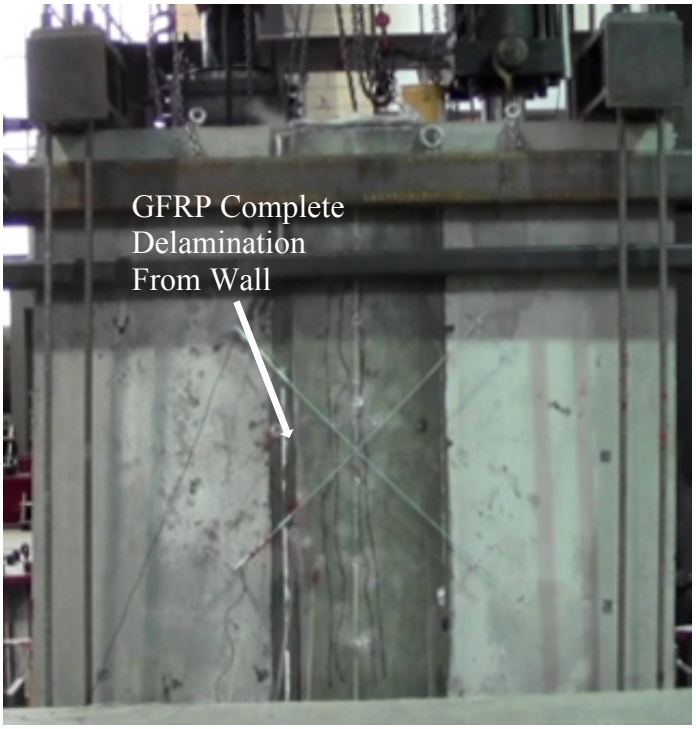

Figure 4.34 – Test #5 connection failure.

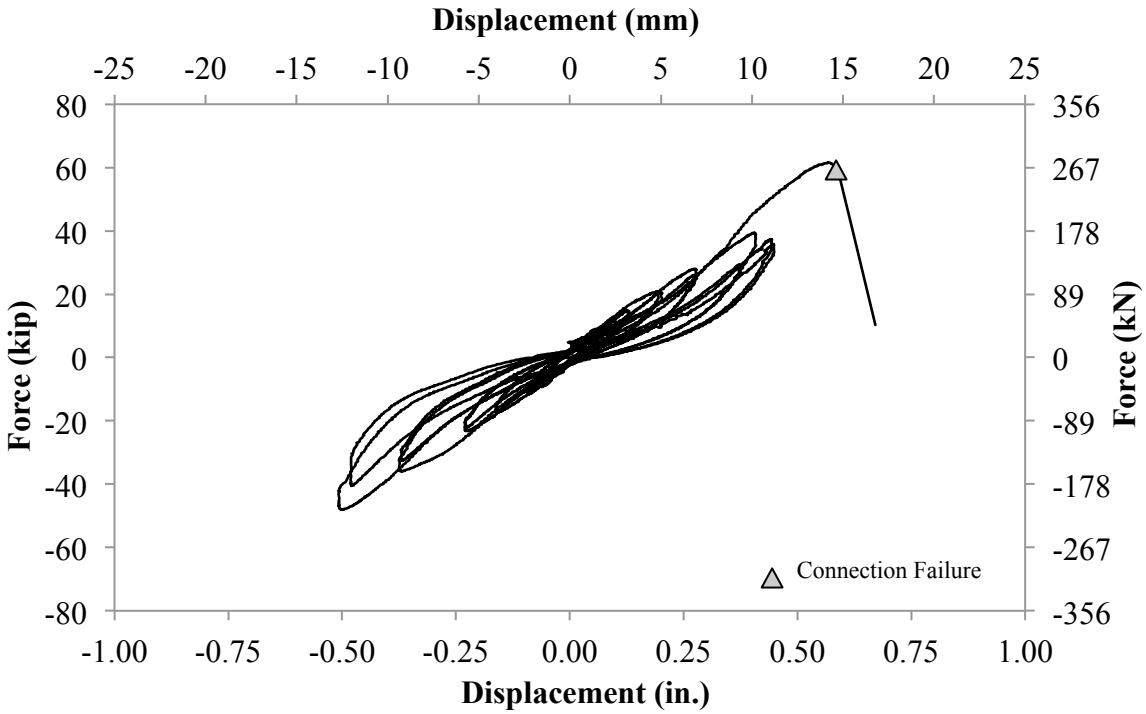

Figure 4.35 – Test #5 hysteresis.

Figure 4.36 – Test #6 connection failure.

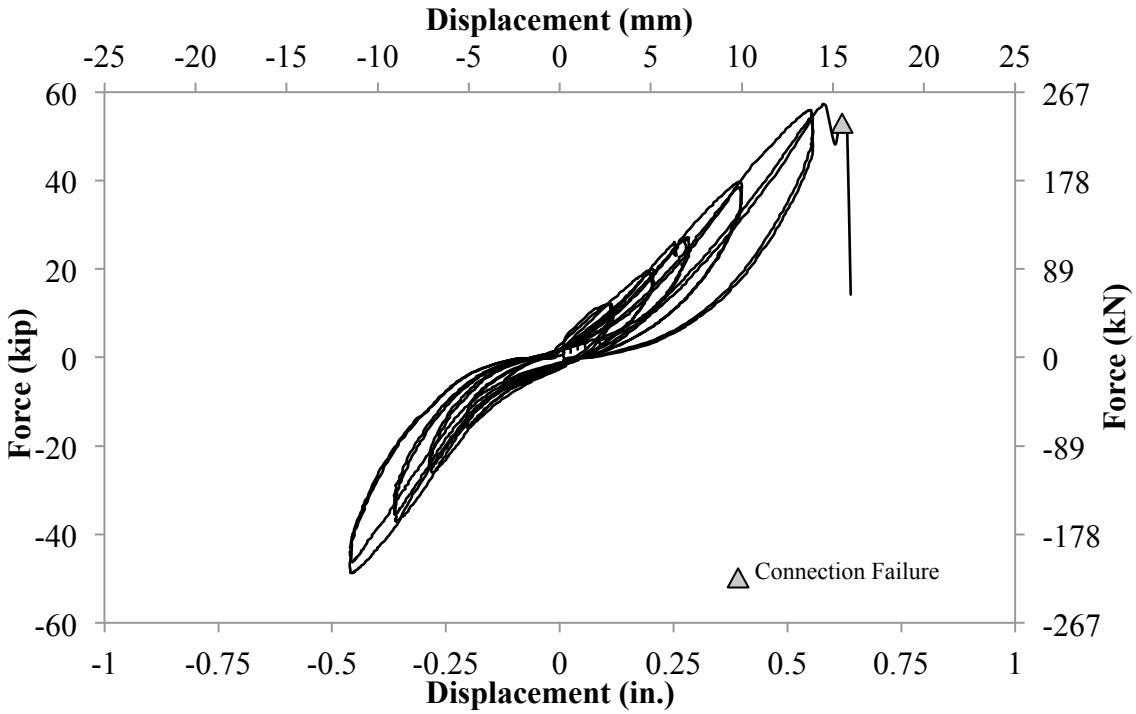

Figure 4.37 – Test #6 hysteresis.

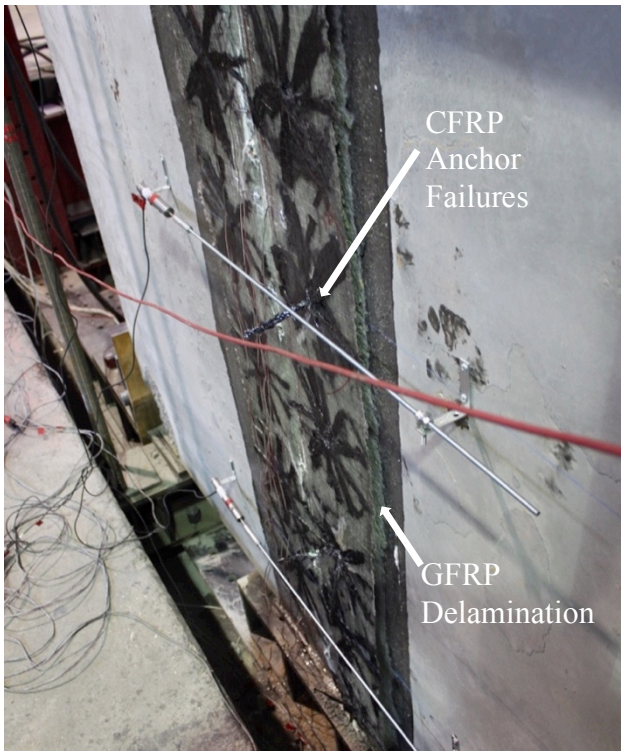

Figure 4.38 – Test #7 connection failure.

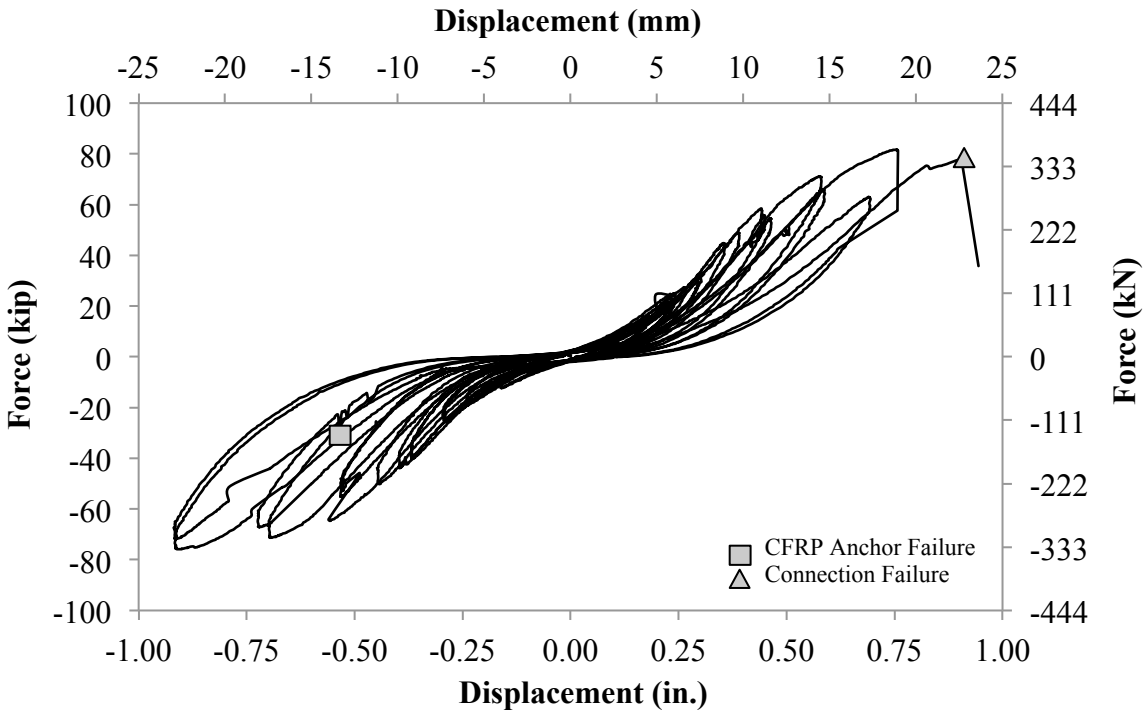

Figure 4.39 – Test #7 hysteresis.

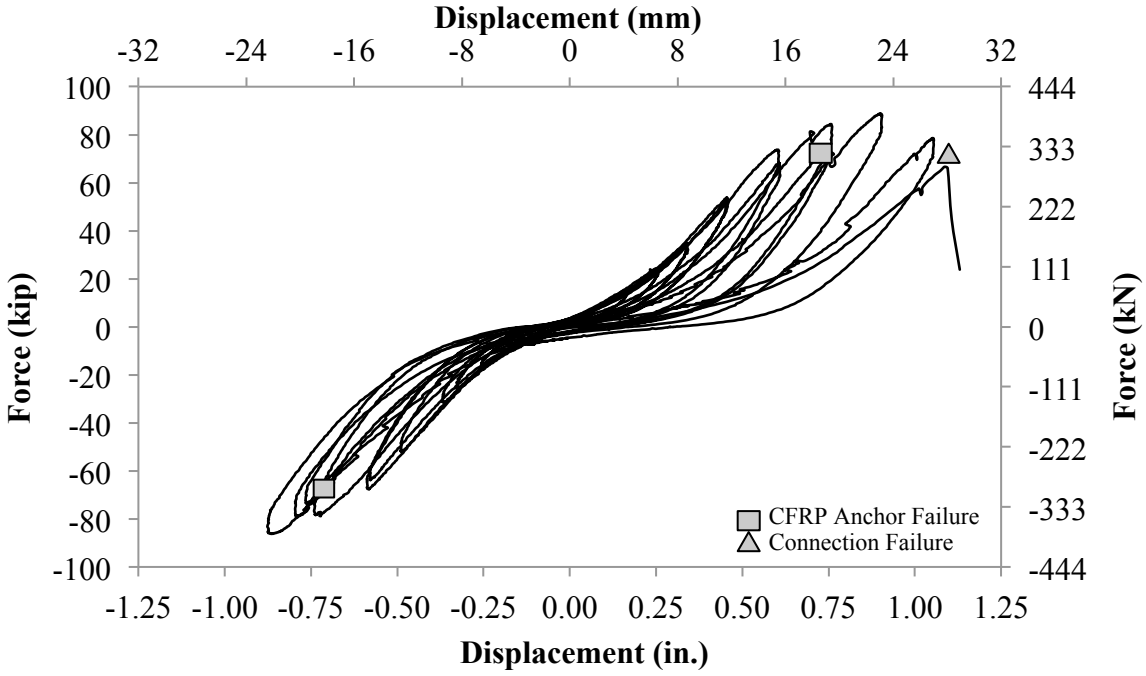

Figure 4.40 – Test #8 hysteresis

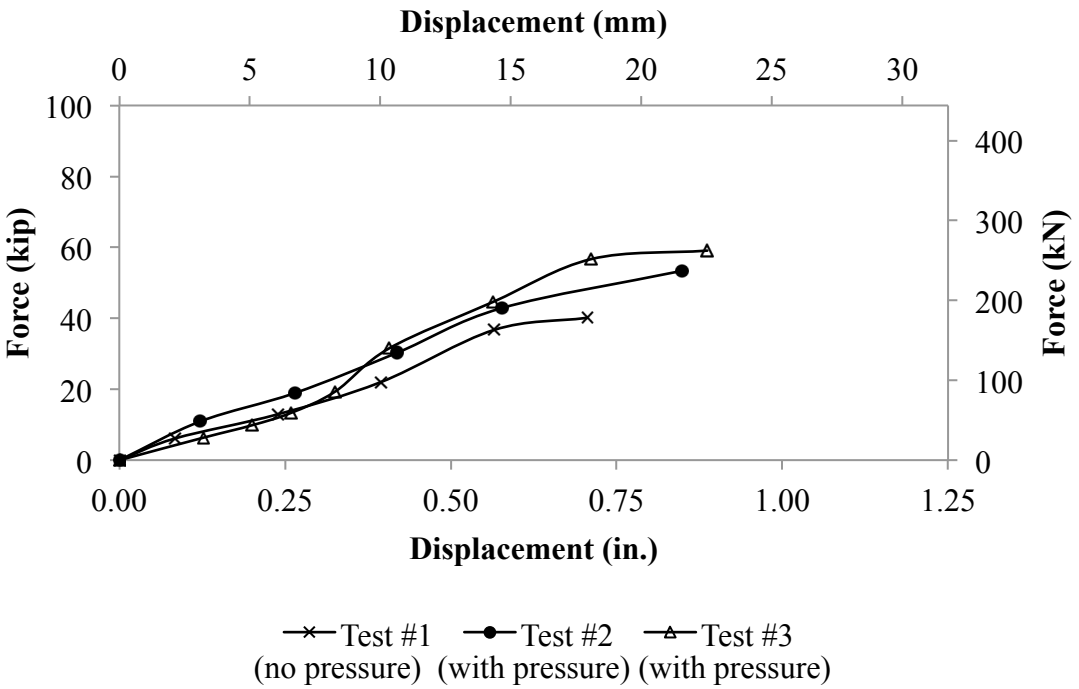

Figure 4.41 – Hysteresis comparing application pressure.

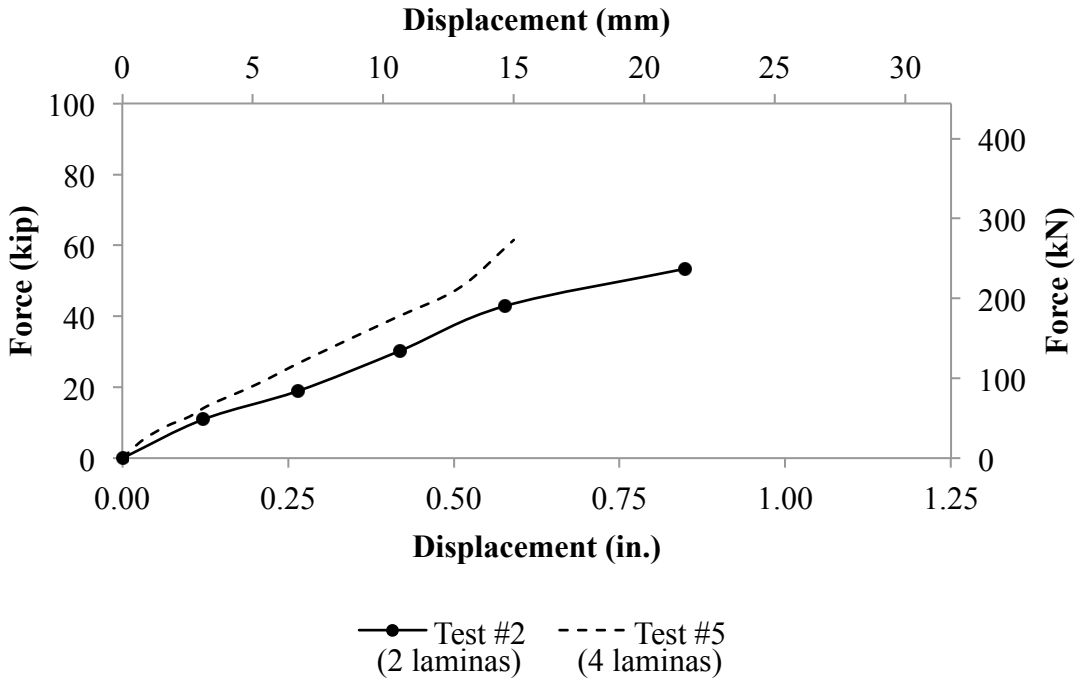

Figure 4.42 – Hysteresis for acid washed tests with two and four GFRP laminas.

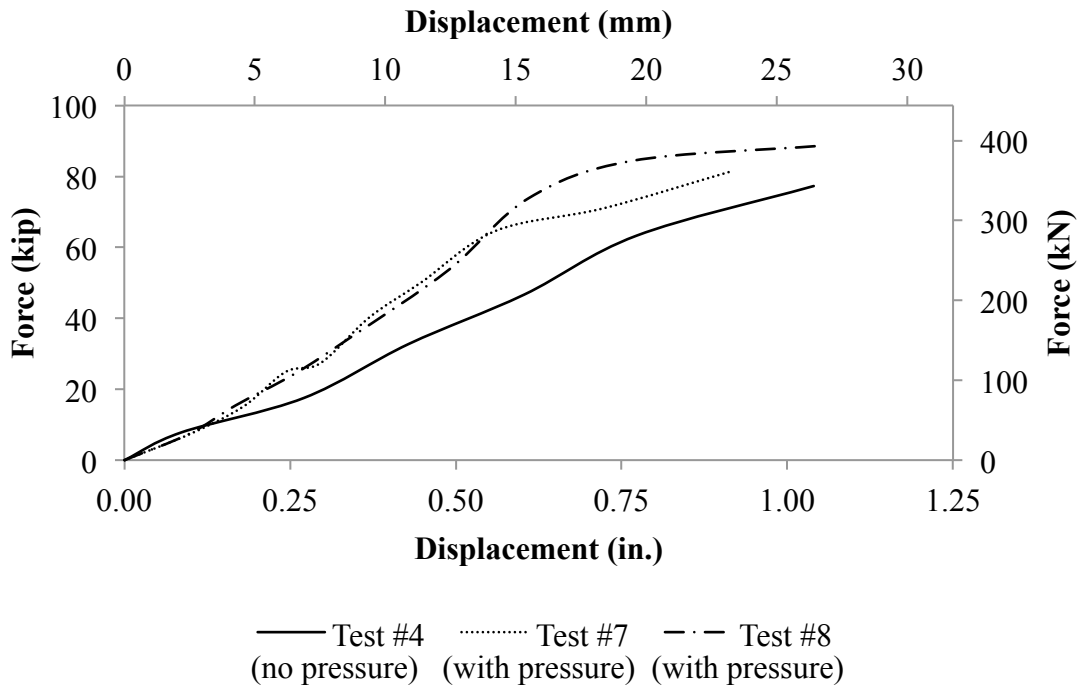

Figure 4.43 – Hysteresis comparing CFRP anchor use.

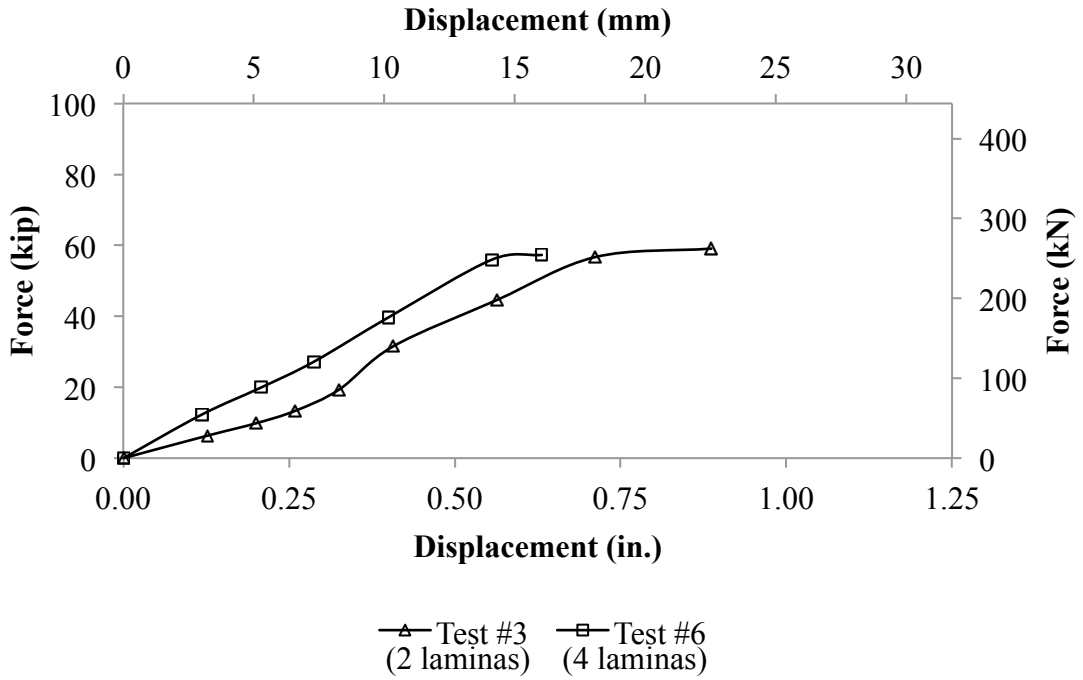

Figure 4.44 – Hysteresis for surface retarder with multiple-pass washed tests with two and four GFRP laminas.

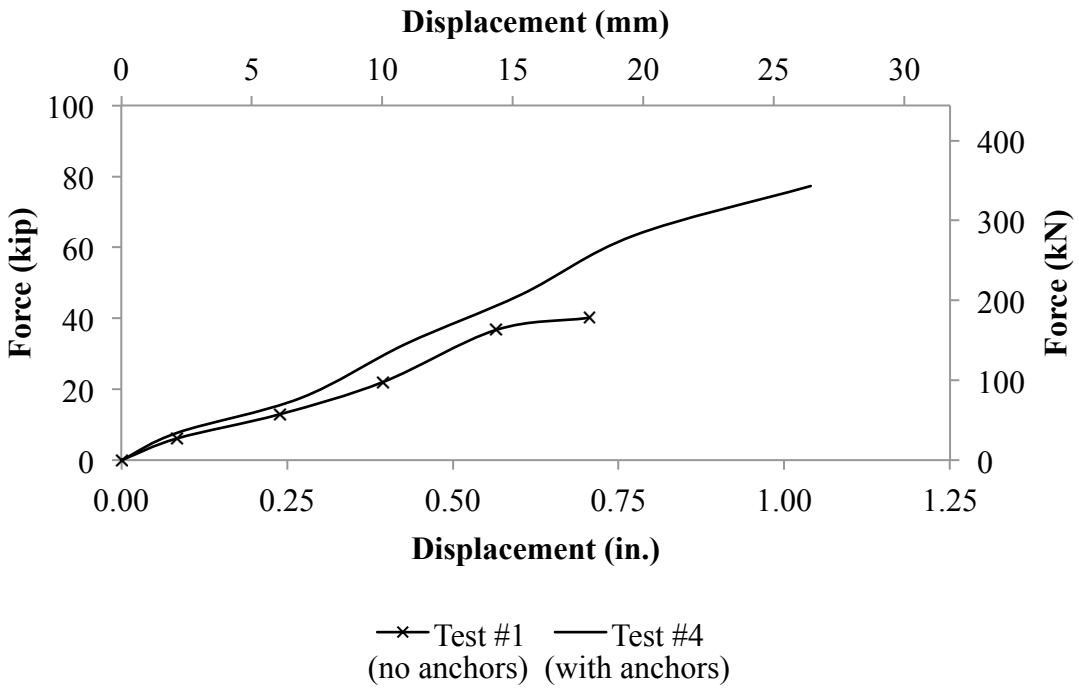

Figure 4.45 – Hysteresis comparing two GFRP laminas and CFRP anchor use.

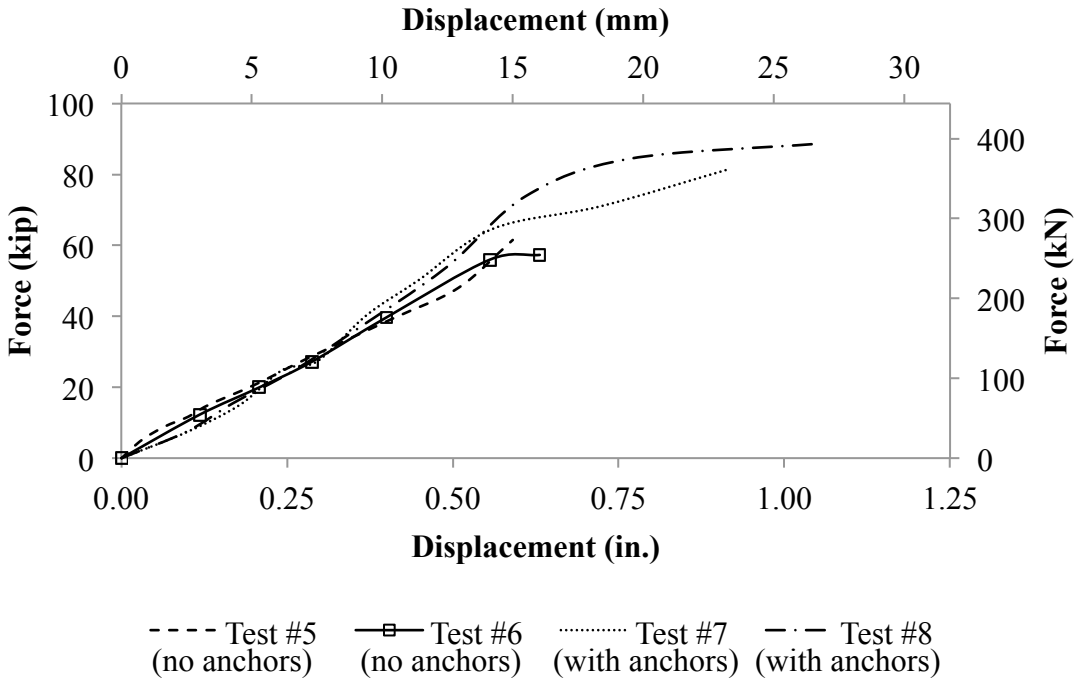

Figure 4.46 – Hysteresis comparing four GFRP laminas and CFRP anchor use.

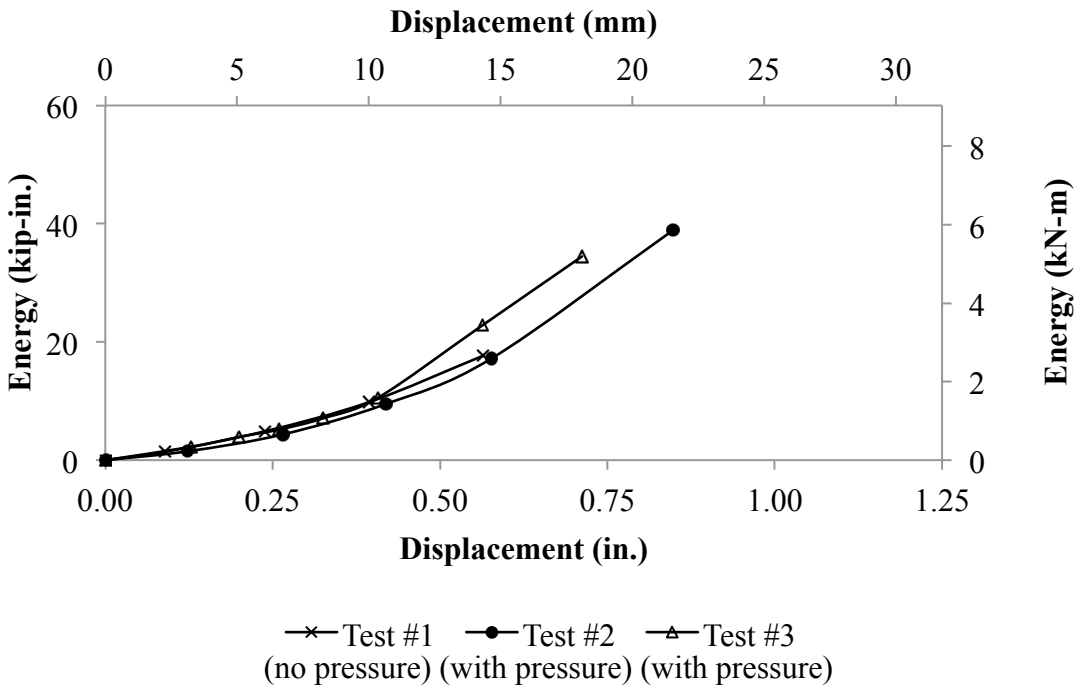

Figure 4.47 – Energy dissipation comparing pressure application.

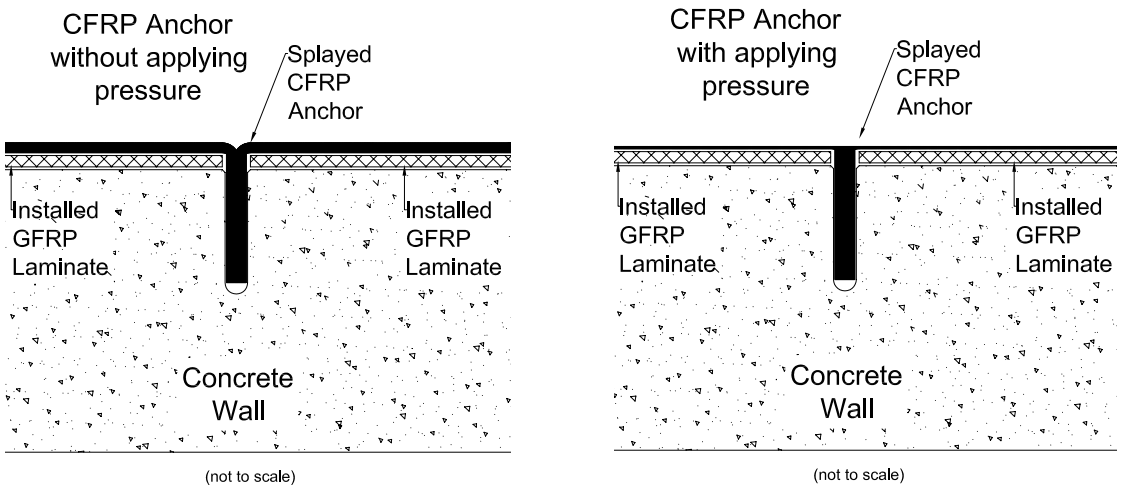

(a) (b)

Figure 4.48 – How pressure potentially damages anchors: (a) without application pressure; (b) with application pressure.

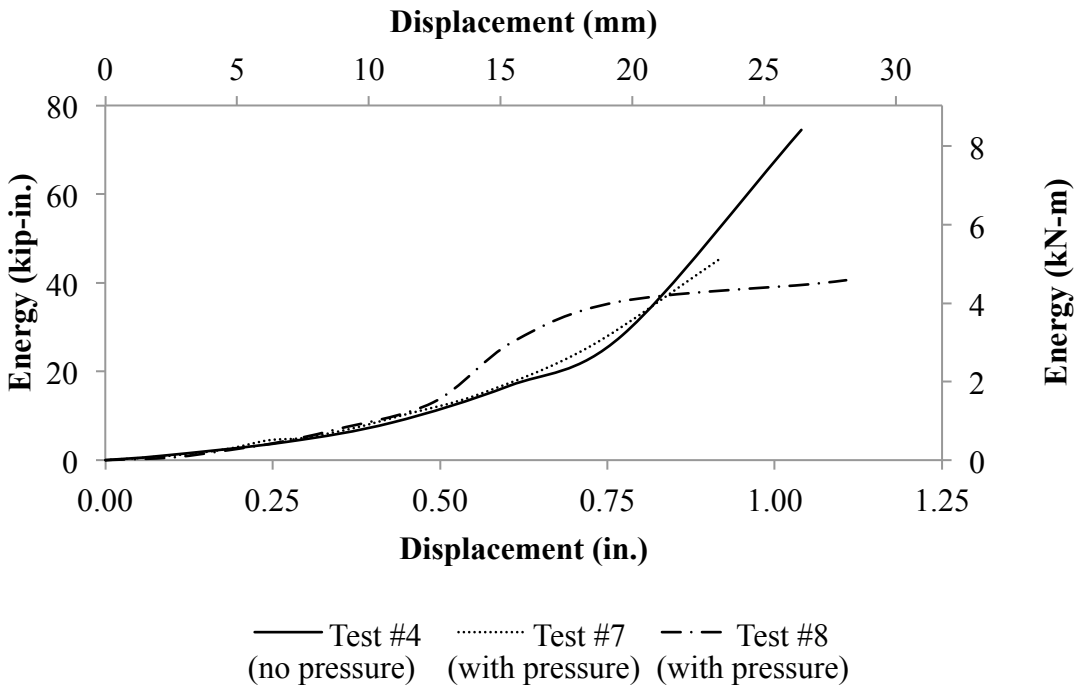

Figure 4.49 – Energy dissipation comparing application pressure when anchors are used.

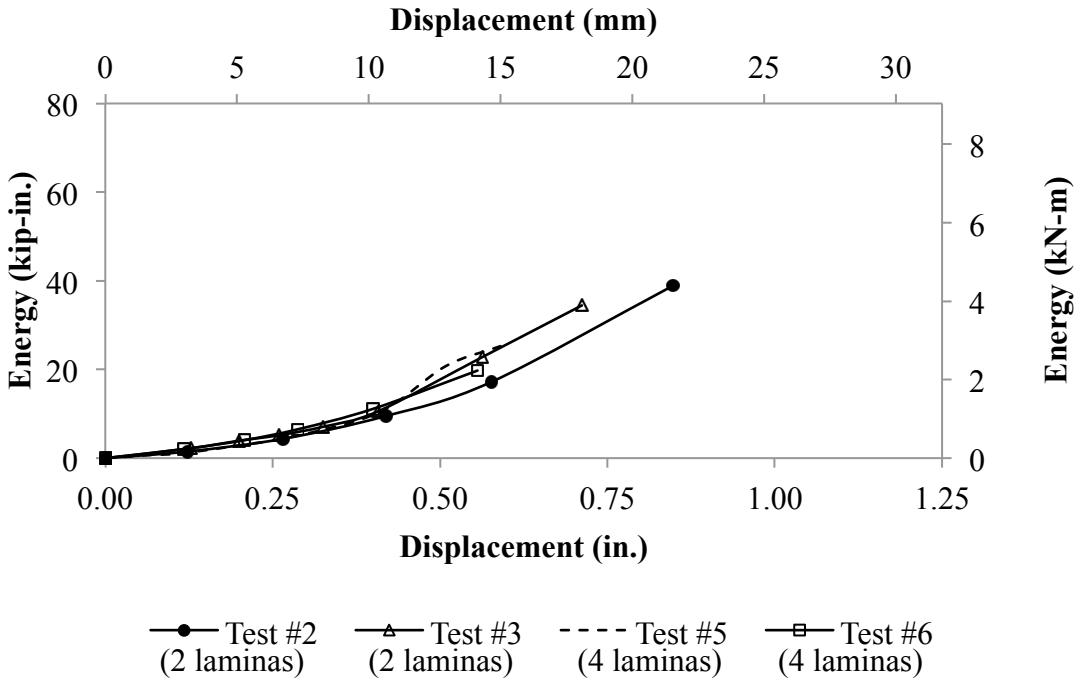

Figure 4.50 – Energy dissipation for two and four GFRP laminas.

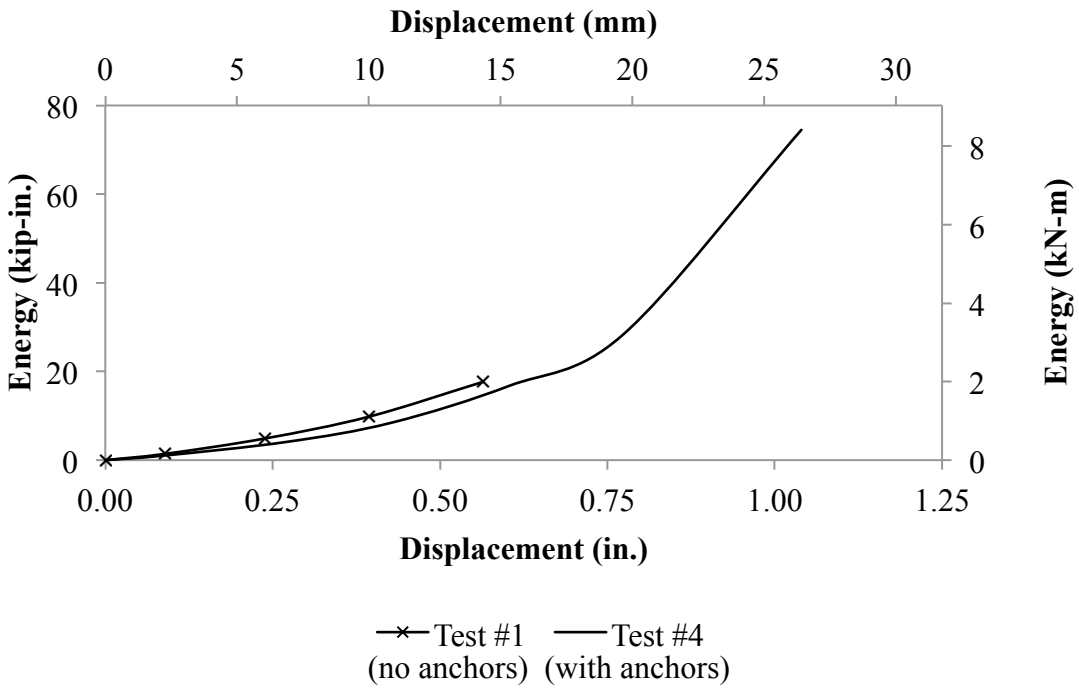

Figure 4.51 – Energy dissipation comparing two GFRP laminas with/without anchors.

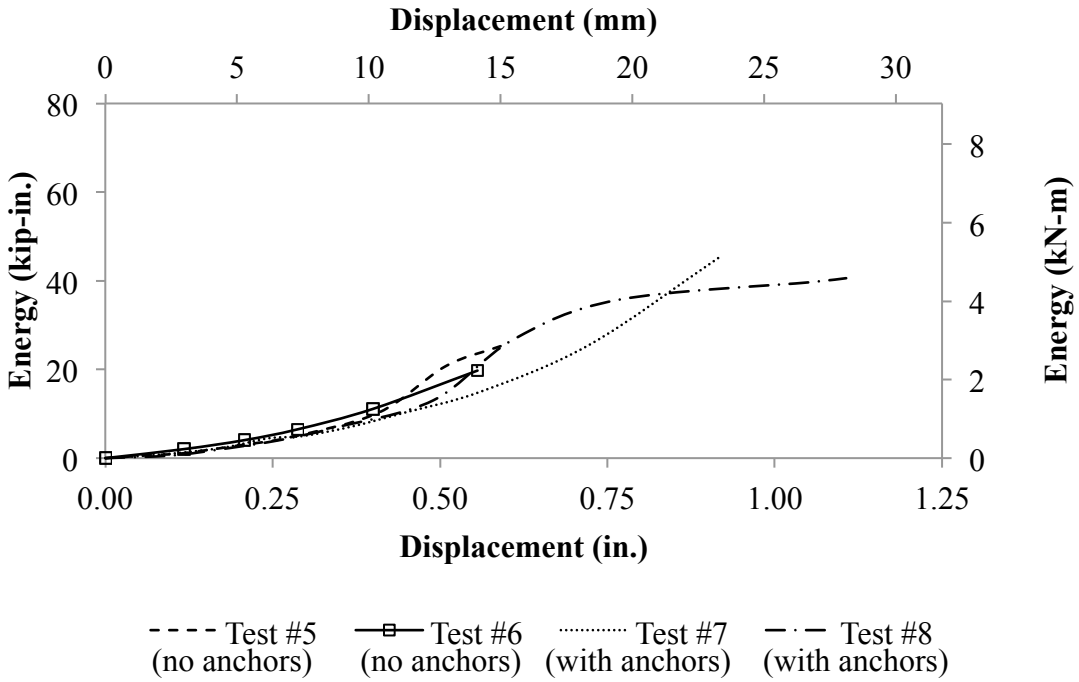

Figure 4.52 – Energy dissipation comparing four GFRP laminas with/without anchors.

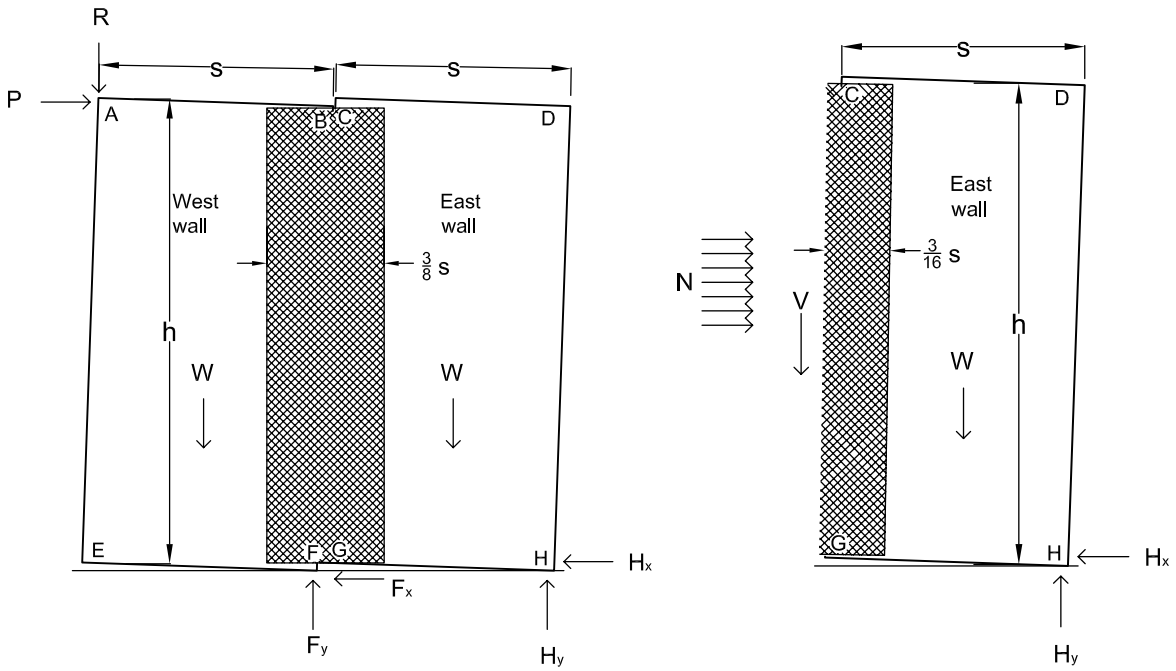

Figure 4.53 – Static analysis of GFRP connection:

(a) two wall panels connected; (b) free-body diagram of east wall.

CHAPTER 5

PERFORMANCE OF BIDIRECTIONAL GFRP CONNECTIONS BETWEEN CONCRETE WALL PANELS UNDER CYCLIC SHEAR

5.1 Introduction

Test specimens were comprised of two erect precast concrete panels side by side connected with one or two laminas of bidirectional GFRP composite. The connection area on each concrete panel was surface prepared by garnet media blasting to ensure a better GFRP to concrete bond. Applying a simulated seismic lateral load at the top of the specimen, and restraining the horizontal and vertical directions, induced cyclic shear in the connection. Six specimens were tested to explore the effects of epoxy-putty adhesive, amount of panel height connected, number of GFRP lamina, and use of GFRP composite anchors. The GFRP composite connection was tested with the purpose of determining shear transfer capabilities across the seam and the seismic performance. Performance of the GFRP connection is determined by the load, displacement, energy dissipation, and shear transfer capacity.

5.2 Testing Program

5.2.1 Test Specimens

One concrete panel has dimensions 4 ft x 8 ft x 8 in. (1.2 m x 2.4 m x 203 mm) as shown in Figure 5.1. Each wall had two 4x4 W4xW4 (102x102 MW25.8xMW25.8)

curtains of steel reinforcement, as shown in Figure 5.1, and corner reinforcement consisting of an 8 x 8 x ½ in. (203 x 203 x 13 mm) steel plate with four welded 12-in. (305 mm) long No. 4 (13M) deformed bar anchor (DBA), as shown in Figure 5.1. Thus, any failure of the specimen was at the GFRP connection.

The erect pair of wall panels was connected using a GFRP composite laminate system. This system includes the application of epoxy resin to the garnet media blasted concrete surface, a thin applied layer of high strength epoxy-putty adhesive, and a wet layup of one or two GFRP lamina of different height. The GFRP composite connections varied based on the presence or absence of a ½ in. (13 mm) gap between the two walls with a 2 in. (51 mm) deep filling of that gap with the epoxy-putty adhesive, the height of the GFRP lamina applied to the wall panels, the number of GFRP lamina, and the presence or absence of GFRP anchors. Table 5.1 shows the test matrix.

Test #1 had a varying gap between the two panels caused in construction. The walls were touching in the front and had a ½" (13 mm) gap in the back. The entire height of this gap, or 8 ft. (2.4 m), was filled with the epoxy-putty adhesive extending to a depth of 2 in. (51 mm). Unlike the other walls tested, the adhesive was applied to the backside of the specimen and not directly beneath the GFRP laminate. For comparative purposes, this test will be referred to as having a ½ in. (13 mm) adhesive in between the wall panels. As shown in Figure 5.2, the total height of the seam was covered with a 2 ft. (0.6 m) wide continuous single lamina of bidirectional (±45º) GFRP composite, evenly applied between the two wall panels.

Test #2 was a repeat of Test #1. As will be shown, the GFRP connection in Test #1 did not fail since the load exceeded the capacity of the hydraulic actuator, so the

epoxy-putty adhesive applied in the gap was completely removed by cutting it out with a grinder and the test was repeated and labeled Test #2. As stated previously, this particular set-up had no gap in the front, and is shown as having no epoxy-putty adhesive (and no gap) between the two wall panels. The total height of the seam had a 2 ft. (0.6 m) wide, single lamina bi-directional (±45º) GFRP composite, evenly applied between the two wall panels as shown in Figure 5.3(a) and Figure 5.3(b). This has the same, undamaged, GFRP composite laminate that was applied in Test #1.

Test #3 had a ½ in. (13 mm) uniform gap between the wall panels and the epoxy-putty adhesive between the two wall panels, at the location that the GFRP was applied. Half of the height of this gap, or a total of 4 ft. (1.2 m), was filled with the epoxy-putty adhesive extending to a depth of 2 in. (51 mm). The adhesive was applied in two different areas. Two areas 2 ft (0.6 m) high by 2 ft (0.6 m) wide were connected using two bidirectional GFRP composite lamina (±45º, ±45º), as shown in Figure 5.4(a). Thus, a total of 50% of the height of the seam had two laminas of bidirectional GFRP, evenly applied between the two wall panels as shown in Figure 5.4(b).

Test #4 was a repeat of Test #3 with some modification. As will be shown, the GFRP connection in Test #3 did not fail since the load exceeded the capacity of the hydraulic actuator, so the high-strength epoxy adhesive applied in the gap and the GFRP composite (±45º, ±45º) laminate spanning the two wall panels were reduced by half, as shown in Figure 5.5(a) and Figure 5.5(b). The 2 ft (0.6 m) by 2 ft (0.6 m) GFRP connections were cut with a grinder down to the concrete surface, both horizontally and vertically through the adhesive-filled seam; effectively reducing the GFRP connection area by half. The test was repeated and labeled Test #4. Thus, Test #4 had a quarter of the

height of the specimen with adhesive in the seam at a depth of 2 in. (51 mm) in two different areas; in addition, 25% of the height or 2 ft (1.2 m) of the seam had two bidirectional GFRP composite laminas that were 2 ft (1.2 m) wide, evenly applied between the two wall panels. This has the same, undamaged, GFRP composite laminate that was applied in Test #3.

Test #5 did not have a gap or epoxy adhesive between the two wall panels and there was concrete-to-concrete contact for the entire height of the seam. Two bidirectional GFRP composite laminas (±45º, ±45º), that were 2 ft (1.2 m) wide, connected 25% of the height of the seam, as shown in Figure 5.6(a). This was accomplished by applying the GFRP in two different locations over the seam, as shown in Figure 5.6(b).

Test #6 had a similar GFRP layup to Test #5, as shown in Figure 5.7(a), differing in the application of GFRP anchors as shown in Figure 5.7(b). Four holes, with a 3/8 in. (9.5 mm) diameter, were predrilled in the concrete wall panels to a depth of 3 in. (76 mm) and 3/8 in. (9.5 mm) diameter GFRP composite anchors were inserted (one on each side of the wall seam per connection) to a depth of 3 in. (76 mm). The anchor was splayed with an 8 in. (203 mm) diameter between the first and second bidirectional GFRP composite laminas (±45º, (splayed anchor), ±45º).

5.2.2 Material Properties

The welded wire mesh (WWM) curtains and four steel plates with welded DBA were 60,000 psi (413,685 kPa) mile steel. The concrete was a structural mix with a design 28-day compressive strength of 10,000 psi (68,950 kPa). Table 5.2 shows the concrete mix design.

The GFRP composite used was V-Wrap™ EG50-B bidirectional fiber fabric with fibers oriented in the ±45° directions. Using a two-part epoxy resin and a two-part high-strength structural epoxy-putty adhesive, a system is formed using the following steps: (i) prime the concrete surface with epoxy resin (Figure 5.8), (ii) apply epoxy-putty adhesive to the primed surface (Figure 5.9), and (iii) wet lay-up GFRP laminas (Figure 5.10). The manufacturer's cured GFRP composite laminate properties are shown in Table 5.3, and the cured epoxy-putty adhesive properties are shown in Table 5.4.

5.2.3 Test Set-up

Specimens consisting of two erect concrete wall panels joined with a GFRP composite connection were subject to simulated seismic loads. The seismic, or cyclic, load was applied using a 150 kip (222 kN) hydraulic actuator near the top of the two walls through two W8x31 (W200x46) steel beams connected with two HSS 4x8x3/8 in. (HSS 102x20x9.5 mm) steel tubes, serving as a yoke; this allowed specimens to undergo horizontal cyclic motion. The system was constrained horizontally by steel blocking, near the base, constructed out of W10x100 (W250x149) steel sections, 1 in. (25 mm) thick steel plates, and ½ in. (13 mm) thick triangular-shaped steel plates. Vertical constraint was introduced using W10x100 (W250x149) steel box sections and four vertical 1 in. (25 mm) diameter steel all thread rods located near the outside extremity of each wall; when these constraints are engaged, a shear force is introduced in the GFRP composite connection. The test set-up is shown in Figure 5.11.

5.2.4 Loading Protocol

A cyclic quasi-static horizontal load was applied to the wall system using displacement control. The displacement was increased by 0.25 in. (6.4 mm) after two

cycles of motion, as shown in Figure 5.12. The rate at which the cyclic force was applied was 1.2 in./min. (30 mm/min.). After two cycles, a pause was programmed into the loading protocol in order to evaluate damage to the GFRP composite connection.

5.2.5 Instrumentation

Displacement was measured with linear variable differential transducers (LVDTs) and string pots. Two LVDTs were externally mounted to the lower west and lower east external sides of the wall setup to measure horizontal displacements. Two string pots were mounted horizontally to the upper west and upper east external sides of the wall setup to measure horizontal displacements. Two string pots were mounted vertically to the upper west and upper east interior sides of the wall setup to measure vertical displacements. The force was measured by a load cell that was in-line with the hydraulic actuator at the upper west external side of the test set-up. Specimen instrumentation is also shown in the test set-up of Figure 5.11.

5.3 Test Results

5.3.1 Introduction

For each tested specimen, the horizontal force versus horizontal displacement hysteresis is presented. A comparison of the hysteretic behavior and energy dissipation are compared among the tests. Static analysis to determine shear in the connection is presented. String pots above each specimen measured negligible displacements before failure and are not reported herein.

5.3.2 Results

The connection performance in terms of horizontal load, horizontal deflection, horizontal drift, and failure mode are presented for each specimen in Table 5.5. Modes of failure included no failure and progressive delamination with and without fiber failure.

Test #1 had a single bidirectional lamina of continuous GFRP composite (±45°) extending over the full seam height and epoxy-putty adhesive in the full seam height on the back side. The system reached a horizontal load of 137 kips (609 kN) and a horizontal displacement of 0.93 in. (24 mm), as shown in the hysteresis curve of Figure 5.13. There was no sign of impending delamination or failure at this load and displacement. The load reached during the test was close to the maximum capacity of the actuator of 150 kips (667 kN), and the test was terminated. This hysteresis curve was utilized to create a hysteretic energy dissipation curve and to compare the load-displacement performance to the remaining tests. After the test was terminated, the epoxy-putty adhesive was removed from the back side seam with a grinder, as shown in Figure 5.14(a) and Figure 5.14(b), and the test was repeated as Test #2.

Test #2 had the same, undamaged, laminate of GFRP composite of Test #1 but with no epoxy-putty adhesive in the wall seam. The two concrete panels were in contact for the entire height of the seam on the front side underneath the composite connection. The system had a horizontal load capacity of 147 kips (654 kN) and a horizontal displacement capacity of 1.49 in. (38 mm), as shown in the hysteresis curve of Figure 5.15. Initial delamination, in the form of 45° shear bands, occurred at a load of 135 kips (601 kN) and a deflection of 1.24 in. (32 mm), as shown in Figure 5.16(a). Progressive delamination transpired until failure, shown in Figure 5.16(b).

Test #3 had two bidirectional laminas of intermittent GFRP composite (±45°, ±45°) extending over half of the seam height and epoxy adhesive in the seam behind the GFRP laminate. The system had a horizontal load of 141 kips (627 kN) and a horizontal deflection of 1.79 in. (46 mm), as shown in the hysteresis curve of Figure 5.17. There was insignificant delamination at this load and displacement. The maximum load reached during the test was close to the maximum capacity of the actuator of 150 kips (667 kN), and the test was terminated. This hysteresis curve was utilized to create a hysteretic energy dissipation curve and to compare the load-displacement performance to the remaining tests. After the test was terminated, the epoxy-putty adhesive and the GFRP laminate coverage was reduced by half with a grinder, as shown in Figure 5.18(a) and 5.18(b), and the test was repeated as Test #4.

Test #4 had the same two bidirectional laminas of the intermittent GFRP composite laminate from Test #3 but reduced to cover 25% of the seam height with epoxy-putty adhesive behind the laminate in the wall seam. The system had a horizontal load capacity of 118 kips (525 kN) and a horizontal displacement capacity of 1.34 in. (34 mm), as shown in the hysteresis curve of Figure 5.19. Initial delamination, in the form of 45° shear bands, occurred at a load of 90 kips (400 kN) and a displacement of 1.14 in. (29 mm), as shown in Figure 5.20(a). Progressive delamination transpired until failure, shown in Figure 5.20(b).

Test #5 had two bidirectional laminas of continuous GFRP composite covering 25% of the seam height and no epoxy adhesive in the wall seam. The two concrete panels were in contact for the entire height of the seam. The system had a horizontal load capacity of 58 kips (258 kN) and a horizontal displacement capacity of 1.53 in. (39 mm),

as shown in Figure 5.21. Initial delamination occurred at a load of 58 kips (258 kN) and a displacement of 0.58 in. (15 mm), and is shown in Figure 5.22(a). Although Test #5 experienced progressive delamination, the connection never completely delaminated but rather remained attached at the connection extreme boundaries; the GFRP composite experienced contortion between the two bonded portions of the laminate. The contortion created shear failure in the GFRP matrix and fibers, as shown in Figure 5.22(b) and Figure 5.22(c).

Test #6 had a similar connection system as that of Test #5, but the connections were enhanced with four GFRP composite anchors. The system had a horizontal load capacity of 87 kips (387 kN) and a horizontal displacement capacity of 2.13 in. (54 mm), as shown in the hysteresis curve of Figure 5.23. Initial delamination occurred at a load of 43 kips (191 kN) and a displacement of 0.45 in. (11 mm), as shown in Figure 5.24(a) and 5.24(b). Although Test #6 experienced progressive delamination from the seam to the outside boundary, the connection never completely delaminated. The GFRP composite laminate remained attached at the connection extreme boundaries and at the centers of the GFRP anchors, as shown in Figure 5.24(c) and Figure 5.24(d). The GFRP anchors allowed the connection to withstand larger displacements than those observed in the other tests. In the same manner as Test #5, the laminate eventually fractured at 87 kips (387 kN), as shown in Figure 5.25.

5.3.3 Hysteresis Summary Curves

The hysteretic envelope shows the horizontal load and horizontal displacement for each cycle. These curves are significant in determining the capacity of each connection. The following connection comparisons are presented: (i) walls with 25% of seam height

connected, (ii) walls without a gap (concrete-to-concrete contact), and (iii) walls where the seam was filled with epoxy-putty adhesive.

When 25% of the seam height is connected with GFRP (±45º, ±45º), Test #4 with the ½ in. (13 mm) adhesive-filled seam resisted the highest lateral load as shown in Figure 5.26. The advantage of using the epoxy-putty adhesive in the seam is due to its strong tensile and compressive strength and excellent adhesion to concrete. However, Test #5 without the adhesive in the seam but with the GFRP anchors reached a higher displacement than Test #4. Comparing Test #5 directly to Test #6, it is shown that GFRP anchors not only increase the load but also the displacement, as shown in Figure 5.26. In Tests #5 and #6 the connection was able to reach the initial delamination load due to sufficient area of bonded GFRP laminate to concrete. Tests #5 and #6 did not have epoxy-putty adhesive in the seam between the walls and thus had concrete-to-concrete contact. In comparing these tests, it is seen that a larger area of GFRP coverage increased the displacement and load as shown in Figure 5.27 for Test #2.

Although Tests #1 and #3 did not fail, their hysteresis summary is shown in Figure 5.28 and is compared with the other test where there was a ½ in. (13 mm) adhesive-filled seam up to a depth of 2 in. (51 mm) (Test #4). These three tests performed expected with increasing load and displacement from an increasing amount of GFRP coverage, as seen in Figure 5.28.

5.3.4 Energy Dissipation Curves

Energy dissipated versus horizontal displacement for each cycle is plotted to show a summary of energy dissipation for each connection. Energy dissipation is also significant in determining the capacity of each connection for seismic applications. The

following connection comparisons are presented: (i) walls with 25% of seam height connected, (ii) walls without a gap (concrete-to-concrete contact), and (iii) walls where the seam was filled with epoxy-putty adhesive.

Figure 5.29 shows that when 25% of the seam height is connected with GFRP (±45º, ±45º), the connection with GFRP anchors dissipated the most energy (Test #6). The next highest dissipation of energy is when epoxy adhesive was used in the seam (Test #4), as shown in Figure 5.29.

Test #5 and #6 did not have a gap between the walls, and thus had concrete-to-concrete contact. Figure 5.29 shows that 25% seam coverage with two bidirectional GFRP laminas and four GFRP anchors (Test #6) dissipated more energy than 25% seam coverage with two laminas but without GFRP anchors (Test #5) and full seam coverage with a single GFRP lamina (Test #2). A 25% GFRP seam coverage (two laminas) without GFRP anchors dissipated more energy than full seam coverage with a single GFRP lamina, as shown in Figure 5.30.

Although Test #1 and #3 did not fail, the energy dissipated is shown and compared with the other test where the ½ in. gap was filled with high-strength epoxy-putty adhesive (Test #4). Figure 5.31 shows that a 50% GFRP seam coverage with two laminas (Test #3) dissipated more energy than both the 25% seam coverage with two laminas (Test #4) and a full seam coverage with one lamina (Test #1). This higher energy dissipation is likely due to the small amount of delamination that occurred during testing.

5.3.5 Shear Transfer

The shear transferred between the two walls was determined for the specimens of Test #5 and Test #6. The wall systems for Test #1 and Test #3 exceeded the 150 kip (667 kN) hydraulic actuator capacity, thus, the shear transfer for these tests could not be determined. The specimens of Test #2 and Test #4 had epoxy-putty adhesive in the seam and shear transfer was influenced significantly, but the participation from the GFRP laminate is unknown. Figure 5.32 shows an idealization of the wall system for Test #5 and Test #6, with the applied lateral load denoted as *P*. The vertical constraint provided by the all-thread rods is denoted as *R*; this force was measured during the tests using strain gauges. Under this system of loads and constraints, the reactions are shown as F_x and F_y on the west wall panel at corner *F* and H_x and H_y on the east wall at corner *H*. Equilibrium of the wall system in Figure 5.32(a) results in the following:

$$F_y = 2(R + W) - P\left(\frac{h}{s}\right) \tag{5.1}$$

$$H_y = P\left(\frac{h}{s}\right) - R \tag{5.2}$$

$$H_x + F_x = P \tag{5.3}$$

where *W* is the weight of one wall panel (3.2 kip (14 kN)), *h* is the wall panel height and *s* is the wall panel width. Equilibrium of the free-body diagram of the east wall in Figure 5.32(b) results on the value of the shear resisted by the GFRP composite connection as:

$$V = P\left(\frac{h}{s}\right) - (R + W) \tag{5.4}$$

$$N = H_x \tag{5.5}$$

where *V* is the shear in the GFRP composite connections and *N* is the distributed horizontal reaction from the concrete-to-concrete interaction. The unit shear, in force per

length, at the GFRP composite connection, v, is given as:

$$v = \frac{V}{(h/4)} \tag{5.6}$$

Using these equations, the unit shears at failure in the GFRP connections are obtained, as shown in Table 5.6. The unit shear at failure in the GFRP connections of Test #5 was 28 kip/ft (409 kN/m). By contrast the unit shear in the GFRP connections of Test #6 with GFRP composite anchors was 42 kip/ft (613 kN/m) at failure. Thus, the connection with GFRP composite anchors resisted 1.5 times the unit shear resisted by an identical composite connection without anchors.

5.4 Summary and Conclusions

5.4.6 Summary

The high-strength epoxy-putty adhesive between the walls increased both the horizontal load and energy dissipation capacity of the connection. The system with 25% seam coverage using two bidirectional GFRP composite laminas and epoxy-putty adhesive in the seam failed at twice the horizontal load capacity and 1.3 times more energy dissipation for the same connections without the adhesive in the seam. The two tests exceeding the capacity of the hydraulic actuator both had the adhesive in the seam.

An increase in the connection strength was observed when a larger percentage of connection height was covered with GFRP composite. The system with full seam height coverage using one bidirectional lamina had a horizontal load capacity of 2.5 times more load and 1.3 times more energy dissipation that the system with 25% seam height coverage using two bidirectional laminas. However, both full seam height coverage using one bidirectional lamina and 25% seam height coverage using two bidirectional laminas had a similar horizontal displacement capacity.

The use of GFRP anchors significantly increased the horizontal load capacity and energy dissipation of the connection. A connection with 25% coverage with two GFRP bidirectional laminas and GFRP anchors increased the horizontal load capacity and shear transfer by 1.5 times more than a similar connection without anchors. Also, a 1.4 times increase in horizontal displacement capacity and double the energy dissipation was seen by the use of GFRP anchors.

5.4.7 Conclusions

The high-strength epoxy-putty adhesive between the walls had a significant effect on the connection system capacity and is recommended for such seismic connection applications. However, the specific impact of the adhesive on hysteretic behavior, energy dissipation, and shear transfer requires further investigation.

The GFRP anchors worked extremely well in improving the hysteretic behavior, shear transfer, energy dissipation, and shear transfer of the system. Another benefit of GFRP anchors is the ability to apply less GFRP laminate. The economical implications should be studied to understand applicability and use.

Table 5.1 – Test matrix

Test	% of Seam Height Connected	*Depth of Adhesive, in. (mm)	GFRP Configuration	†Total GFRP Laminas
1	100	2	(±45º)	1
2	100	N/A	(±45º)	1
3	50	2	(±45º, ±45º)	2
4	25	2	(±45º, ±45º)	2
5	25	N/A	(±45º, ±45º)	2
6	25	N/A	(±45º, ±45º)	2

* Adhesive width is ½ in. (13 mm)
N/A – Not Applied
† 1 = 0.034 in. (0.864 mm); 2 = 0.068 in. (1.728 mm)

Table 5.2 – Concrete mix design

Concrete Materials	Density, lbs/ft^3 (kg/m^3)
Grey Cement	24.07 (385.63)
Flyash Class F	6.04 (96.70)
Fine Aggregate	41.41 (663.28)
Coarse Aggregate	56.48 (904.75)
Water	9.63 (154.25)
High Range Water Reducer	0.25 (4)
Air Entrainment	0.009 (0.148)

Table 5.3 – Cured GFRP lamina properties

Cured Laminate Properties	Average Values
Tensile Strength	89,800 psi (620 MPa)
Modulus of Elasticity	4.6×10^6 psi (18,600 MPa)
Elongation at Break	1.94%
Thickness	0.034 in. (0.864 mm)
Strength per Unit Width	1,527 lbs/in. (0.27 kN/mm)

Table 5.4 – Cured epoxy-putty adhesive properties

Cured Adhesive Properties	Average Values
Tensile Strength	8,800 psi (60.7 MPa)
Tensile Modulus	400,000 psi (2,760 MPa)
Elongation at Break	4.40%
Flexural Strength	13,780 psi (95 MPa)
Flexural Modulus	380,000 psi (2,620 MPa)
Compressive Strength	12,450 psi (85.8 MPa)
Compressive Modulus	387,000 psi (2,670 MPa)

Table 5.5 – Test results

Test	Max. Horizontal Load, kip (kN)	Max. Horizontal Deflection, in. (mm)	Max. Horizontal Drift %	*Failure Mode	Energy Dissipated kip-in. (kN-mm)
1	136.7 (608)	0.99 (25)	1.03	NF	47 (5.3)
2	146.5 (652)	1.49 (38)	1.61	PD	101 (11.4)
3	141.3 (629)	1.85 (47)	1.93	NF	138 (15.6)
4	118.0 (525)	1.34 (34)	1.40	PD; FF	79 (9.0)
5	56.5 (251)	1.53 (39)	1.59	PD; FF	59 (6.7)
6	84.6 (376)	2.13 (54)	2.22	PD; FF	117 (13.3)

* Failure Mode Types:
NF – No Failure
PD – Progressive Delamination
FF – Fiber Failure

Table 5.6 – Shear transfer values

Test	Applied Lateral Load *P*, kip (kN)	Restraining Vertical Force *R*, kip (kN)	Shear *V*, kip (kN)	Unit Shear *v*, kip/ft (kN/m)
2	147 (654)	151 (673)	146 (649)	73 (1,065)
5	58 (258)	63 (278)	57 (252)	28 (414)
6	87 (387)	93 (415)	84 (373)	42 (613)

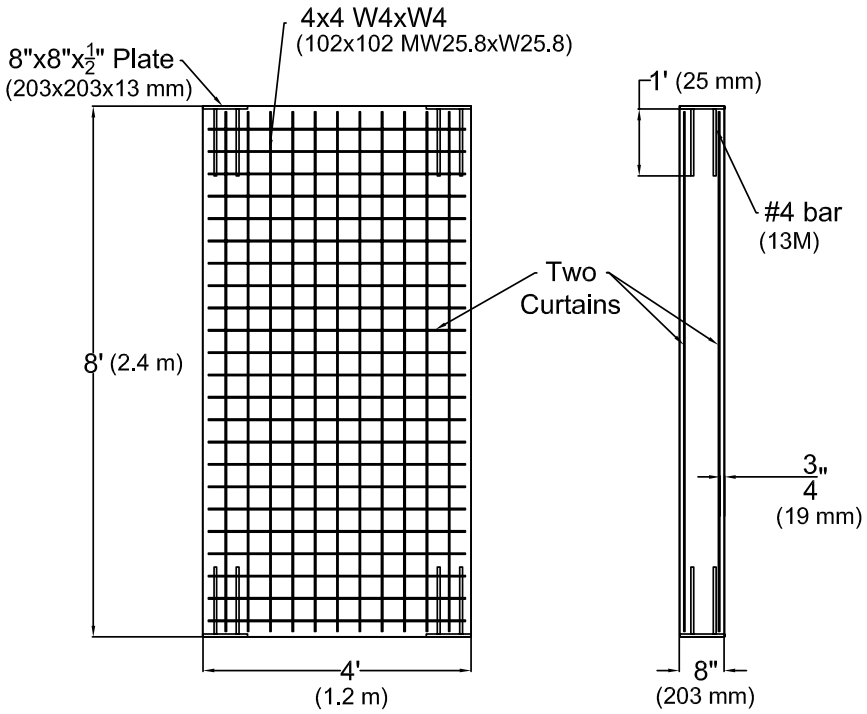

Figure 5.1 – Individual concrete wall panel dimensions and reinforcement details.

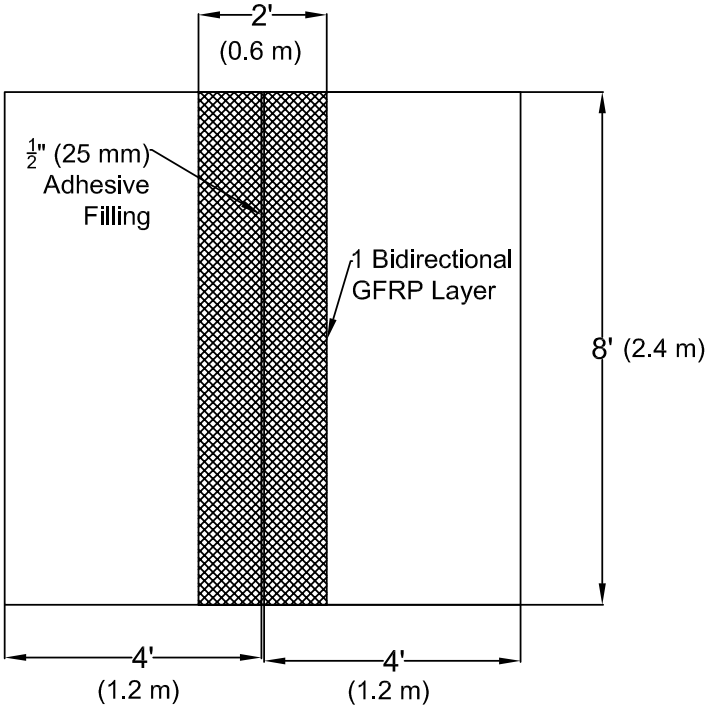

Figure 5.2 – Test #1 details.

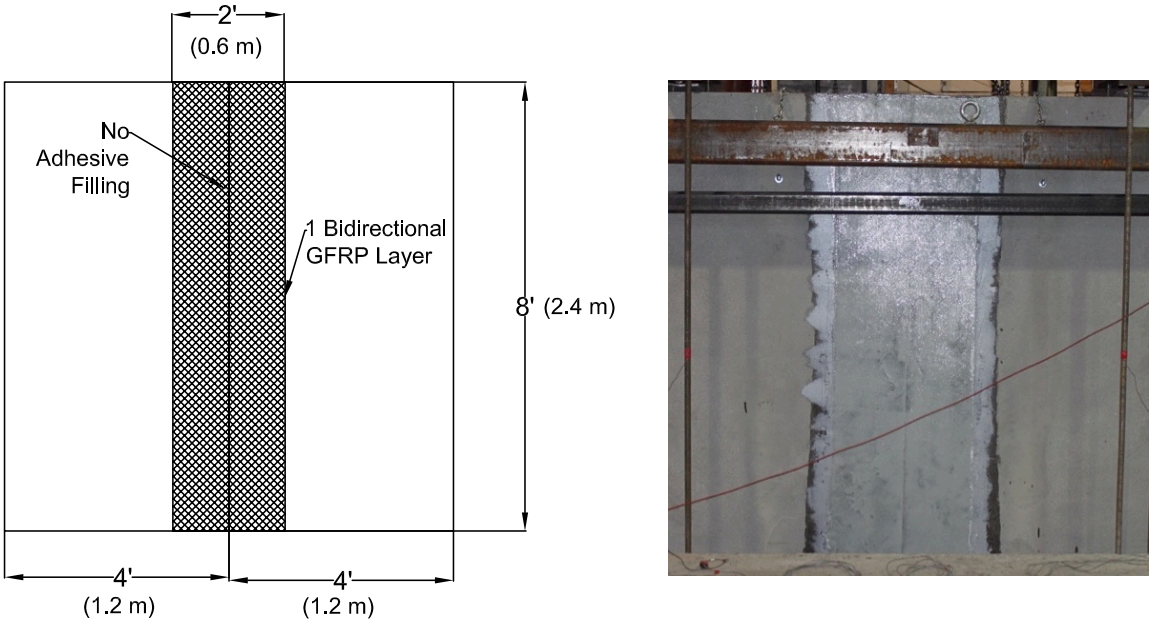

(a) (b)

Figure 5.3 – Test #2: (a) specimen details; (b) test specimen

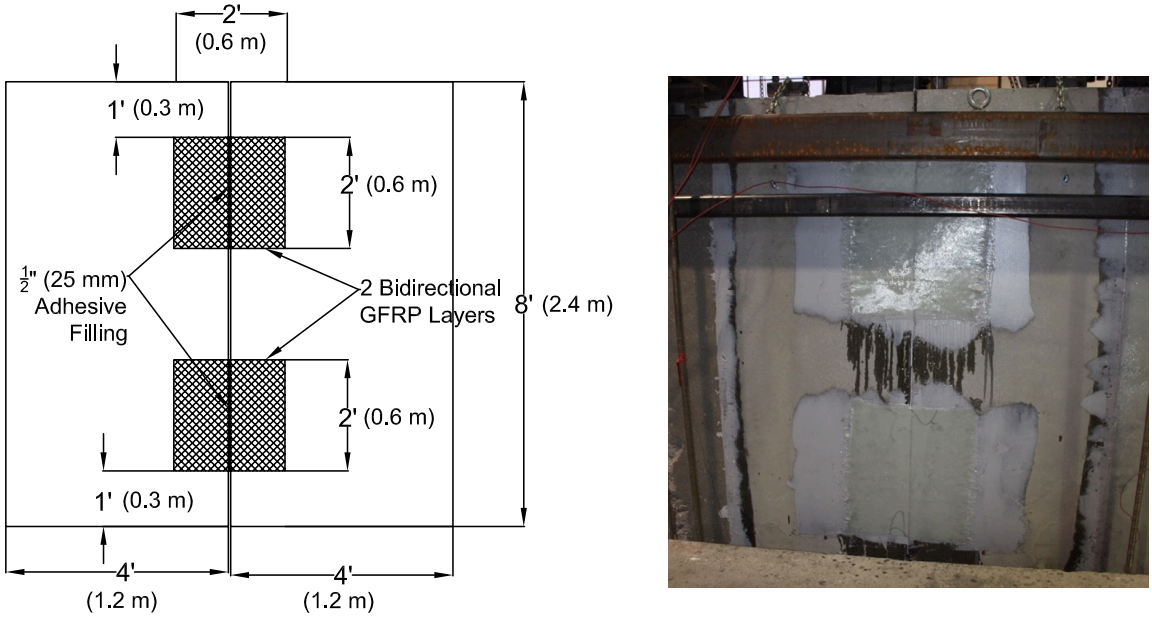

(a) (b)

Figure 5.4 – Test #3: (a) specimen details; (b) test specimen

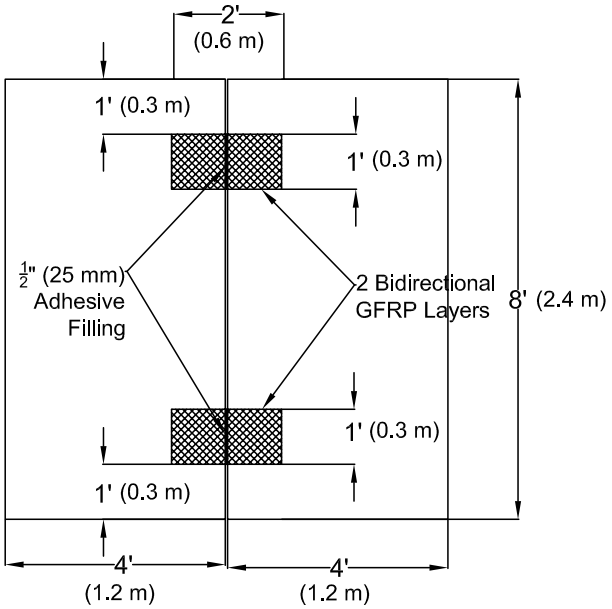

(a) (b)

Figure 5.5 – Test #4: (a) specimen details; (b) test specimen

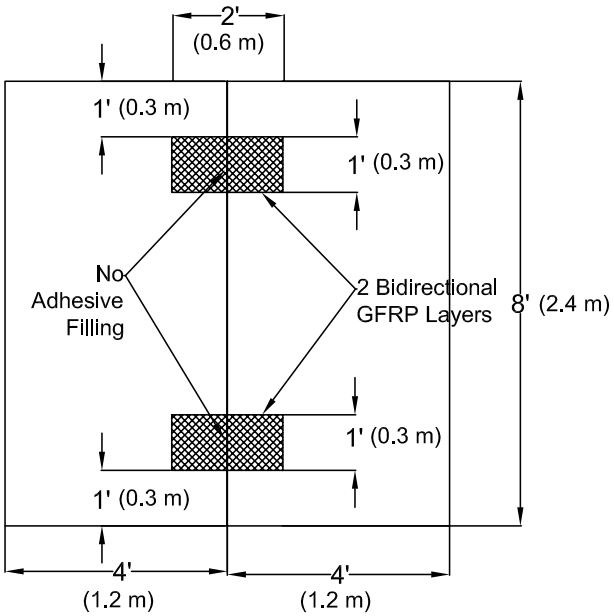

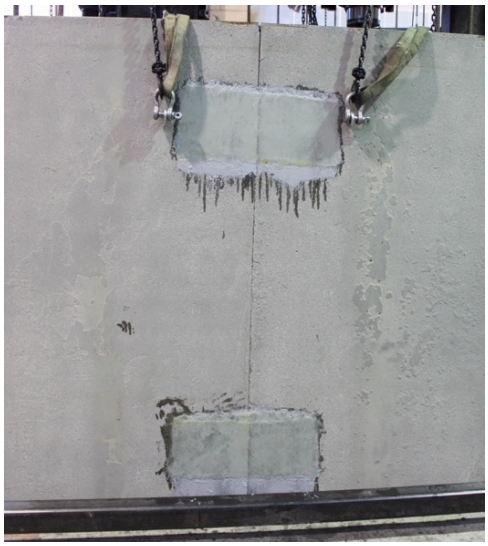

(a) (b)

Figure 5.6 – Test #5: (a) specimen details; (b) test specimen

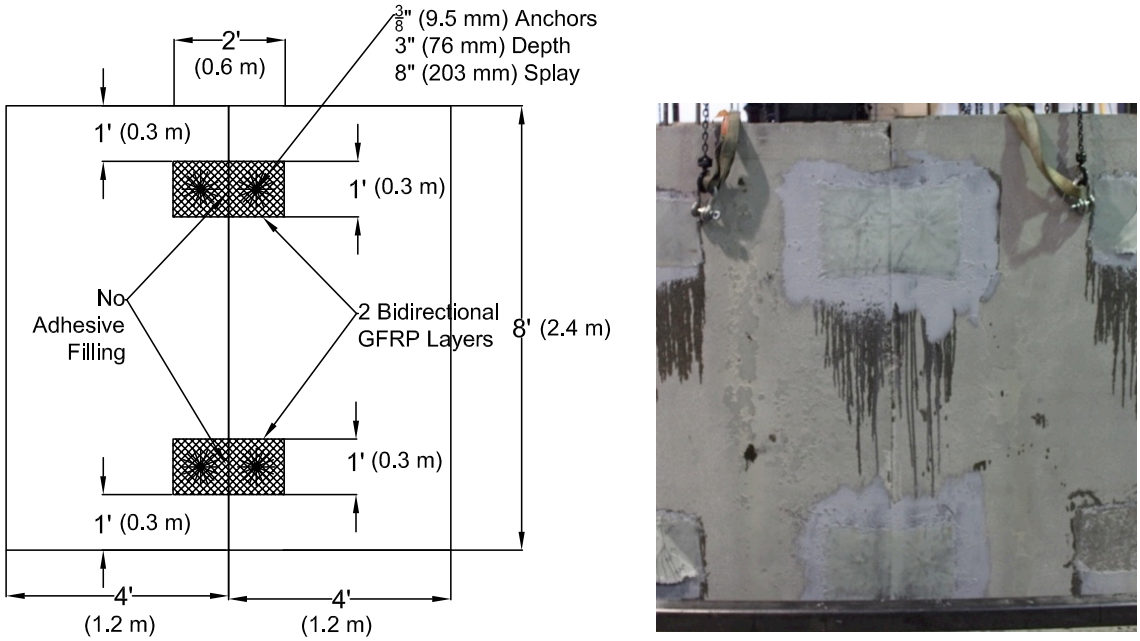

(a) (b)

Figure 5.7 – Test #6: (a) specimen details; (b) test specimen

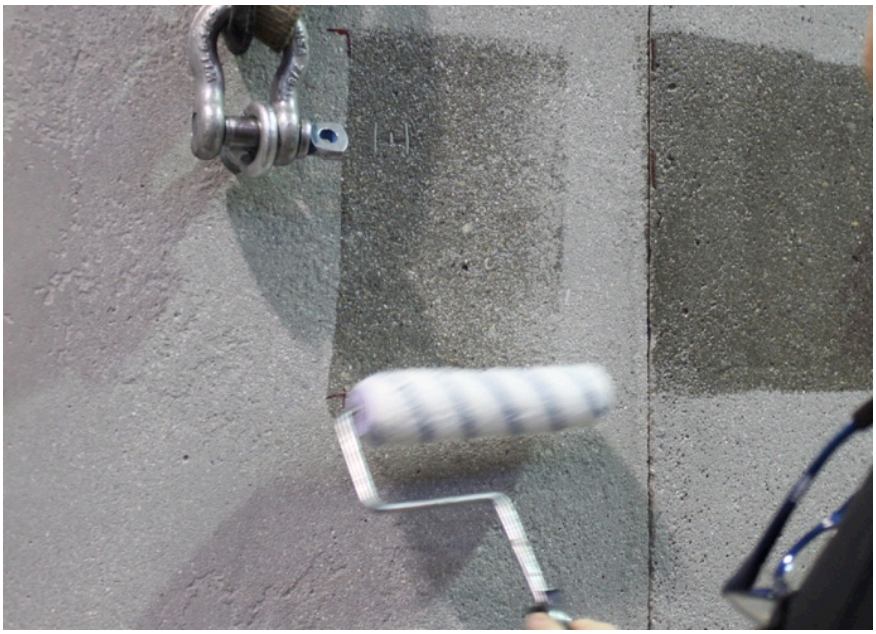

Figure 5.8 – Step 1: Prime concrete surface with epoxy resin.

Figure 5.9 – Step 2: Apply epoxy-putty adhesive to primed surface.

Figure 5.10 – Step 3: Lay-up wet GFRP laminas.

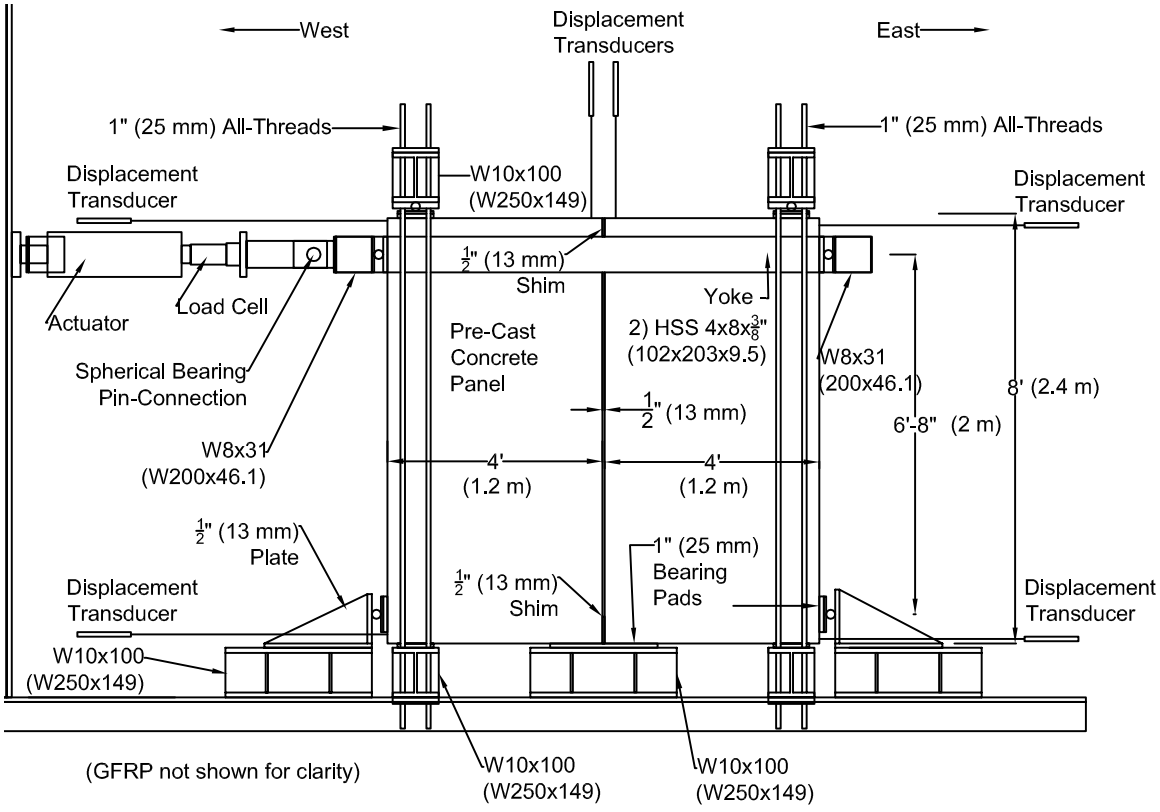

Figure 5.11 – Test set-up.

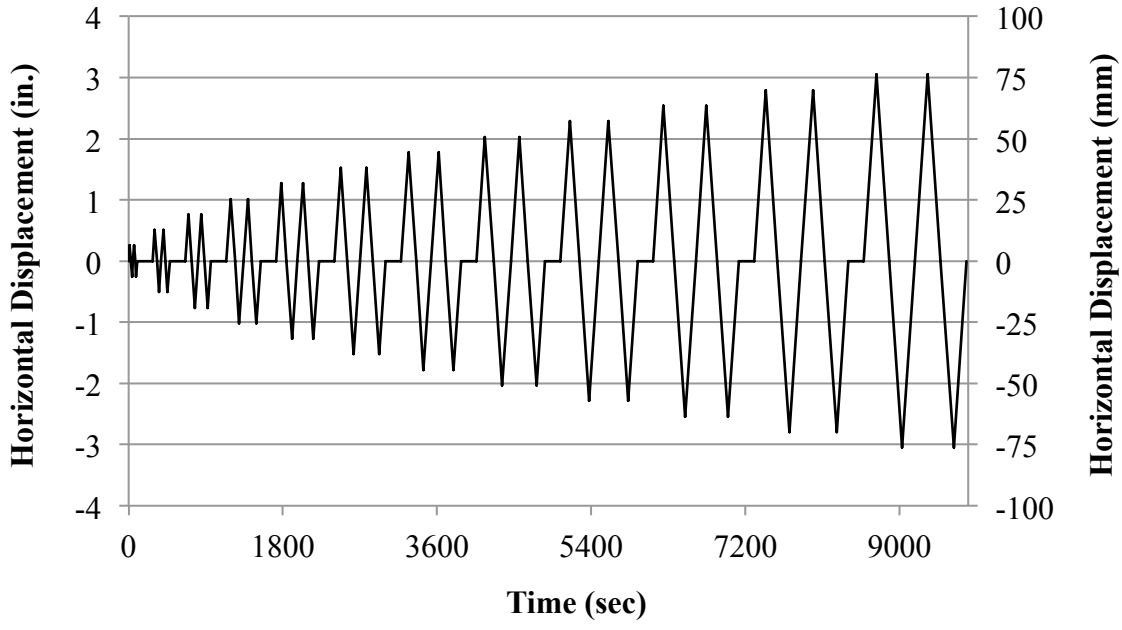

Figure 5.12 – Loading protocol.

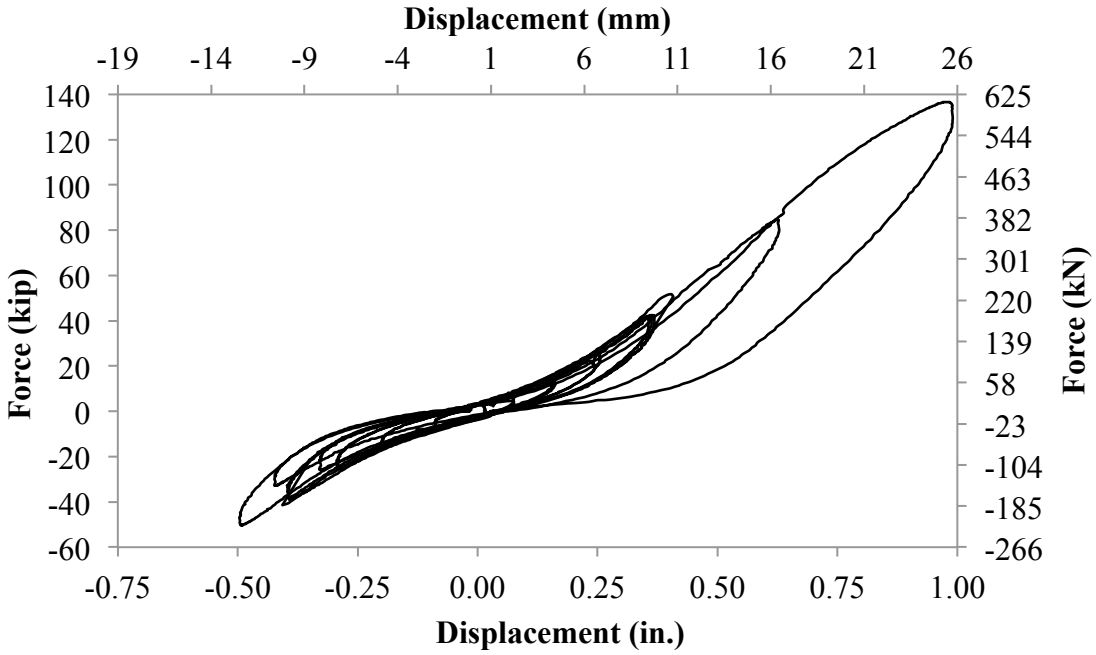

Figure 5.13 – Test #1 hysteresis.

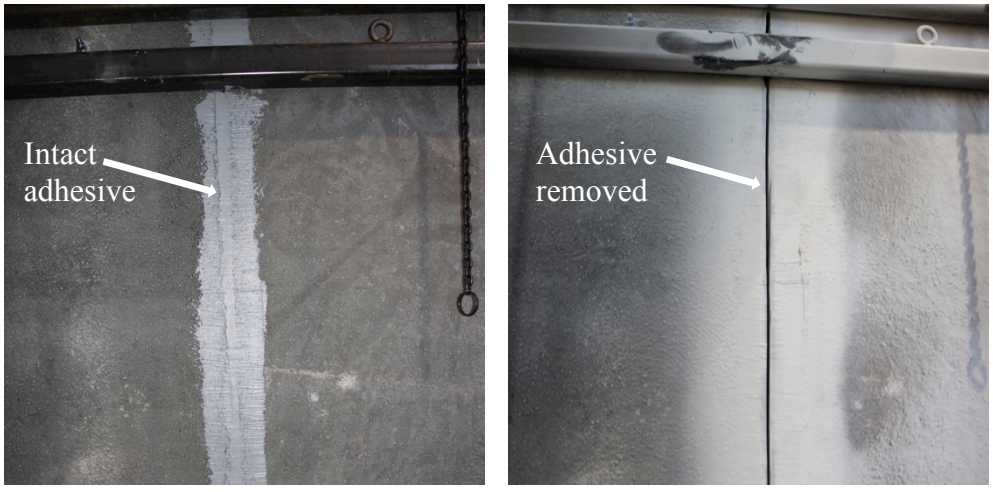

(a) (b)

Figure 5.14 – Epoxy-putty adhesive removal: (a) back side of Test #1 with intact adhesive; (b) back side of Test #2 with adhesive removed with grinder.

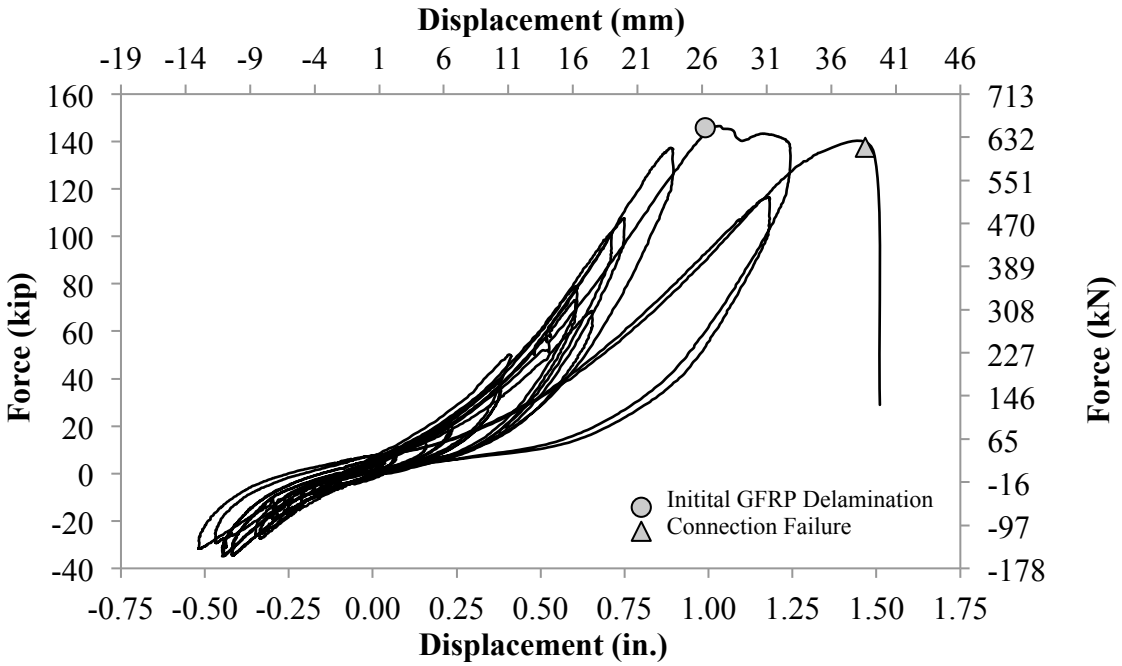

Figure 5.15 – Test #2 hysteresis.

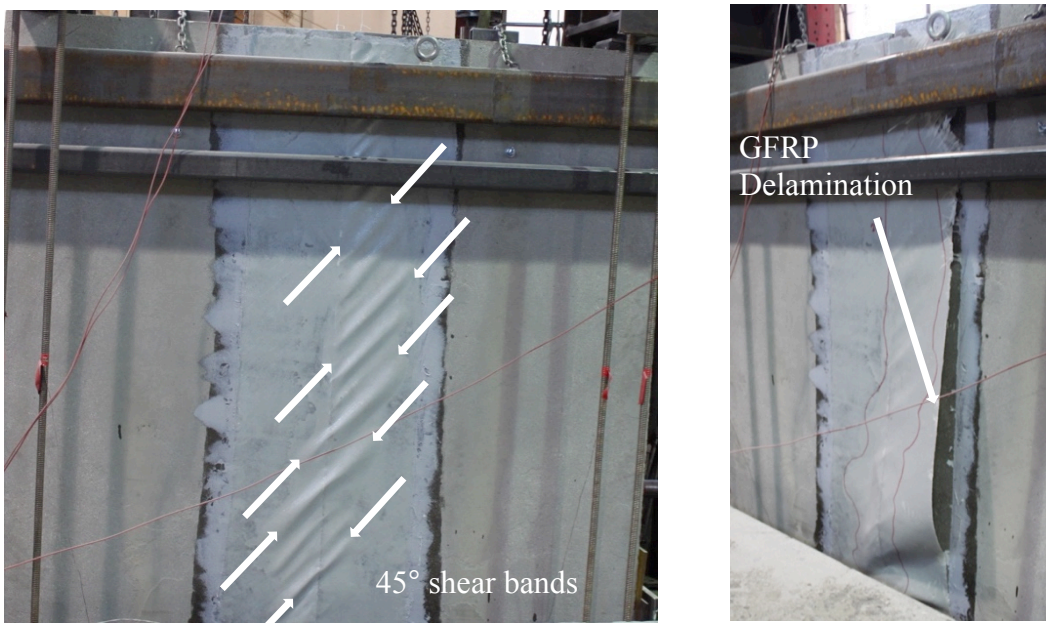

(a) (b)

Figure 5.16 – Test #2: (a) initial GFRP composite delamination; (b) connection failure.

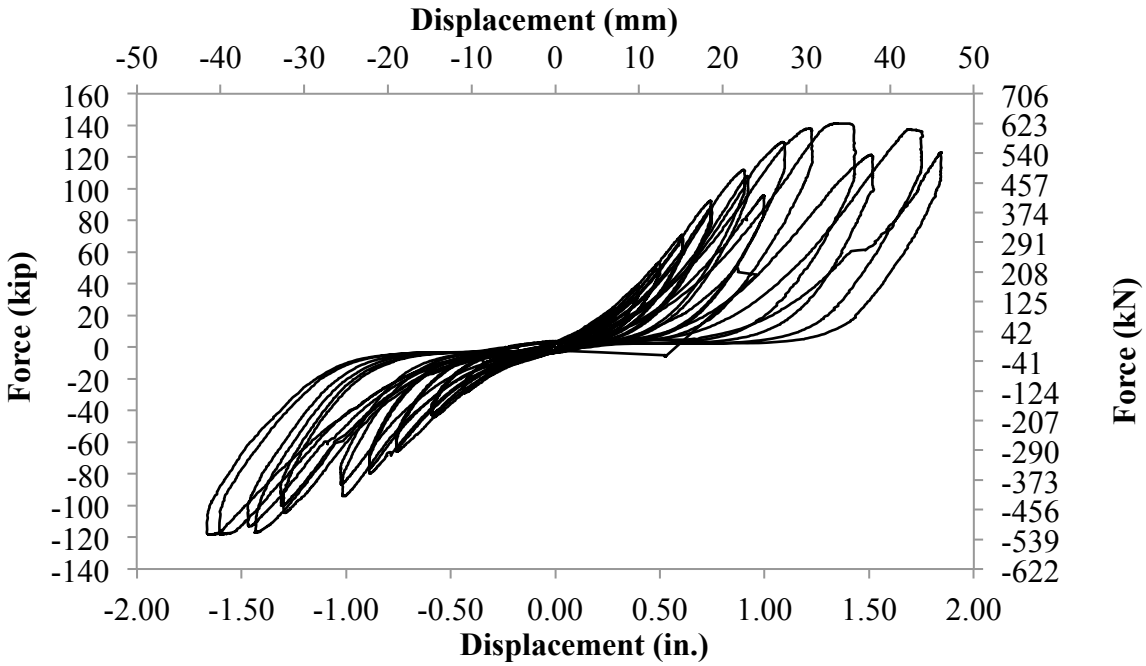

Figure 5.17 – Test #3 hysteresis.

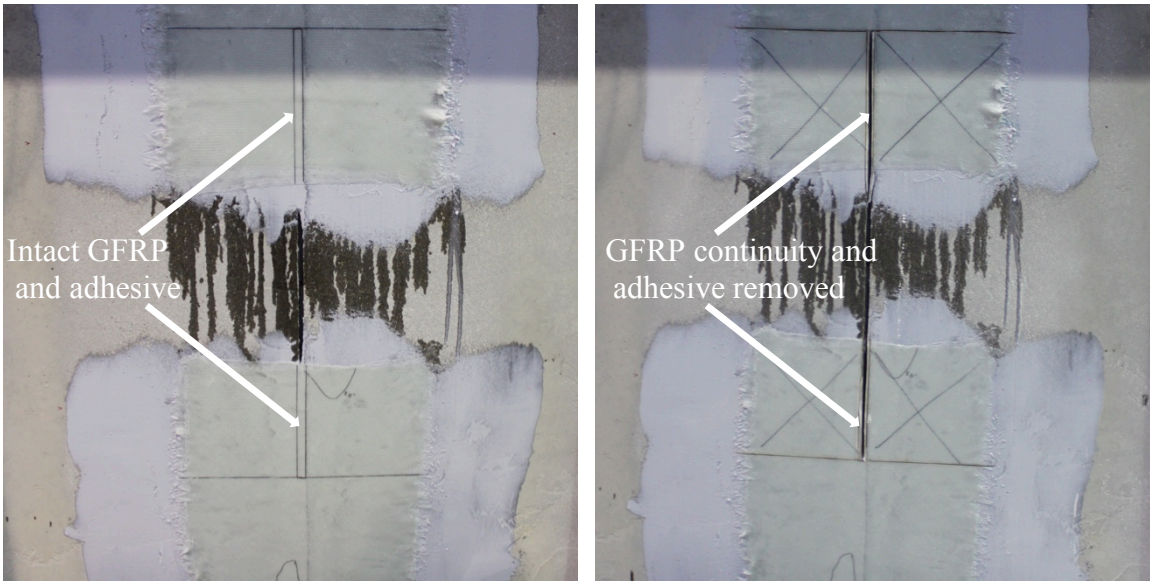

(a) (b)

Figure 5.18 – Connection reduction: (a) Test #3 with intact adhesive and GFRP laminate;

(b) Test #4 with reduced adhesive and GFRP laminate.

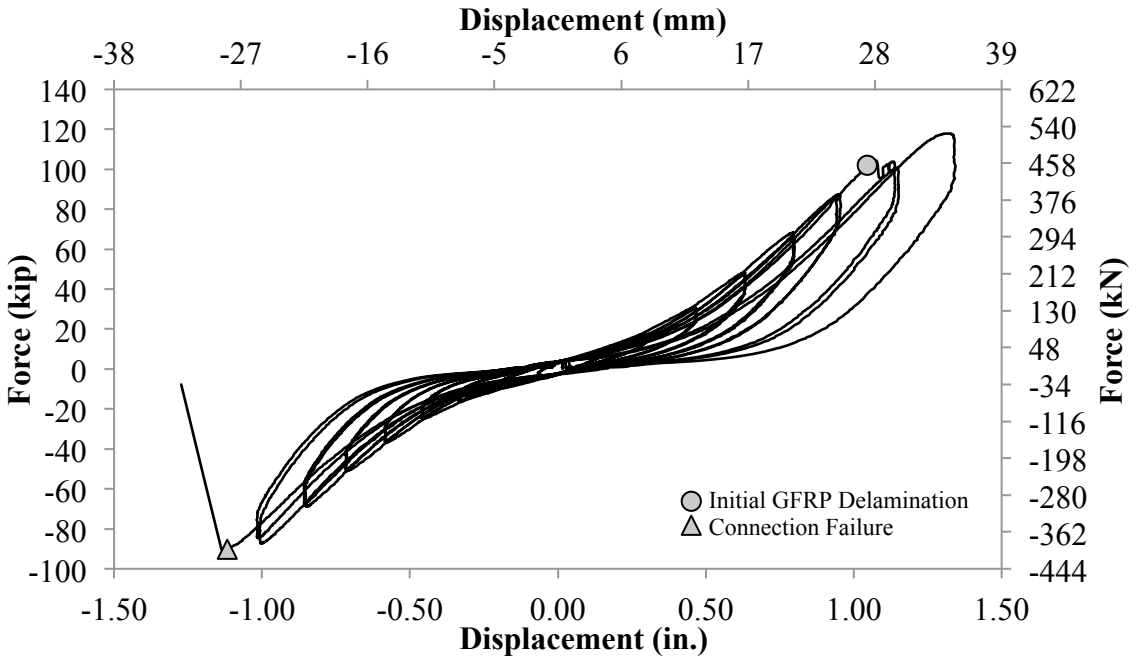

Figure 5.19 – Test #4 hysteresis.

(a) (b)

Figure 5.20 – Test #4: (a) initial GFRP delamination; (b) connection failure.

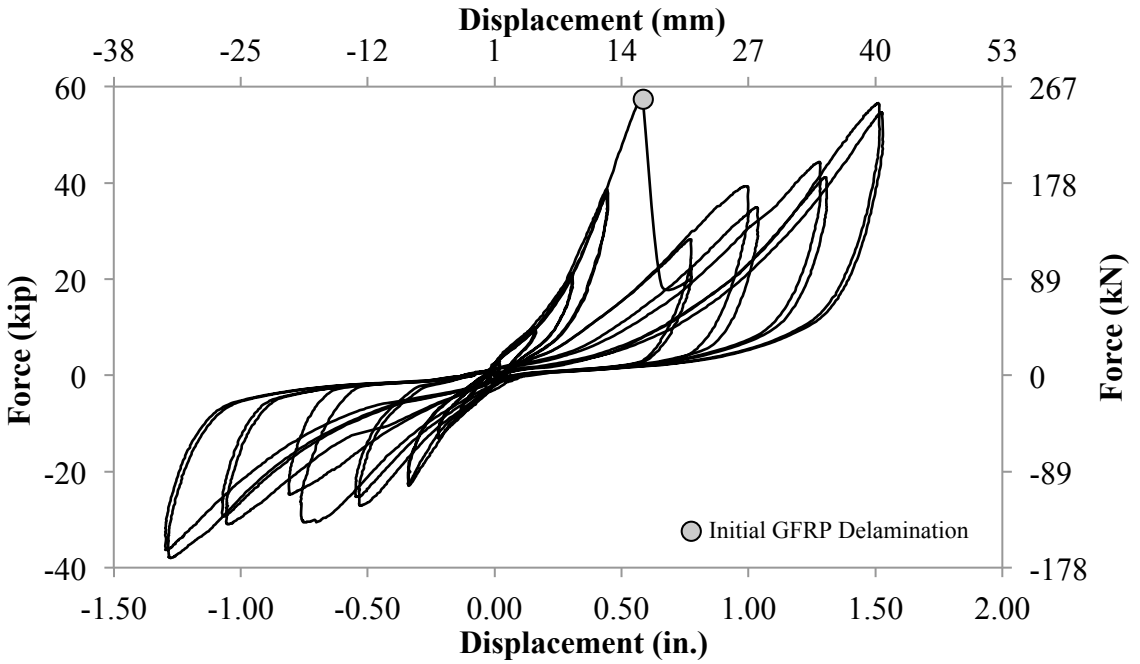

Figure 5.21 – Test #5 hysteresis.

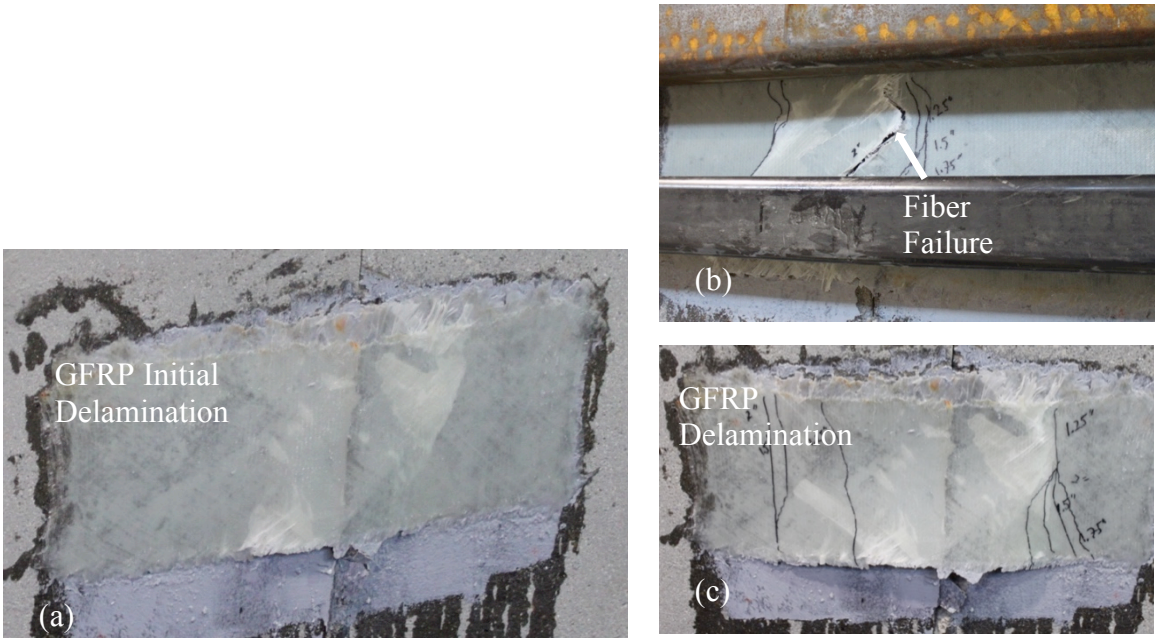

Figure 5.22 – Test #5: (a) lower connection initial delamination; (b) upper connection failure; (c) lower connection failure.

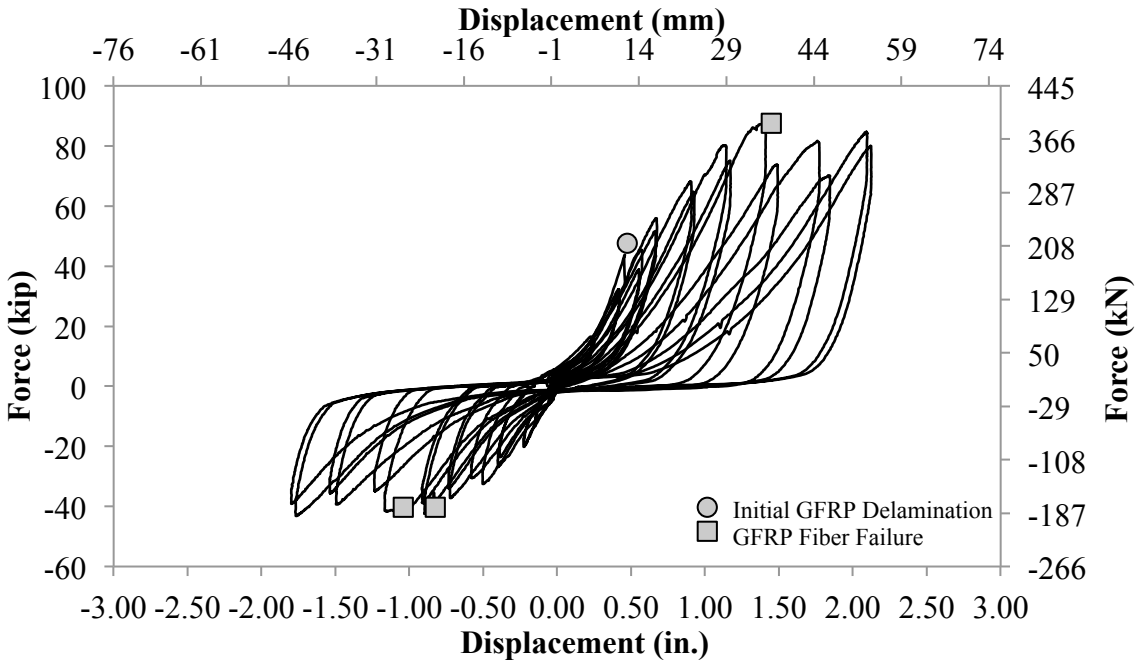

Figure 5.23 – Test #6 hysteresis.

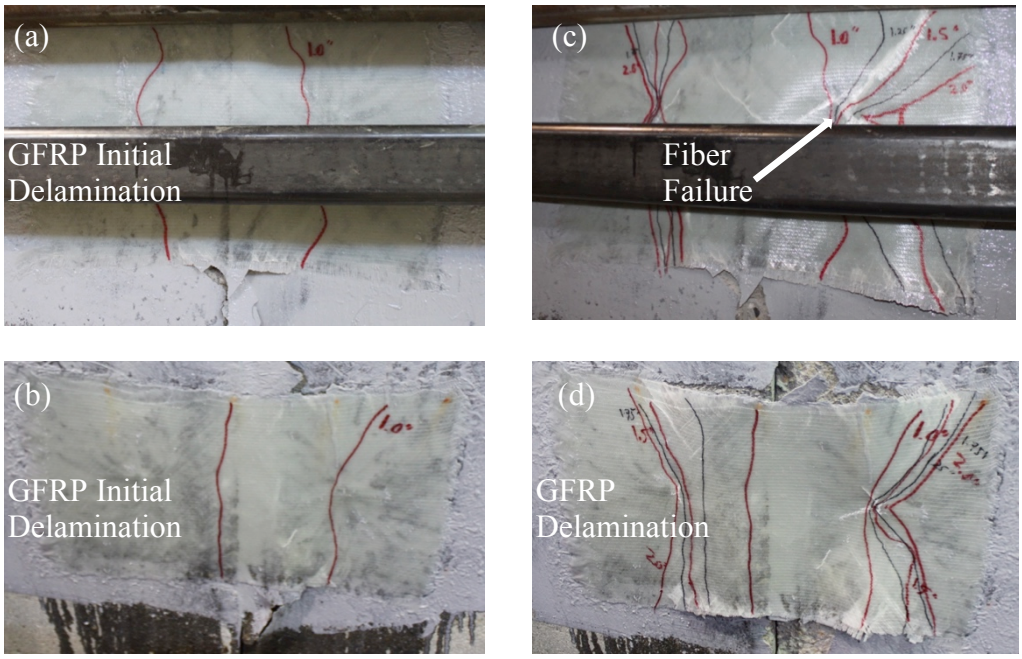

Figure 5.24 – Test #6: (a) upper connection initial delamination; (b) lower connection initial delamination; (c) upper connection progressive delamination; (d) lower connection progressive delamination.

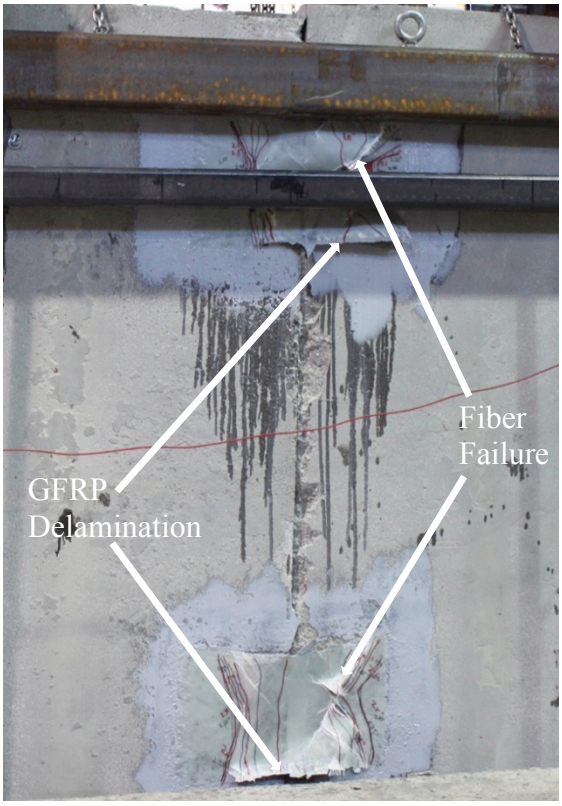

Figure 5.25 – Test #6 connection failure.

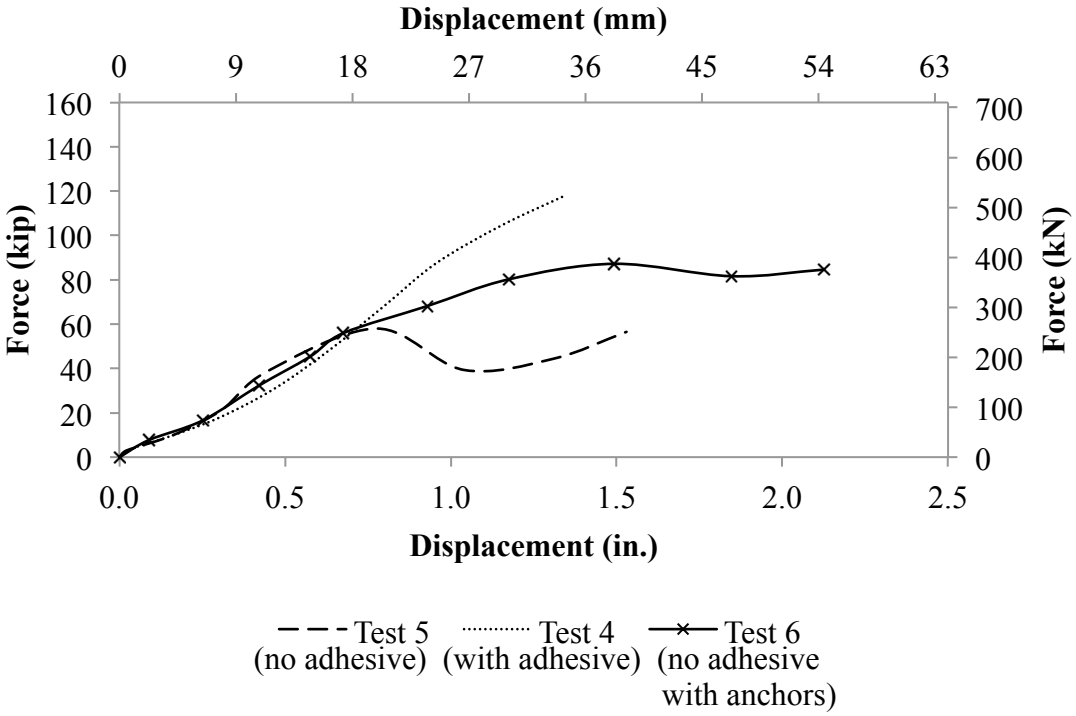

Figure 5.26 – Hysteresis for specimens with 25% of seam height covered.

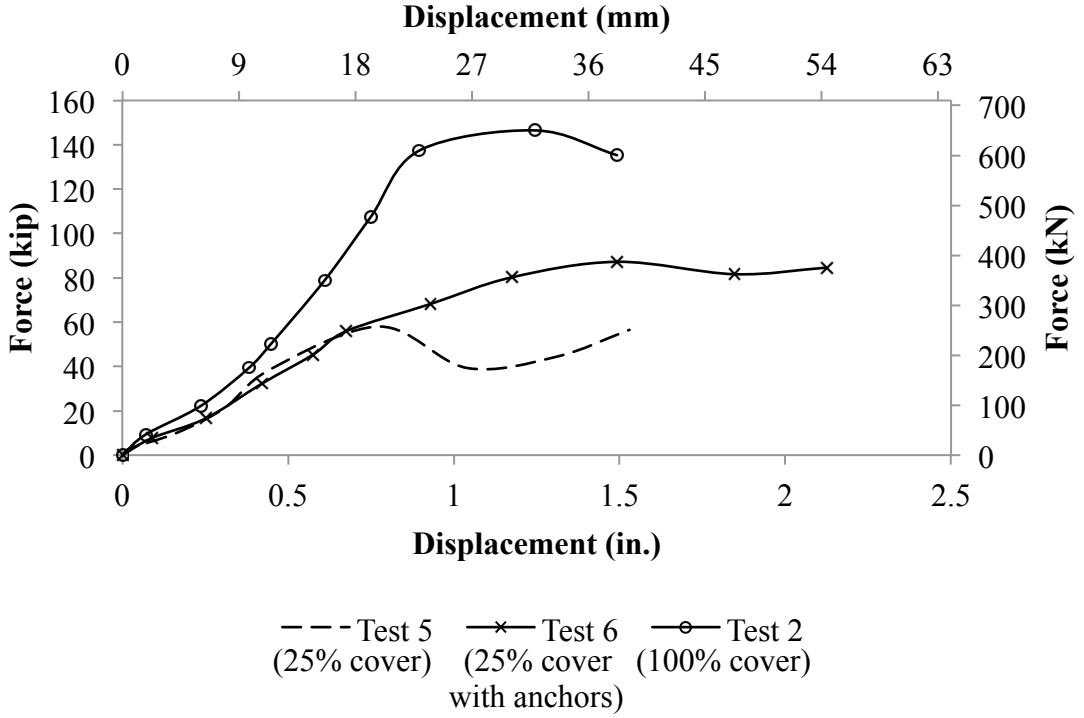

Figure 5.27 – Hysteresis for specimens with no epoxy-putty adhesive in the seam (concrete-to-concrete contact in the seam).

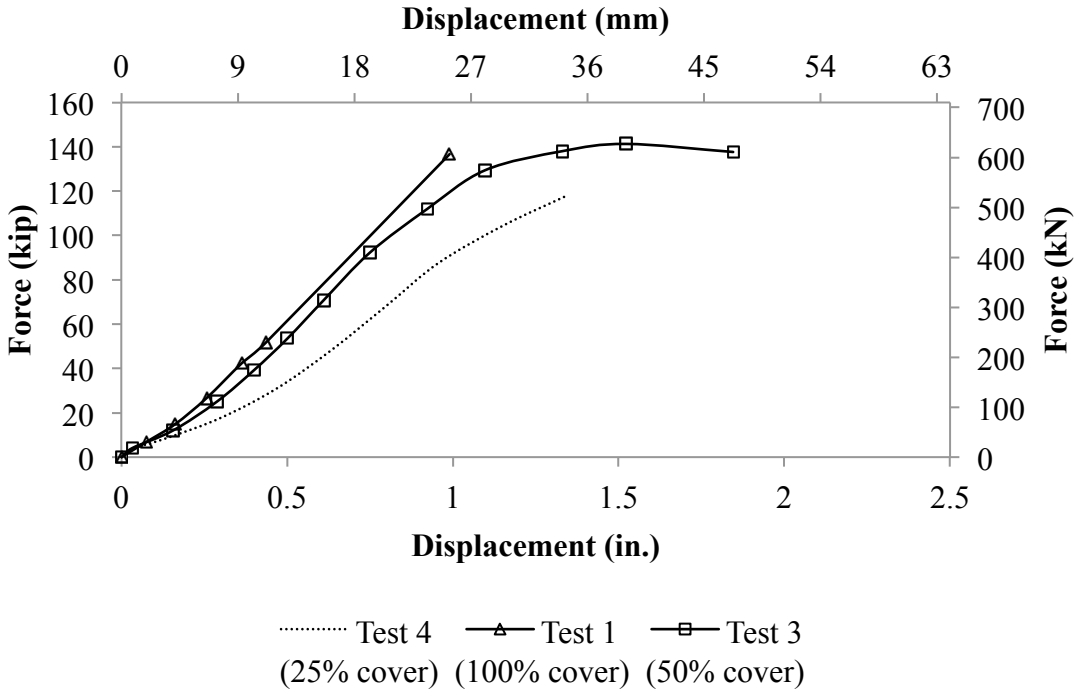

Figure 5.28 – Hysteresis for specimens with epoxy-putty adhesive in the seam.

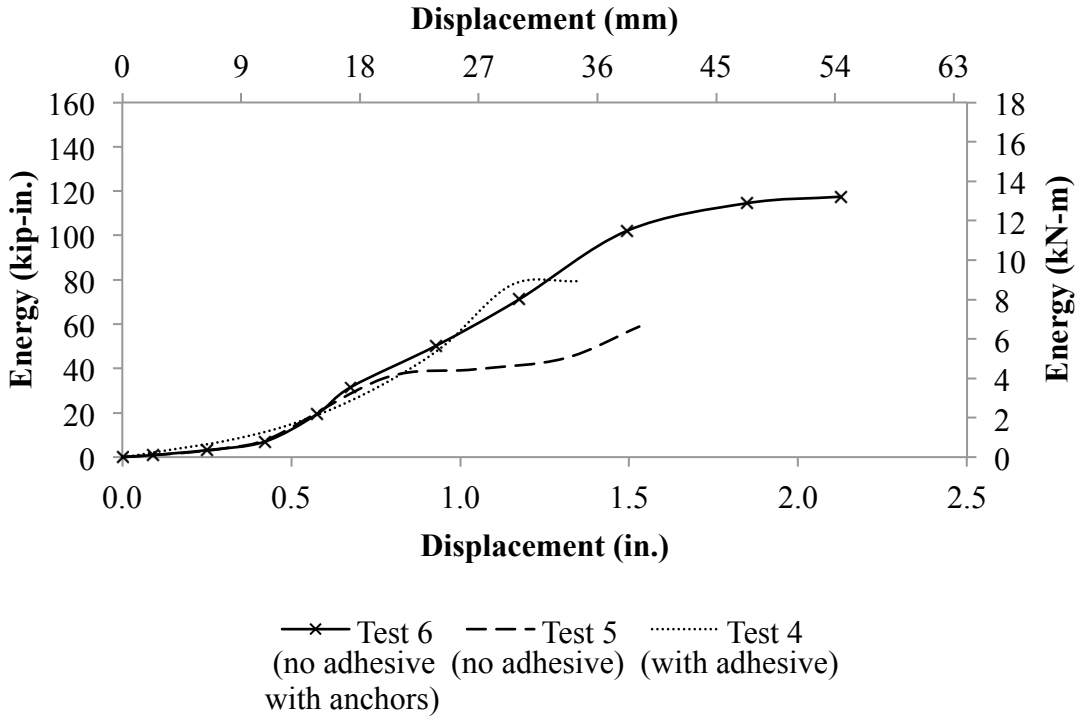

Figure 5.29 – Energy dissipation for specimens with 25% of seam height covered.

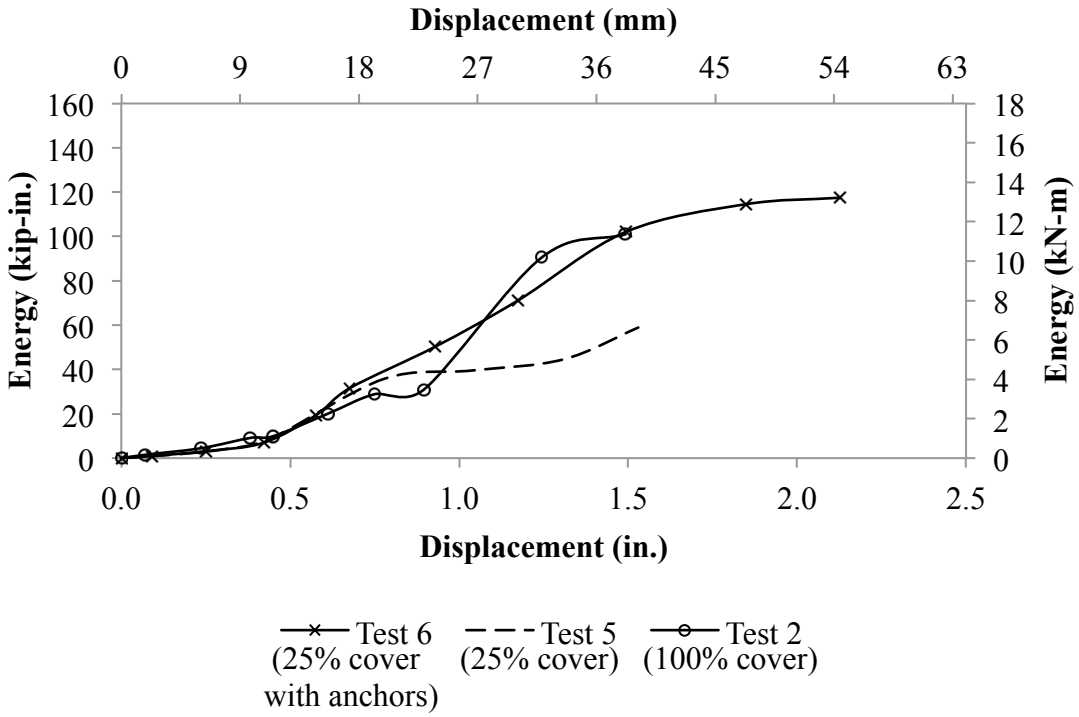

Figure 5.30 – Energy dissipation for specimens with no epoxy-putty adhesive in the seam (concrete-to-concrete contact in the seam).

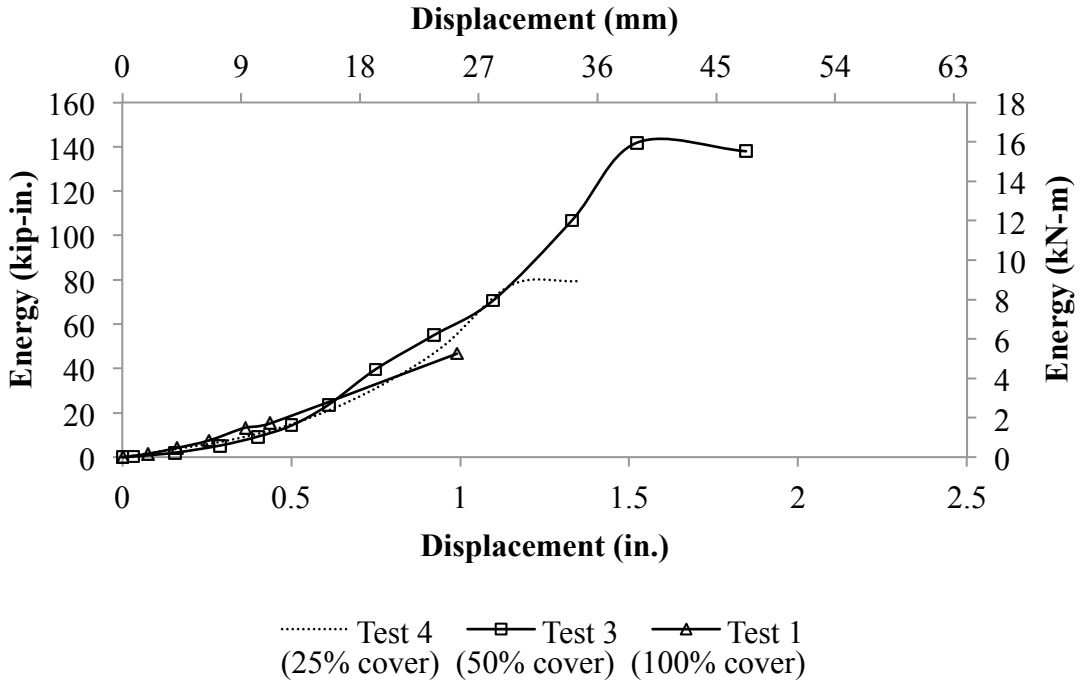

Figure 5.31 – Energy dissipation for specimens with epoxy-putty adhesive in seam.

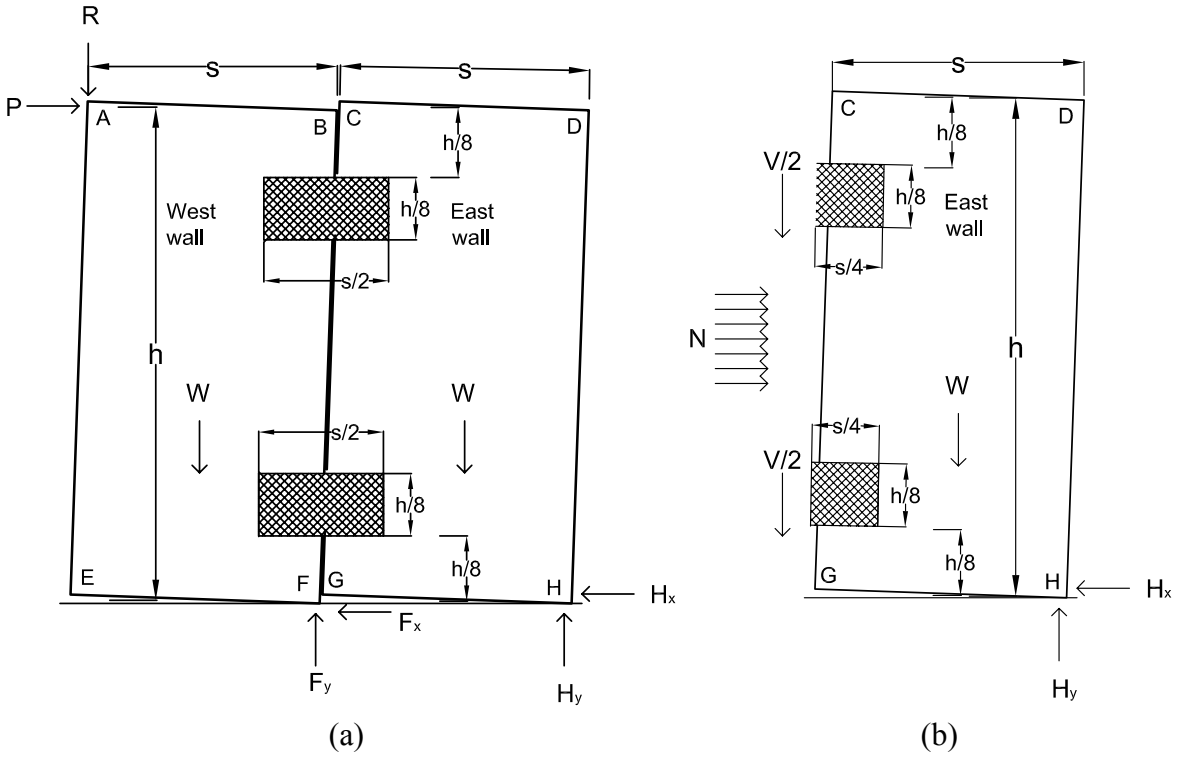

Figure 5.32 – Static analysis of 25% of seam height GFRP connection:

(a) two wall panels connected; (b) free-body diagram of east wall.

CHAPTER 6

SUMMARY AND CONCLUSIONS

The application of GFRP composite as a connection between concrete elements was investigated. The investigation began with an evaluation of different surface preparation methods for a GFRP composite connection, applied between concrete elements, in a direct shear transfer application. The following conclusions can be drawn:

1. Acid wash and surface retarder with multiple-pass pressure wash were determined to be the most practical surface preparation methods. Acid wash is applicable for retrofit and new construction scenarios, where surface retarder with multiple-pass wash is applicable for new construction applications. Although specimens with multiple-pass washed surfaces (without the use of surface retarder) obtained a higher vertical load capacity of 1.5 times more than other methods, the technique could produce varying results depending on how hard the curing surface is when washing 18 hours after casting. Surface retarder can mostly provide consistent results for surface preparation preceding the GFRP composite connection application.
2. GFRP fiber failure was only observed with the scrabbling surface preparation method, where all other tests showed a delamination behavior or a combination of both delamination and GFRP fiber failure. However, scrabbled specimens showed some of the lowest load capacity. This indicates that the bond between the GFRP

connection and the concrete was likely better than the other specimens and resisted early delamination, which delamination immediately propagates with vertical slip. A more thorough investigation is required to determine the effects of scrabbling on GFRP bond to concrete elements.

3. Pressure washing the concrete early in the curing process (without the use of surface retarder) proved to increase the bond strength of the GFRP to concrete, which increased the vertical load capacity of the connection. High-pressure washing has been observed to improve bond strength with concrete (Pantelides et al 2003). However, the method is highly dependent on the concrete strength at the particular time during curing. The early strength is affected by several factors that were not controlled in this testing program.

The performance of precast concrete wall panels connected using a unidirectional GFRP composite connection was investigated under a cyclic quasi-static lateral load simulating seismic excitation. The objective of the tests was to evaluate the load capacity, displacement capacity, energy dissipation, and shear transfer between the walls. The GFRP connections varied in terms of the number of GFRP laminas and were applied to differently prepared concrete surfaces with or without GFRP application pressure and with or without CFRP anchors. The orientation of all GFRP layups was either at (+45°, -45°) or (+45°, -45°, 90°, 0°) with respect to the vertical (90°) seam between the two walls. The following conclusions can be drawn:

1. An increase of horizontal load, horizontal displacement, energy dissipation, and shear transfer was observed when pressure was applied during curing of the GFRP composite connection. Horizontal load capacity increased by 1.4 times,

horizontal displacement capacity increased by 1.5 times, energy dissipation doubled, and shear transfer increased by 1.4 times when pressure was applied. Pressure reduces the thickness of the bond line and increases fiber-aggregate interaction.

2. An increase in lateral load of 1.2 times was observed when four GFRP laminas were used in the connection instead of two GFRP laminas. However, a higher displacement by 1.4 times and a higher energy dissipation of 1.8 times was observed when two GFRP laminas were used in the connection instead of four GFRP laminas. Four GFRP laminas created a stiffer connection and a more brittle failure mechanism. CFRP anchors help improve and preserve the bond of the GFRP laminate to concrete and do not allow for complete delamination. Two GFRP laminas have a lower horizontal load capacity as four laminas, but create a connection with a higher displacement capacity and energy dissipation potential.
3. An increase in horizontal load capacity and horizontal displacement capacity was observed when the concrete surface was prepared using a surface retarder with multiple-pass wash. The horizontal load capacity was increased by 1.1 times more and the horizontal displacement capacity was increased by 1.2 times more. The surface retarder with pressure wash technique exposed a bigger area of large aggregates in the connection area. However the muriatic acid washed surface dissipated 1.3 times more energy.
4. Application pressure improves the bond of the GFRP composite laminate to the concrete surface by allowing the fibers to follow the contours of the concrete surface. Application of pressure also reduces the bond line thickness that creates a

stronger bond between the GFRP laminate and concrete. However, the applied pressure is potentially damaging to fibers of the CFRP anchors when splayed above the outermost lamina. An increase of energy dissipation of 1.7 times was observed when application pressure on GFRP connections with CFRP anchors was used.

5. The use of CFRP anchors increased the strength and displacement capacity of the connection. A GFRP composite connection with CFRP anchors and without applying pressure resisted 1.4 times the load of a similar connection without anchors and with applying pressure. A GFRP composite connection with CFRP anchors and without applying pressure resisted 1.9 times the load of a similar connection without anchors and without applying pressure. A GFRP composite connection with CFRP anchors and with applying pressure resisted 1.5 times the load of similar connections without anchors. Tests with CFRP anchors had the highest displacement capacity of all tests by 1.6 times. The use of approximately one CFRP anchor per 1 ft (0.3 m) of seam height connected demonstrated that anchorage of the GFRP laminate to the concrete increases the lateral load and displacement capacity. In addition, the hysteretic energy dissipation of the connection with anchors was 2.2 times that of the connection without anchors.
6. Different surface preparations showed different added benefits. Acid wash successfully removes the cement paste in the outermost layer from cured concrete, without introducing any new, loose, materials such as media debris. Larger aggregates were exposed when using a surface retarder with multiple-pass wash. The larger aggregates were directly engaged in the connection and contributed to

a moderate increased lateral load and displacement capacity.

The performance of precast concrete panels connected using a bidirectional GFRP composite connection was investigated under lateral quasi-static cyclic load simulating seismic excitation. The objective of the tests was to evaluate the lateral load capacity, displacement capacity, energy dissipation, and shear transfer between the walls. The GFRP connections varied in laminas and were applied in different configurations with or without GFRP composite anchors. The following conclusions can be drawn:

1. The epoxy adhesive in the seam between the two walls increased the strength of the connection significantly. The system with 25% seam coverage using two bidirectional GFRP composite lamina and adhesive in the seam failed at twice the load and dissipated 1.3 times more energy than the system without epoxy adhesive in the seam.
2. For systems without epoxy adhesive in the seam, the wall connection with 100% seam coverage using one bidirectional GFRP composite lamina resisted a horizontal load 2.5 times the horizontal load and dissipated 1.3 times more energy than a system with 25% seam coverage using two laminas of bidirectional GFRP composite sheets. This shows that the seam coverage area by GFRP composite is very influential in determining horizontal load capacity.
3. Use of GFRP composite anchors significantly increased the horizontal load capacity of a connection with identical GFRP composite seam coverage. A connection with 25% seam coverage using two bidirectional GFRP composite laminas and four GFRP composite anchors resisted 1.5 times the horizontal load capacity and shear transfer capability reached by a similar connection without

GFRP anchors. The specimen with GFRP anchors had the highest horizontal displacement capacity of all tests. In addition, the hysteretic energy dissipation of the connection with anchors was twice as much as the connection without anchors.

4. GFRP composite anchors are recommended for use in the seismic retrofit of wall panel connections with bidirectional GFRP composite laminas. The system with two bidirectional GFRP composite laminas over 25% of the seam was able to resist a unit shear equal to 28 kips/ft (409 kN/m). A system with identical details and GFRP composite anchors was able to resist a unit shear 1.5 times that of the system without anchors.

The application of GFRP as a connection between precast wall panels as a new construction connection and a retrofit application proved viable. This composite connection has little ductility and suggested seismic design of R=1. For new construction, and especially when waterproofing is involved, a full height connection of two laminas of unidirectional GFRP with CFRP anchors roughly every 1 ft (0.3 m) is suggested for highest horizontal load capacity and horizontal displacement capacity. For retrofit, when the seam has full concrete-to-concrete interaction, a 25% seam coverage using GFRP anchors is suggested for highest horizontal load capacity and horizontal displacement capacity. Also, for retrofit, when the seam can be filled, a 25% seam coverage using epoxy-putty adhesive in the gap is suggested for highest horizontal load capacity. Although no direct comparison between specimens using unidirectional and bidirectional GFRP laminates can be made, respective test results revealed that a

connection system using bidirectional GFRP laminas demonstrated an overall better seismic performance than a connection system using unidirectional GFRP laminas.

CHAPTER 7

FUTURE RESEARCH CONSIDERATIONS

A successful investigation on a GFRP composite connection between concrete elements has been performed. The effects of surface preparation, application pressure, epoxy adhesive, and CFRP and GFRP anchors on horizontal load capacity, horizontal displacement capacity and shear transfer ability has been described in this thesis. The following additional research should be considered:

1. Surface preparation of concrete in preparation for bonding with a GFRP composite connection could be better understood when using the scrabbling technique and pressure washing (without surface retarder) the surface of concrete elements. Both techniques showed superior connection behavior in shear transfer.
2. It is recommended that in future research GFRP anchors should be considered in a full-height seam coverage situation, since they have a higher strain capacity than CFRP anchors. However, because of their lower ultimate strength more research is required to determine applicability. It is also recommended that in a full-height coverage situation, splaying of GFRP or CFRP anchors should be performed in-between GFRP laminas to create a more integrated anchorage system; this would potentially reduce damage to splayed anchor fibers from application of pressure during curing as well.
3. The full-height seam coverage application of a bidirectional laminate (±45°)

potentially decreases installation efforts when compared to unidirectional laminates and the welded plate connection. However, further research is recommended to observe if agreeable results would be obtained with less installation effort.

4. The direct effect on shear transfer of high-strength epoxy-putty adhesive between wall panels should be further investigated, so that its contribution can be determined.

REFERENCES

ACI Committee 374. (2013). “Guide for Testing Reinforced Concrete Structural Elements under Slowly Applied Simulated Seismic Loads.” (ACI 374.2R-13), Farmington, MI.

Hofheins, C.L., Reaveley, L.D., and Pantelides, C.P. (2002). “Behavior of welded plate connections in precast concrete panels under simulated seismic loads.” *PCI J.*, 47(4), 122–133.

Lin, F., Hua, J., and Dong, Y. (2016). “Shear Transfer Mechanism of concrete Strengthened with External CFRP Strips.” *J. Compos. Constr.,* 10.1061/(ASCE)CC. 1943-5614.0000751 , 04016089

McMullin, P.W., Pantelides, C.P., and Reaveley, L.D. (2003). “CFRP composite connector for concrete members.” *J. Compos. Constr.*, 7(1), 73–82.

Pantelides, C.P., Volnyy, V.A., Gergely, J., and Reaveley, L.D. (2003). “Seismic retrofit of precast concrete panel connections with carbon fiber reinforced polymer composites.” *PCI J.*, 48(1), 92–104.

Pantelides, C.P., Reaveley, L. D., and McMullin, P.W. (2004). “Design of CFRP composite connector for precast concrete elements.” *J. Reinf. Plast. Compos.*, 22(15), 1335–1351.

Saenz, N. and Pantelides, C. (2005). "Shear Friction Capacity of Concrete with External Carbon FRP Strips." *J. Struct. Eng.*, 10.1061/(ASCE)0733-9445(2005)131:12(1911), 1911-1919.

Smith, S.T., Hu, S., Kim, S.J., and Seracino, R. (2011). “FRP-strengthened RC slabs anchored with FRP anchors.” *Engineering Structures*, 33, 1075-1087.

Strigel, R.M., Pincheira, J.A., and Oliva, M.G. (2000). “Reliability of 3/8 in. stud-welded deformed bar anchors subject to tensile loads.” *PCI J.*, 45(6), 72–83.

Tape, W.D., Kennedy, J. B., and Madugula, M.K.S. (2007). “Proposed design of a CFRP flange-to-flange connection for precast prestressed double tee systems.” *J. Compos. Constr.*, 11(1), 91–98.

Volnyy, V.A., and Pantelides, C.P. (1999). “Bond length of CFRP composites attached to precast concrete walls.” *J. Compos. Constr.*, 3(4), 168–176.